CHALMERS

Application of FRP materials in Culvert Road Bridges

A feasibility study with focus on mechanical behavior and life-cycle cost analysis

Master of Science Thesis in the Master's Programme Structural Engineering and Building Technology

JINCHENG YANG
LINA KALABUCHOVA

Department of Civil and Environmental Engineering
Division of Structural Engineering
Steel and Timber Structures
CHALMERS UNIVERSITY OF TECHNOLOGY
Göteborg, Sweden 2014
Master's Thesis 2014:123

Application of FRP materials in Culvert Road Bridges

A feasibility study with focus on mechanical behavior and life-cycle cost analysis

Master of Science Thesis in the Master's Programme Structural Engineering and Building Technology

JINCHENG YANG

LINA KALABUCHOVA

Department of Civil and Environmental Engineering
Division of Structural Engineering
Steel and Timber Structures
CHALMERS UNIVERSITY OF TECHNOLOGY

Göteborg, Sweden 2014

Application of FRP materials in Culvert Road Bridges

A feasibility study with focus on mechanical behavior and life-cycle cost analysis

Master of Science Thesis in the Master's Programme Structural Engineering and Building Technology

JINCHENG YANG

LINA KALABUCHOVA

Department of Civil and Environmental Engineering
Division of Structural Engineering
Steel and Timber *Structures*
Chalmers University of Technology
SE-412 96 Göteborg
Sweden
Telephone: + 46 (0)31-772 1000

Cover:
Stresses distribution in the FRP culvert structure and FRP culvert bridge, ABAQUS model

Application of FRP materials in Culvert Road Bridges

A feasibility study with focus on mechanical behavior and life-cycle cost analysis

Master of Science Thesis in the Master's Programme Structural Engineering and Building Technology

JINCHENG YANG

LINA KALABUCHOVA

Department of Civil and Environmental Engineering

Division of Structural Engineering

Steel and Timber Structures

Chalmers University of Technology

ABSTRACT

The aim of the thesis is to investigate the feasibility of using FRP materials in culvert road bridges. A literature study is carried out to identify the shortcomings of traditional steel culverts and advantages of FRP materials as a construction material for manufacture of culverts. A parametric study is carried out on design of a number of traditional steel culvert bridges and equivalent design is done using FRP sandwich. Finite element modelling is performed to verify and optimize the preliminary design of FRP culverts. Furthermore, a life-cycle-cost analysis of two types of culvert that investigated in this thesis is performed to represent economic advantages of FRP culverts.

Key words: Culvert, Pettersson-Sundquist design method, FRP, Mechanical behavior, FE-analysis, Life-cycle cost analysis

II

Contents

Preface

The master thesis was carried out in the Division of Structural Engineering at Chalmers University of Technology from January 2014 to June 2014.

We would like to give a great thanks to our supervisor and examiner, Assistant Professor Reza Haghani at Chalmers, for his consistent help during the whole thesis project. We would also like to thank the supervisor from WSP at Göteborg, Kristoffer Ekholm, for giving us precious support for the design of steel culverts. Thanks to the supervisor, Associate Professor Mohammad Al-Emrani, for his critical comments and constructive suggestions in future. We also express our gratitude to our supervisor Valbona Mara, the Ph.D. student in the Division of Structural Engineering who shared her experience and ideas about FRP materials and the life-cycle cost analysis.

Finally, a special thanks to our opponent group Chanthoeun Chiv and Yubath Vocal Vasquez. We get lots of inspiration from the discussion and idea-sharing about the design of FRP materials through the entire thesis work.

Göteborg July 2014

Jincheng Yang & Lina Kalabuchova

Notations

Notations in the structural design of culverts

Roman letters

A_{bolt}	Cross-sectional area of the bolt
a_{bolt}	Distance between two parallel rows of bolts (center to center)
A_s	Cross-sectional area of steel profile
$A_{s.cor}$	Cross-sectional area of steel profile in the corner region of the culvert
$A_{s.top}$	Cross-sectional area of steel profile in the top region of the culvert
$C_{my.0}$, C_{my}	Calculation parameter for uniform moment factor
C_{yy}	Equivalent uniform moment factor according to EN 1993-1-1
c_{sp}	Corrugation length of steel profile
C_u	Uniformity coefficient
D	Span of the culvert
d_{bolt}	Diameter of the bolt
d_{10}	Aggregate size at 10% passsing
d_{50}	Aggregate size at 50% passsing
d_{60}	Aggregate size at 60% passsing
e_1	Soil void ratio
E_s	Elastic modulus of steel material
$E_{soil.d}$	Design value of the tangent modulus of soil material
$E_{soil.k}$	Characteristic value of the tangent modulus of soil material
e_{sp}	Calculation parameter of steel profile
$F_{b.Rd}$	Bearing resistence per bolt
F_{st}, $F_{t.Ed}$	Tension in the bolt due to external bending moment
F_{sv}, $F_{v.Ed}$	Shear in the bolt due to external normal force
$F_{t.Rd}$	Tensile force resistance per bolt
f_{ub}	Ultimate strength of steel material for bolts
$F_{v.Rd}$	Shear resistence per bolt
f_{yb}	Yielding strength of steel material for bolts
f_1	Calculation parameter for bending moment
$f_{2.cover}$	Calculation parameter for bending moment
$f_{2.surr}$	Calculation parameter for bending moment
$f_{4'}$, $f_{4''}$, $f_{4'''}$, f_{4IV}	Calculation parameters for bending moment

f_{uk}	Characteristic value of ultimate strength of steel material
f_{yd}	Design value of yielding strength of steel material
f_{yk}	Characteristic value of yielding strength of steel material
H	Vertical distance between the crown of the culvert and the height at which the culvert has its greatest width
h_f	Vertical distance between bolted connection and surface of soil cover
h_c	height of soil cover
$h_{c.red}$	Reduced height of soil cover
h_{corr}	Profile height
I_s	Moment of inertia of the cross-section
$I_{s.cor}$	Moment of inertia of the cross-section in the corner region of the culvert
$I_{s.top}$	Moment of inertia of the cross-section in the top region of the culvert
k_v	Calculation parameter of soil material
k_{yy}	Interaction factor according to EN 1993-1-1
m_1	Soil modulus number
$M_{d.SLS.1}$	Design value of bending moment when the backfilling reaches crown level in SLS
$M_{d.SLS.2}$	Design value of bending moment when the backfilling completed in SLS
$M_{d.ULS.2}$	Design value of bending moment when the backfilling completed in ULS
$M_{s.cover}$	Bending moment due to soil cover
$M_{s.surr}$	Bending moment due to backfilling soil till crown level
M_t	Bending moment due to live traffic
$M_{t.fatigue}$	Bending moment due to live traffic considering fatigue
m_{tt}	Tangential length of steel profile
M_u	Plastic moment capacity of the steel profile
M_{ucr}	Plastic moment capacity of the steel profile considering buckling
$M_{y.Ed}$	Bending moment in the maximum loaded section
$M_{y.Ed.cor}$	Bending moment in the corner region
n_{bolt}	number of bolts
$N_{d.u}$	Design value of the maximum normal force in ULS

N_{obs}	Number of heavy vehicles per year per slow lane
n_{pl}	Calculation parameter for uniform moment factor
N_{Ed}	Normal force in the maximum loaded section
$N_{Ed.cor}$	Normal force in the corner region
N_{cover}	Normal force due to soil cover
N_{cr}, $N_{cr.y}$	Critical buckling load
$N_{cr.el}$	Critical buckling load under idea elastic conditions
$N_{d.SLS.1}$	Design value of normal force when the backfilling reaches crown level in SLS
$N_{d.SLS.2}$	Design value of normal force when the backfilling completed in SLS
$N_{d.ULS.2}$	Design value of normal force when the backfilling completed in ULS
N_{surr}	Normal force due to surrounding soil
N_t	Normal force due to live traffic load
$N_{t.fatigue}$	Normal force due to traffic load considering fatigue
N_u	Plastic normal force capacity of the steel profile
$p_{traffic.fatigue}$	Equivalent line load due to fatigue
$p_{traffic}$	Equivalent line load due to traffic group
Q_0, N_0	Traffic volume values according to EN 1993-2
Q_{m1}	Average gross weight of lorries in the slow lane
r	Radius of curvature of steel profile to section center
R_b	Bottom radius of the culvert
R_c	Corner radius of the culvert
r_d	Dynamic amplification factor
RP	Degree of compaction
R_s	Side radius of the culvert
R_{sp}	Radius of curvature of steel profile
R_t	Top radius of the culvert
$Stiff_{soil}$	Calculation parameter of stiffness
$Stiff_{steel}$	Calculation parameter of stiffness
$S_{v.1}$	Calculation parameter considering arching effect of soil
t_{Ld}	Design life of the culvert bridge
t_s	Thickness of the corrugated steel plate
w_y	Ratio of plastic to elastic section modulus according to EN 1993-1-1

W_s	Elastic section modulus of the cross-section
$W_{s.cor}$	Elastic section modulus of the cross-section in the corner region of the culvert
$W_{s.top}$	Elastic section modulus of the cross-section in the top region of the culvert
Z_s	Plastic section modulus of the cross-section
$Z_{s.cor}$	Plastic section modulus of the cross-section in the corner region of the culvert
$Z_{s.rein}$	Plastic section modulus of the cross-section with one more reinforcement plate
$Z_{s.top}$	Plastic section modulus of the cross-section in the top region of the culvert

Greek letters

α	Corrugation Angle of steel profile
α_{bu}	Imperfection factor according to EN 1993-1-1
α_c	Calculation parameter according to BSK 99
β	Soil stress exponent
γ_{Ff}	Partial factor for fatigue load
$\gamma_{G.s}$	Partial factor for permanent load in SLS
$\gamma_{G.u}$	Partial factor for permanent load in ULS
$\gamma_{m.soil}$	Partial factor for soil material according to SDM manual
$\gamma_{m.steel}$	Partial factor for steel material according to SDM manual
γ_{M1}	Partial factor for steel material according to Eurocode
γ_{Mf}	Partial factor for steel material considering fatigue
γ_n	Safty class factor
$\gamma_{Q.s}$	Partial factor for live load in SLS
$\gamma_{Q.u}$	Partial factor for live load in ULS
δ_{max}	Maximum theoretical deflection
$\Delta F_{d.t}$	Design value of tensile force in each bolt
$\Delta F_{d.v}$	Design value of shear force in each bolt
$\Delta M_{t.f}$	Design value of fatigue moment
$\Delta N_{t.f}$	Design value of fatigue normal force
$\Delta \sigma_{bott}$	Effective stress range for bottom fiber

$\Delta\sigma_c$	Detail category for tension
$\Delta\sigma_{c.p}$	Plate section category
$\Delta\sigma_{E.2.b}$	Tensile stress per bolt for fatigue
$\Delta\sigma_{E.2.p}$	Damage equivalent stress range related to 2 million cycles
$\Delta\sigma_p$	Effective stress range
$\Delta\sigma_{top}$	Effective stress range for top fiber
$\Delta\tau_c$	Detail category for shear
$\Delta\tau_{E.2.b}$	Shear stress per bolt for fatigue
H	Ratio of plastic to elastic section modulus
K	Calculation parameter considering arching effect of soil
$K, \xi, \eta_j, \mu, \omega$	Calculation parameters for buckling in the maximum loaded region
λ	Damage equivalence factor for fatigue according to EN 1993-2
λ_1	Factor for damage effect of traffic
λ_2	Factor for traffic volume
λ_3	factor for design life for the bridge
λ_4	Factor for traffic in the other lanes
λ_{buk}	Relative slenderness according to EN 1993-1-1
λ_f	Relative stiffness between culvert structure and the surrounding soil
ν	Poisson ratio of soil material
ρ_1	Density of the soil material up to crown height
ρ_2	Mean density of the soil material within region (h_c+H)
ρ_{cv}	Mean density of the soil material above crown
ρ_{opt}	Optimum density of backfilling soil
$\sigma_{SLS.1}$	Design value of normal force when the backfilling reaches crown level in SLS
$\sigma_{SLS.2}$	Design value of normal force when the backfilling completed in SLS
$\sigma_{SLS.max}$	Design value of normal force in the most unfavorable case in SLS
Φ	Calculation parameter for flexural buckling
ϕ_2	Damage equivalent impact factor
φ_k	Characteristic value of friction angle of the soil material
$\varphi_{k.d}$	Design value of friction angle of the soil material
χ_y	Reduction factor for flexural buckling according to EN 1993-1-1

Notations in the design of FRP materials

Roman letters

[A]	Extensional stiffness matrix for the FRP sandwich
[B]	Coupling stiffness matrix for the FRP sandwich
[D]	Bending stiffness matrix for the FRP sandwich
[Q]	Stiffness matrix for one FRP ply
d	Thickness of the core part of the FRP sandwich
E_{11}	Design elastic modulus of FRP material in the longitudinal direction
E_{22}	Design elastic modulus of FRP material in the transversal direction
$E_{k.11}$	Characteristic longitudinal elastic modulus of FRP material
$E_{k.22}$	Characteristic transverse elastic modulus of FRP material
EA	The equivalent membrane elastic constants
EI_{FRP}	Bending stiffness of the designed FRP sandwich in the span direction
EI	The equivalent bending elastic constants
G_{12}	Design in-plane shear modulus of FRP material
$G_{k.12}$	Characteristic in-plan shear modulus of FRP material
M	Bending moment applied on the designed cross-section of FRP sandwich
NF	Normal force applied on the designed cross-section of FRP sandwich
no	Number of plies used for the FRP laminate face
t	Thickness of the FRP plies
t_{face}	Thickness of the FRP laminate face

Greek letters

γ_M	Partial factor for FRP material
γ_{M1}	Partial factor for FRP material considering derivation of properties
γ_{M2}	Partial factor for FRP material considering method of manufacturing
γ_{M3}	Partial factor for FRP material considering loading conditions
ΔN	Increment value of applied load
ε_{mid}	Midplane strains
θ	Fiber orientation angle of each ply
κ_{mid}	Midplane curvature
$\sigma_{d.11.c}$ / $\sigma_{d.11.t}$	Design strength of FRP material in the longitudinal direction under compression / tension

$\sigma_{d.22.c}$ / $\sigma_{d.22.t}$	Design strength of FRP material in the transverse direction under compression / tension
$\sigma_{k.11.c}$ / $\sigma_{k.11.t}$	Characteristic strength of FRP material in the longitudinal direction under compression / tension
$\sigma_{k.22.c}$ / $\sigma_{k.22.t}$	Characteristic strength of FRP material in the transversal direction under compression / tension
$\tau_{d.12}$	Design shear strength of FRP material
$\tau_{k.12}$	Characteristic shear strength of FRP material
υ_{12}	Major Poisson's ratio of FRP material

Notations in the life-cycle cost analysis

Δt	Driver delay time due to detouring
L	Length of affected roadway the cars are driving
N	Number of days of roadwork
n	Number of the year considered in LCC
r	Hourly vehicle operating cost
r	Discount rate
S_a	Traffic speed during bridge work activity
S_n	Normal traffic speed
w	Hourly time value of drivers

Abbreviations

BaTMan	Swedish Bridge and Tunnel Management
BRO 2011	Swedish Design regulations for bridges
BSK 99	Swedish Design regulations for steel structures
BV	Swedish National Rail Administration (Banverket)
CFRP	Carbon Fibre Reinforced Polymer
FE	Finite Element
FRP	Fiber Reinforced Polymer
GFRP	Glass Fiber Reinforced Polymer
KTH	The Royal Institute of Technology
LCC	Life-Cycle Cost
NPV	Net Present Value
SCI	Soil Culvert interaction

SDM	Swedish Design Method
SLS	Serviceablility Limit State
TRVK	Swedish Transport Administration Requirement (Trafikverkets Krav)
ULS	Ultimate Limit State
UV	Ultraviolet radiation

Example of indices

b	bolt
bott	bottom
c	compression
cor	corner
corr	corrugation
d	design value
f	fatigue
k	characteristic value
rein	reinforcement
s	steel
t	tension/traffic
u	ultimate
v	shear
y	yielding

1 Introduction

1.1 Background

Steel culvert bridges are already used for more than one hundred years. The versatility of culverts assert due to their low initial investment, fast manufacture and installation time, simplicity in the construction methods, aesthetical look and their geometrical adaptability. Since the application of culvert structures are greatly miscellaneous they can function as pedestrian, highway, railway and road bridges as well as for the passage of water and traffic via conduit.

Despite the number of advantages, the steel culvert structures have some shortcomings regarding maintenance and repair. Most common problems are corrosion, abrasion of galvanized steel coating, which lead to degradation and weakening of the structure. Repair and protection against both local and general scour become a routine for the steel culvert bridges. Many culvert bridges in Sweden have deteriorated to the point where replacement or repair is required.

In addition, the fatigue problem coming from the live traffic loads is realized to be one of the governing issues that limit the use of steel culvert structures. In the condition with shallow soil cover above the culvert, the fatigue becomes even dominant.

Considering the problems involved with traditional steel culverts, substantial demand of a better solution comes from the construction field.

In this master thesis fibre reinforced polymer (FRP) materials, as a promising alternative for the culvert structure, are investigated, due to its significant properties and satisfying performance regarding deterioration and fatigue.

1.2 Aims and objectives

The brief introduction of background gives a clear goal of the thesis, which aims to investigate whether the application of FRP materials in culvert bridge structures is a feasible alternative to the traditional corrugated steel plates.

In order to achieve the goal, the following objectives are determined to capture in terms of mechanical behaviour and economic performance.

Objectives

Structural feasibility of FRP culvert structures in terms of mechanical behaviour

1. Design the representative cases with steel culverts and find out the governing issues.
2. Design the same cases with FRP and study the performance of FRP culvert against the issue involved in the steel design.

Cost efficiency of FRP culvert structures in terms of economic performance

3. Perform a life-cycle cost (LCC) analysis of a selected case designed with two alternatives and compare the costs.

1.3 **Methodology and approach**

Practical approaches are discussed in order of these three objectives.

Objective 1: Design of the steel culvert structure (see **Chapter 3**)

- Determine a collection of design cases with representative conditions
- Design the cases with the Swedish Design Method [1]

Objective 2: Design of the FRP culvert structure (see **Chapter 4**)

- Choose a proper case for further design with FRP
- Propose a practical design method for the FRP culvert
- Verify the results from proposed design method by FE modelling in ABAQUS
- Improve the proposed design method based on the verification

Objective 3: LCC analysis (see **Chapter 5**)

- For the same design case, carry out the LCC analysis of using steel culvert and FRP culvert, respectively
- Compare and analyse the economic performance of these two alternative

1.4 **Limitations**

Limitations of this thesis generally come from two aspects proposed design method for FRP culvert structures and assumptions in the LCC analysis.

Due to the complexity of FRP materials and lack of developed design manuals for FRP structures, the thesis mainly focuses on the design and calculation of the FRP material in the culvert structure. Thus, the verification part of the FRP culvert design includes: 1) the checks of capacity of FRP material in the ultimate limit state (ULS) and 2) the deflection in the serviceability limit state (SLS). More checks need to be taken into account in the future verification, for instance the creep of FRP material, the capacity of core material and interface between the face and core (Figure 2.30)

Sustainability such as environmental issues and social aspects of alternatives are not discussed in the life-cycle study.

2 Literature Review

2.1 Steel culverts

2.1.1 Steel culverts in Sweden

The concept of corrugated profile steel pipes was presented in the mid 1950's. The design was based on primitive diagrams and standard drawings, which operated with two types of conduits only: low-rise culverts and vertical ellipses. By then, the standard drawings were only applicable for the structures with a span up to 5 m. However, several culverts with a span over 5 meters were also erected.

With an increasing industry, technologies and therefore knowledge about culverts, the more advanced and accurate design methods were developed, that are able to consider different soil materials, larger spans and various cover heights. The first full-scale test of pipe arch was performed by The Royal Institute of Technology (KTH) in 1983 supported by Swedish Road Administration (Figure 2.1). The structure had as span of 6,1 meters with a cover height of 1 meter. In addition, the other field test of the culvert with span of 6 meters and 0,75-1,5 meters cover height was carried in 1987-1990 (Figure 2.2).

The tests were followed by a newly proposed Swedish Design Method (SDM) in 2000. Thereafter, The Swedish Road Administration (Vägverket) implemented the method in the code Bro 2002 and National Rail Administration (Banverket) accepted it in BV Bro. After introducing the box culvert to Swedish marked in 2002, actualizing the full-scale field tests, improving the design methodologies and introducing certain modifications the 4th edition of the handbook by Pettersson and Sundquist [1] was published in 2010.

There existed about 4430 culvert bridges in 2012, 4100 whereof are made of steel according to Swedish Bridge and Tunnel Management (BaTMan). The vast majority of culverts were built in 50's and 60's, which implies that they are in the poor condition and require rehabilitation or replacement. Moreover, according to the report Safi, 2012 [2] the common span length for culverts in Sweden are 5 meters and less.

According to TRVK Bro 11 (2011) culverts are commonly designed for the technical life of 80 years; however culverts are constantly exposed to adverse environment, thus making the inspection and maintenance frequent and service life shorter.

Figure 2.1 The first full-scale test in Sweden in 1983 [3]

Figure 2.2 The field test of pipe arch culvert in Sweden in 1987-1990 [3]

2.1.2 General information of steel culverts

The steel culvert can be defined as a flexible corrugated structure forming a pipe or an arch, gaining its load bearing capacity by the interaction between conduit wall and surrounding soil. A common configuration of the culvert can be indicated as in Figure 2.3 and Figure 2.4 represents parts of the culvert ridge. The extensive usage of the culverts can be easily explained by pointing their advantages:

- Low initial cost
- Fast manufacturing and assemblage
- Aesthetics: natural exterior because of the overfill
- Simple construction methods
- Adjustment to a possible extension or widening of the road

A culvert is a burred bridge construction which requires a very thorough soil compaction, therefore a great attention should be paid in the proper backfill [4] in order to obtain a preferred strength, prevent wash-outs and settling.

Another important parameter to evaluate is the soil height above the culvert [4]. This covert height is greatly important when concentrated live loads are considered: for lower cover heights live loads has more significant effect on the structural behaviour of the culvert introducing bending moments in the conduit wall as well as enhancing the fragility to fatigue damage. For this reason, a minimum cover height of 0, 6 m is adopted in Sweden.
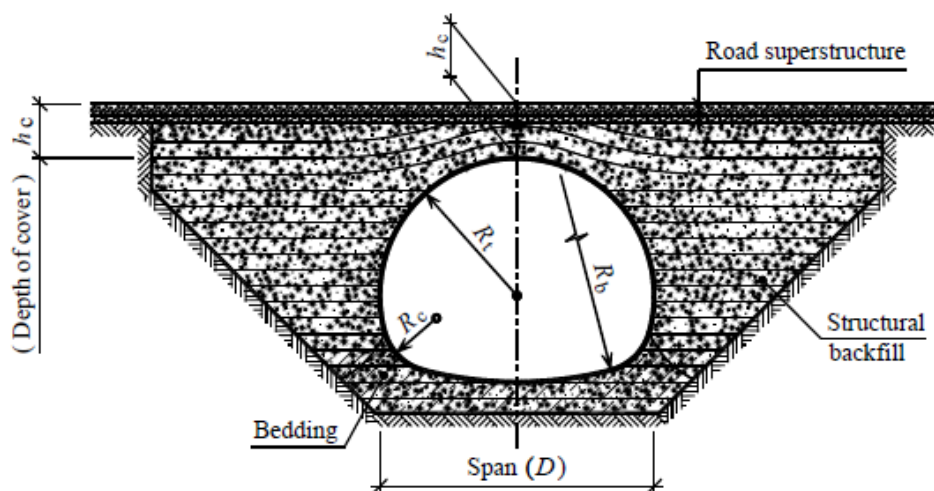

Figure 2.3 Typical configuration of a corrugated steel pipe arch culvert [1]
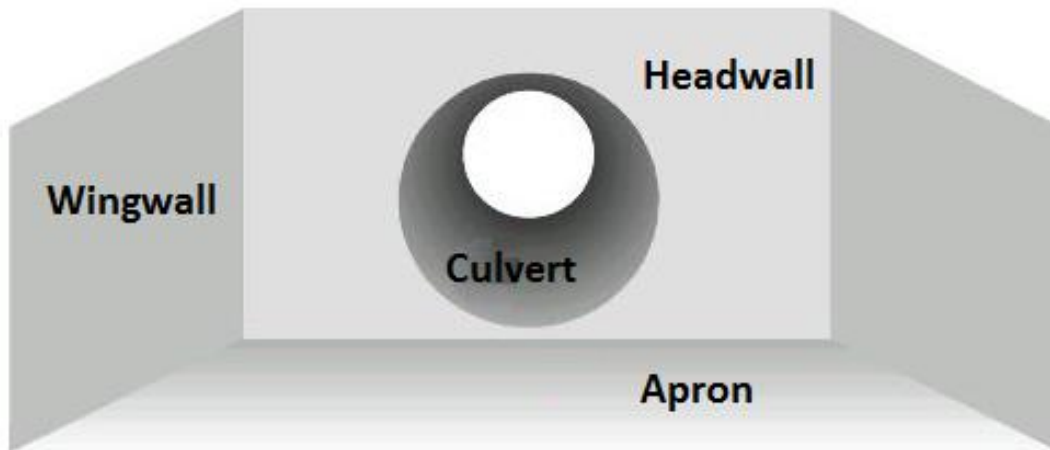
Figure 2.4 Different parts of the culvert ridge [5]

2.1.2.1 Culvert profiles

The design of culvert shape considers: 1) the site conditions, such as span and cover height, 2) flow capacity and fish passage for the river-passage-culvert bridges. The proposal should also be cost-effective and durable. According to 4th edition of the handbook by Pettersson and Sundquist [1], sever types of culvert profile are classified as:

Closed profiles (Figure 2.5 - Figure 2.8)**:**

    A. Circular with constant radius
    B. Horizontal ellipse
    C. Vertical ellipse
    D. Pipe-arch, defined by three radii

Arch-type profiles (Figure 2.9 - Figure 2.11):

    E. Circular with single radius
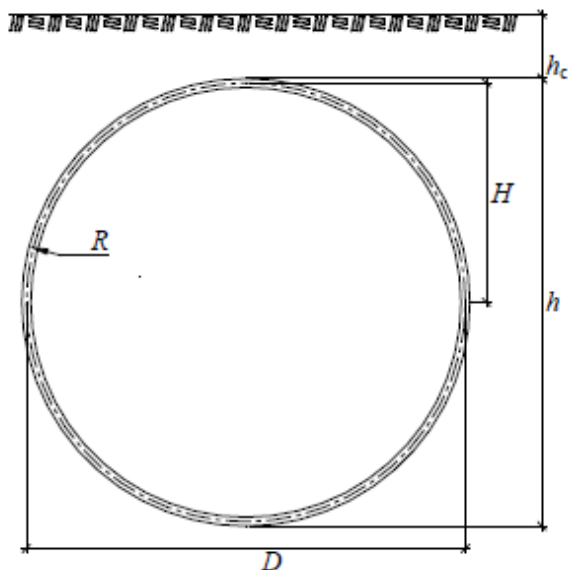   F. Two or three radii
    G. Box culvert

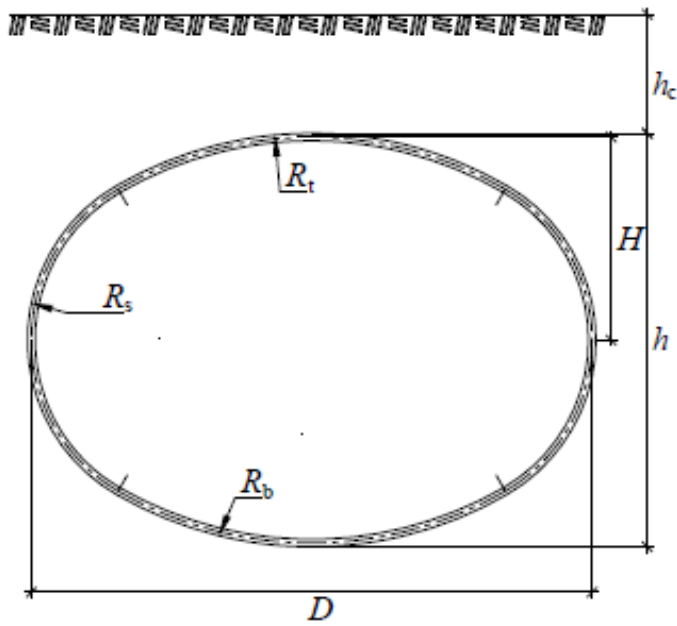*Figure 2.5 A. Circular profile with constant radius R [1]*

Figure 2.6 B. Horizontal ellipse. The relationships between top/bottom and side radii should be $R_t/R_s{\leq}4$ and $R_b/R_s{\leq}4$ [1]
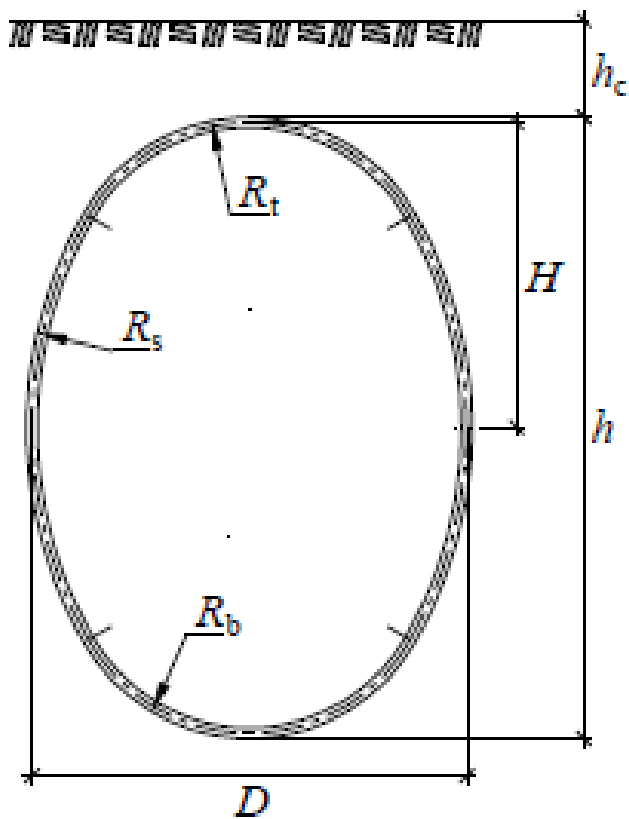
Figure 2.7 C. Vertical ellipse usually with a ratios $R_t/R_s{\approx}0{,}95$ and $R_b/R_s{\approx}0{,}95$ [1]
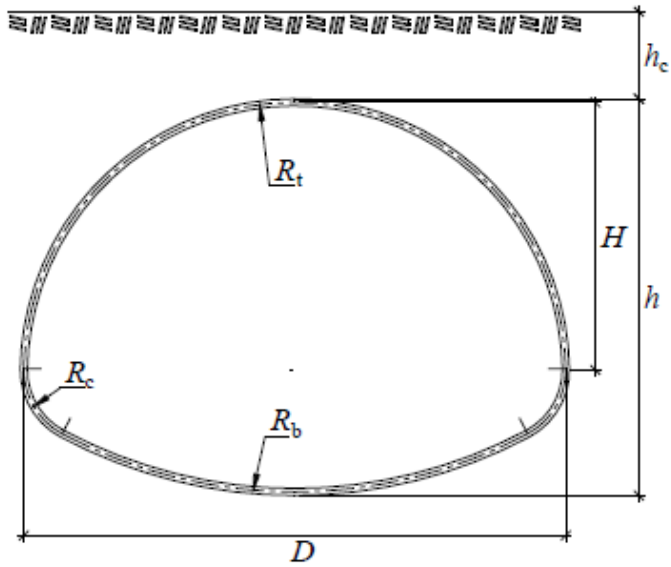
Figure 2.8 D. Pipe-arch, having three different radii. The conditions of top/bottom and corner radii such that $R_t/R_c \leq 5.5$ and $R_b/R_c \leq 10$ [1]
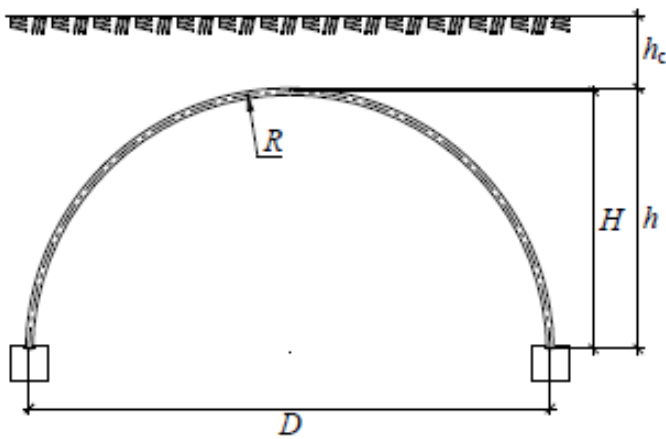
Figure 2.9 E. Circular profile with single radius R [1]
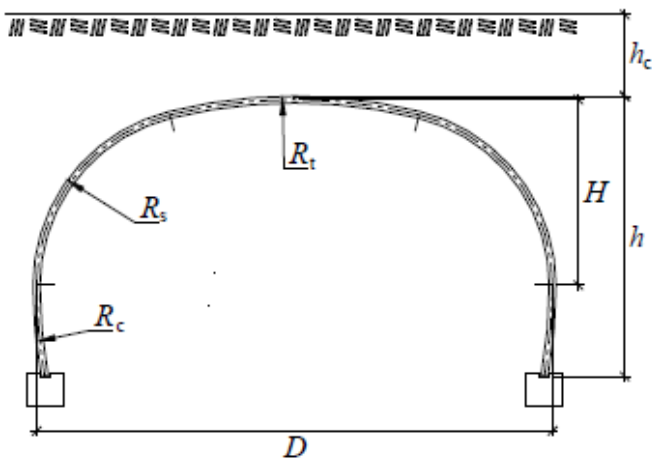
Figure 2.10 F. Arch-type profile with three different radii. The conditions of top and side radii so that $Rt/Rs \leq 4$ and of corner and side radii so that $1 \leq Rc/Rs \leq 4$ [1]
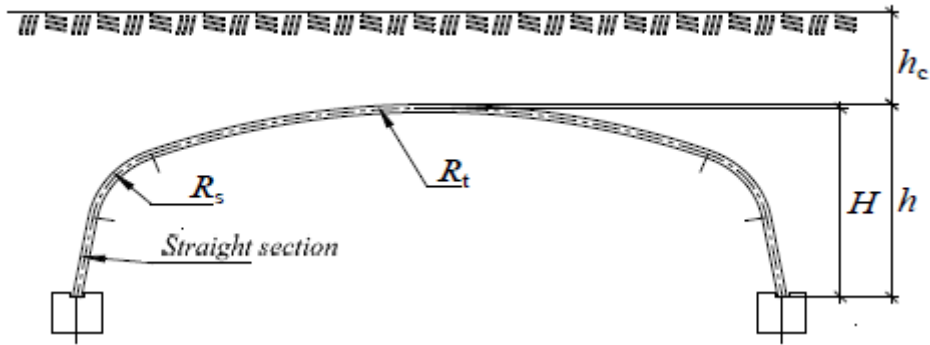
Figure 2.11 G. Box culvert with a relationship Rt/Rs≤12 [1]

The box culverts for strengthening purposes due to critical sections might be reinforced with plates (Figure 2.12).
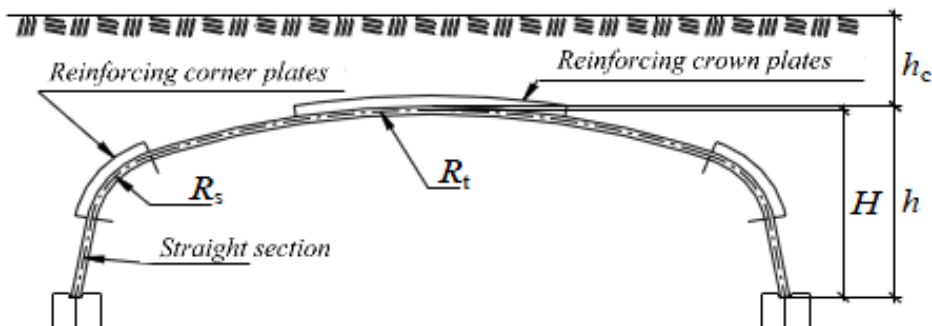

Figure 2.12 Box culvert with reinforcing plates [1]

2.1.2.2 Corrugation profiles

Manufacturers offer a wide range of corrugation profiles, but according to the 4th edition of the handbook by Pettersson and Sundquist [1], the most typically used are illustrated in Figure 2.13 and the thicknesses vary between 1,5-7 millimetres.
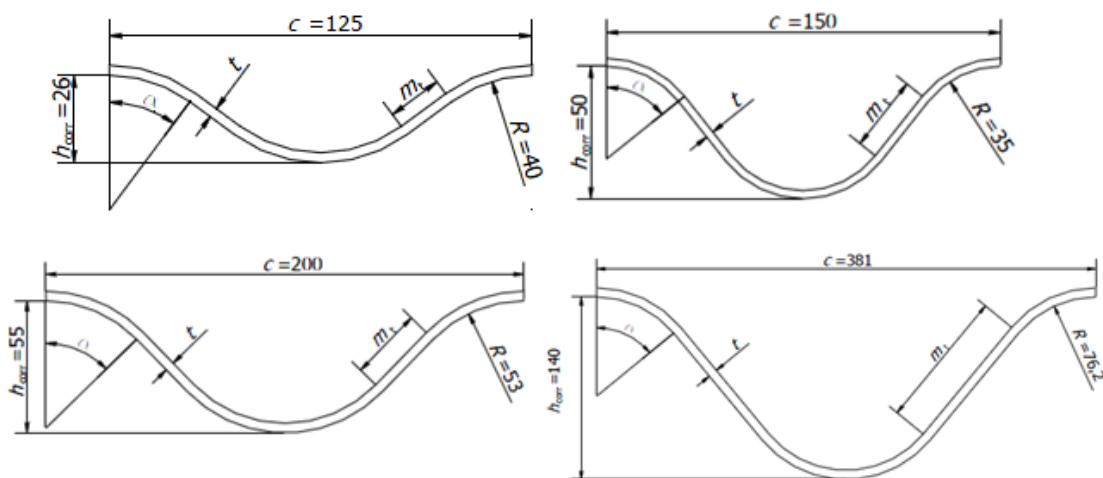
Figure 2.13 Common steel corrugation profiles [1]

2.1.3 **Problems of steel culverts**

Nowadays, a critical problem of the existing culvert is a threat of sink holes, flooding or road collapse. The development of a more durable material is much-needed, since replacement or repair of steel culverts is costly, time-consuming and traffic interruptive. As mentioned previously, culverts can be used in a variety of conditions, for instance for a road bridge and stream crossing, aquatic fauna passage and drainage (Figure 2.14), thus the most concerning issue is corrosion having a significant effect on service life of the structure. The most exposed location and prone to deteriorate is the invert (Figure 2.15, Figure 2.16), in addition to this, the damage of protective layer due to road salts might appear especially for aged structures, allowing the corrosion and annihilation of base metal. Moreover, increased traffic, low quality of structural members and insufficient maintenance makes the culverts structurally deficient and/or functionally obsolete. In addition, under certain circumstances, repair might be even more expensive than replacing with a new one.

Figure 2.14 Culverts for stream crossing and drainage [6]

Figure 2.15 Deteriorated invert and perched end of pipe culvert [7]

Figure 2.16 Corrugated steel culvert invert corrosion [8], [9]

In order to restore the integrity of the structure, one practical example of steel culvert rehabilitation in 2009 in Orono, Maine, USA using invert lining FRP composites can be mentioned (Figure 2.17). The corrugated metal was eroded due to abrasion and corrosion, which leads to degradation and weakened culvert invert. The project was "first-of-its-kind" and included initial analysis and design, testing, manufacturing and installation, though the project proceeded quickly.

Figure 2.17 Corrosion of corrugated culvert and completed installation [10]

Another example is an entire diameter culvert re-lining with GFRP done by Erie Country Department of Public Works, Division of Highways, in western New York in 2002 (Figure 2.18). The replacement or repair was essential because of deterioration, resulting in severe corrosion and strength loss and incapacity to no longer maintain the heavy traffic (38,500 vehicles per day).

Inverting the culverts is an effective rehabilitation solution, however the service life of such hybrid structure is not investigated thoroughly and depends on many factors. Taking into consideration the exposition to the environment, it is estimated that the service life of composite materials should exceed that of steel, so repair will be likely required for the primary steel conduit, resulting in increased maintenance cost. Another solution is a replacement of the structures with FRP composite sandwiches, which should have lower life cycle cost in a long time perspective.

Figure 2.18 An entire culvert re-lining in Buffalo, New York, USA [11]

Even though culverts made of steel has a number of positive aspects, both regarding production, construction and structural performance, the most pronounced problem is the material deterioration due to aggressive environment and construction degradation due to fatigue. Despite the protective layer that steel is covered, the service life sometimes cannot by fully utilized, this entails expensive and frequent inspection and repair.

Additionally, due to loading-unloading cycles on the bridge, fatigue is one of the dominant factors that influence the performance of steel culverts. Therefore, in order to avoid these time- and money-consuming issues a new alternative of FRP culverts is further studied in this thesis.

2.2 Application of FRP materials in civil engineering

2.2.1 Historical perspective of FRP

Although the history of FRP composites can be observed back thousands of years ago to Mesopotamia (present – Iraq), bringing under the use of straw as a reinforcement in mud brick, it is referred to a more recent times, when the usage of short glass fibre reinforcement in cement in the United States in the early 1930's started and the development of FRP, the composition that we know today, were not developed until the early 1940's.

As the name of the material itself suggests, FRP is composed from at least two materials: high-strength fibres embedded in a polymer matrix, thus giving a great-performance composite material. After World War II, when the FRP was used mainly for defence industries, the polymer-based composites spread broadly when the fibre reinforcements and resins became commercially available and affordable. Primarily, FRP automotive industry introduced composites into vehicle frames in early 1950s. The greatest advantages of the material are high strength characteristics, corrosion resistance, easy-shaping and lightness, therefore research emphasized on developing new and improving manufacturing techniques, such as filament winding and pultrusion, which helped to introduce the usage of composites into new applications. Other industries such as aerospace started producing pressure vessels, containers and non-structural aircraft components, marine market applied the material in mine sweeping vessels, submarine parts and brew boats and recreation industry adopted composites very well for tennis, golf, fishing and skiing equipment.

The main growth in the application and development of the FRP composites in civil engineering started in the 1960's. Two major structures made of glass fibre-reinforced polymer were built: the dome structure in Benghazi in 1968 and the roof structure in Dubai in 1972, and the other structures followed deliberately. By late 1980's the military market begin to vanish and in the early 1990's the need for old infrastructure to be repaired or replaced

increased as FRP cost decreased simultaneously. Currently the interest in the appliance of the material is growing, including the research of full-scale experiments, because the long –term behaviour is still not explored conclusively, also focusing on the optimisation of structures using finite element analysis approaches.

2.2.2 Applications of FRP in structural engineering

Nowadays the interest of development and application of FRP structures in structural engineering is greatly increasing. Because of its' superb material characteristics, quick and easy erection, long service life, low maintenance and geometrical diversity (Figure 2.19) the materials is gaining recognition amongst structural engineers, architects, contractors and clients. The most obvious potential usage of FRP composites is to fabricate entire structure or installing particular structural element. The latter application as well as durability of the material is illustrated in Figure 2.20 the Mondial House on the River Thames banks in London. It was entirely cladded with FRP panels more than 30 years ago remaining the same surface colour and exterior.

When it comes to hybrid bridge structures, conventional materials are usually used for girders or pylons and decks, cables/tendons are usually made of composites. In Figure 2.21 the first composite bridge in Scandinavia is presented – the Fiberline Bridge in Kolding, Denmark which was officially opened in 1997. Fiberline Bridge is a pedestrian bridge, with a span of 40 meters, representing the material as a future perspective for lightweight, maintenance-free and rapid erection (the bridge was installed in 18 hours during 3 nights). The 38 m span and 3 meter width Lleida Footbridge in Spain (2004) is the longest arch bridge made of standard GFRP pultruded profiles (Figure 2.22).

Figure 2.19 Fibreglass reinforced plastic composite digester dome [12]

Figure 2.20 Mondial House in London [13]

Figure 2.21 The Fiberline bridge at Kolding, Denmark [14]

Figure 2.22 Lleida Footbridge in Spain [14]

Figure 2.23 illustrates steel pedestrian bridge replacement with FRP composite bridge in Devon railway station in United Kingdom. The original bridge was reconstructed in 1930's and in 2012 was replaced because of deterioration due to proximity to aggressive environment, i.e. seafront. An existing steel bridge suffered from severe corrosion damage, the timber decking was all rotted and protective coatings were all worn out and damaged. The new FRP composite bridge is 18 meters span, weighs only 5 tonnes and an expected service life is 120 years [15].

Figure 2.23 Dawlish railway station steel bridge replacement [15] with FRP composites [16]

2.2.3 Applications of FRP in drainage and sewage systems

The durability and long-term behaviour of FRP culverts might be referred to the serviceability to sewage, drainage, etc. piping (as an example see Figure 2.24), since both structural systems are buried underground and exhibit same environmental impacts.

FRP pipes are designed for a variety of applications such as carrying water under roads, railways or other obstacles as well as for waste/potable/fire water piping (

Figure 2.25, Figure 2.26), drainage and sewage systems, geothermal piping, food industry piping and bridge drainage. The systems from FRP material are very applicable for chemical and sea water piping, abrasion piping, industrial waste and when a high quality and purity of water is a prerequisite [17]. Depending on the required application pipes can be either smooth or perforated [18]. Such systems are also buried under specific required depth of the soil, therefore the pipes must provide structural resistance to withstand acting loads and evinces the durability because of the capacity to withstand aggressive environment [17].

Figure 2.24 FRP underground pipe installation [17]

Figure 2.25 FRP pipe versus steel pipe for water applications [17]

Figure 2.26 FRP water piping system at an Oregon cogenerating power facility [19]

There are considerable number of advantages for usage FRP pipes [20]:

- Fatigue endurance
- Corrosion resistant in comparison with ordinary steel
- High mechanical and impact strength
- Temperature resistant
- Smooth internal pipe surface (low friction coefficient)
- Abrasion resistant
- Lightweight, therefore easy handling, lower transportation costs and fast installation
- Low service life cost, due to reduced installation and maintenance investments
- Increased serviceability
- Shape complexity

The general inspection of FRP pipes are similar to steel piping when checking positional deviation, mechanical damage (mainly in the area of invert, resulting in reduced wall thickness), erosion wear, deformation, flow obstacles, connections. However the maintenance of FRP piping includes specific controls (containing particular tools and methods) [21]:

- Flange and bottom flatness
- Laminate and ply thickness
- Aging damage: delamination, cracking, etc.
- Heat-related damage

The durability of FRP piping are already well known and proven [17], therefore with the reference to advantages stated above, a stable foundation can be placed for further research in application of FRP material, which in this thesis study-case is the culvert structure.

2.3 Introduction of FRP materials

Fibre Reinforced Polymer (FRP) composites can be defined as combination of at least two individual materials (Figure 2.27): a matrix, either thermoset or thermoplastic, and a fibrous or other reinforcing material with a certain aspect ratio (length to thickness) to provide a considerable reinforcement in one or more directions. Each of these different agents has its own function to perform, i.e. the fibres provide strength and stiffness and matrix contributes in a rigidity and environmental protection, hence the composite system performs sufficiently as one unit (Figure 2.28). FRP may also contain fillers which reduce cost and shrinkage as well additives that improve mechanical and physical properties and workability of the final composite [22].

Moreover, FRP composites are anisotropic, meaning that the best mechanical properties are in the direction of the fibre arrangement, whilst other construction materials, e.g. steel is isotropic.
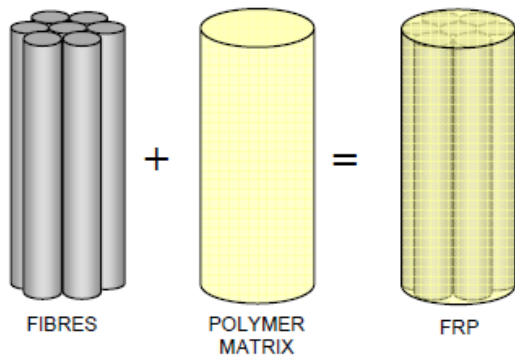
Figure 2.27 Basic components to create FRP composite [23]
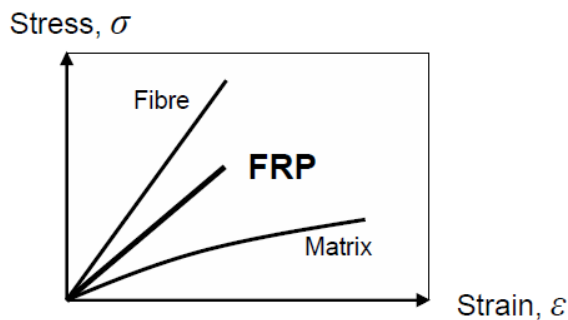
Figure 2.28 The combination of matrix and fibres gives a composite material with superior properties [23]

Advantages

The selection and usage of FRP composites includes such advantages [24], [25]:

- High strength
- Lightweight (75% less than steel)
- Electromagnetically neutral
- UV resistant
- Withstands freeze-thaw cycles
- Anisotropic; the ability to obtain required mechanical properties
- Low maintenance
- Durable: high corrosion and fatigue resistance
- Geometrical diversity
- Dimensional stability
- Simple and rapid installation, therefore cost effective
- Compatible with conventional construction materials

2.3.1 Manufacturing processes

The manufacturing process, as well as the composites constituents, plays a very important part in assessing the characteristics of the final product. In addition, such manufacturing process should be chosen so that optimal properties of the composite and economical alternative are attained. Purchaser demands, structural and architectural requirements, production rate and assembly/erection possibilities should be considered as well. According to "The International Handbook of FRP Composites in Civil Engineering" by Zoghi [22], manufacturing processes can be classified into three categories:

- Manual processes, i.e. wet lay-up and contact moulding

- Semi- automated processes, i.e. compression moulding and resin infusion.
- Automated processes, i.e. pultrusion, filament winding, injection moulding

2.3.2 **Matrix constituents**

As a matrix for the composites, resins are used and functions as a binder for the reinforcement, transfers stresses between the reinforcing fibres and protects the fibres from mechanical or environmental damage. Resins are classified into thermoplastics and thermosets [22]. Thermoplastic resins remain solid at room temperature, become fluid when temperature increase and solidifies when cooled. There is no chemical reaction; the material change is totally physical. Thermoset resins undergo an irreversible chemical reaction; after curing they cannot be converted back to the original liquid form, therefore being a desirable agent for structural applications. Resins should be chosen taking into account the application field, the extent that structure is exposed to environment and temperature, manufacturing method, curing conditions and required properties. The most common thermosetting resins used in the composite market [25]:

- Unsaturated polyester
- Epoxy
- Vinyl ester
- Phenolic
- Polyurethane

Unsaturated polyester

The vast majority of composites applied in industry are unsaturated polyesters which is approximately 75 % of the total resins used. During the building of the polymer chains, polyesters can be formulated and chemically tailored to provide desired properties and process compatibility, hereby making the material greatly versatile. The advantages of the unsaturated polyester are its affordable price, dimensional stability, easy to handle during manufacturing process, corrosion resistant and can serve as a fire retardant.

Epoxy

Epoxy resins are well-known for their extensive application of composite parts, structures and concrete repair. The utmost merit of the resins over unsaturated polyesters are their workability, low-shrinkage, environmental durability and have a higher shear strength than polyesters. Binding the agent with different materials or incorporating with other epoxy resins specific performance characteristics can be achieved. Epoxies are used in the production of high performance composites with improved mechanical, electrical and thermal properties, better environment and corrosion resistance. Nevertheless, epoxies have poor UV resistance and due to higher viscosity post-curing (elevated heat) is required to attain the ultimate mechanical properties. Epoxies are operated along with fibrous reinforcing materials, e. g. glass and carbon.

Vinyl ester

Vinyl esters were developed taking the advantages of workability of the epoxies and fast curing of the polyesters. An outcome of such material is that it is cheaper than epoxies but has a higher physical performance than polyesters. Moreover, this composite is mechanically stiff, very workable and offers superb corrosion, heat and moisture resistance and fast curing.

Phenolic

Phenolic resins performs well in elevated temperatures, low emission of toxic fumes, they are creep and corrosion resistant, excellent thermal and effective sound insulation. The resins have lower shrinkage in comparison with polyesters.

Polyurethane

Polyurethanes arise in an astonishing diversity of forms; they are used as adhesives, foams, coatings or elastomers. Advantages of polyurethane adhesives are impact and environmental resistant, rapid curing and well binding with various surfaces. Polyurethane foams optimize the density for insulation, architectural and structural components, such as sandwich panels. Polyurethanes used for coatings are stiff, but flexible, chemical-proof and fast curing. Elastomers can be characterized as especially tough and abrasive in wheels, bumper components or insulation.

2.3.3 Reinforcements

Fibres are used to convey structural strength and thickness to a composite material. The fibres commonly occupies 30 – 70 % of the matrix volume in the composite, thence a considerable amount of effort was put in the research and development of the performance in the types, orientation, volume fraction and composition. Obviously, the most desirable characteristics for the composites are strength, stiffness and toughness, which are highly dependent on the type and geometry of the reinforcement.

Reinforcements can be either type of natural and man-made, however most commercial are man-made; correlating to the price respectively, glass, carbon and aramid fibres are usually used for composites in the structural applications [25].

In order to improve the handling, the surface treatment of the fibres can be done with sizings such as gelatine, starch, oil or wax [26]. The arrangement of the fibres governs the directional and the level of strength of the composite. Three basic fibre distributions might be excluded: unidirectional, bidirectional and multidirectional, that are illustrated in Figure 2.29.

Figure 2.29 Basic orientation of the fibres [27]

Glass Fibres

Glass fibres are the lowest-cost and high strength reinforcement thus making them predominant and very applicable when there is a demand for large amounts of materials.

Along with these advantages glass fibres are also corrosion resistant, tough and chemical inert. However, the fibres possess some disadvantages:

- Low modulus of elasticity
- Poor abrasion resistance, therefore manufactured with various surface covers
- Poor adhesion to resins, requiring chemical coupling agents, e.g. silane

Even though the material creeps under sustained loading, the design can be made so that the composite performance would be satisfactory. In the application where stiffness is crucial, the design of the glass fibres must be specially treated.

There are various types of glass fibres for different kinds of application:
- "A" or "AR" stands for alkane resistance
- "C" may be selected when better chemical resistance is required, but they have a slightly lower strength compared to "E" type
- "E" used to improve electrical properties; most extensively used for its high tensile strength and durability
- "S" or "R" stands for higher strength, stiffness and elevated temperature resistant, but more expensive than "E" fibres

Glass fibres are regarded as an isotropic material, having equal or better characteristics than steel in particular forms. The material weights more than carbon or aramid, but generally has a fine impact resistance.

Carbon Fibre

Despite high specific strength and stiffness, the applications in construction of carbon fibres are quite limited because of their high cost. However, the first two properties makes it an ideal material where the lightweight is important, e.g. aircraft applications. Carbon fibres are also very convenient to use in a critical applications such as concrete beam/column or seismic rehabilitation and retrofitting. The fibres are assumed as anisotropic; stronger and stiffer in longitudinal direction than in transverse, in addition to high fatigue and creep resistance as well as favourable coefficient of thermal expansion.

Similarly to glass fibres, carbon fibres' surface is also chemically treated with coatings and chemical coupling agents before any further processing. Carbon composites shows higher performance when adhesively bonded rather than mechanically fastened, because of phenomenon when the composite exhibits stress concentrations that are caused by material brittleness due to higher modulus. Moreover, when used together with metals carbon fibres can cause corrosion, therefore a barrier materials such as glass or resin are used to overcome this.

Aramid Fibre

Aramid fibres are the best known organic fibres and are often used for ballistic and impact applications. Aramid characteristics:
- Good mechanical properties at low density
- Tough and damage resistant
- Quite high tensile strength
- Medium modulus of elasticity
- Very low density in comparison with glass and carbon
- Electrical and heat insulator
- Resistant to organic solvents, fuels, lubricants
- Ductile

- Good fatigue and creep resistance

In comparison with glass, aramids offers higher tensile strength and approximately 50% higher modulus, however has a low-performance regarding compressive strength in comparison with two latter fibres, it is also costly, susceptible to UV light and temperature changes.

2.3.4 **Fillers**

Fillers are used to fill up the voids in a matrix, because of the high price of resins, therefore enhancing mechanical, physical and chemical performance of the composite. The main types of fillers [26] used in the market:

- *Calcium carbonate* is a low-cost material available in a variety of particle size, therefore the most widely used inorganic filler.
- *Kaolin* can also be offered in a wide range of particle size, thus the second mostly used filler.
- *Alumina trihydrate* is commonly used to enhance the performance of the composite during fire and smoke. The principle is that that when this filler is exposed to high temperatures it gives off water (hydration), hereby reducing the spread of the flame and smoke.
- *Calcium sulphate* is the major flame/smoke decelerator, releasing water at lower temperatures.

If the fillers are used properly, improved characteristics may include:

- Better performance during fire or chemical action
- Higher mechanical strength
- Lower shrinkage
- Stiffness
- Fatigue and creep resistance
- Lower thermal expansion and exothermic coefficients
- Water, weather and temperature resistance
- Surface smoothness
- Dimensional stability

However, when the high strength composites are formulated, they should not contain fillers, because of the difficulty to fully wet out the heavy fibre reinforcement, due to increased viscosity of the resin paste.

2.3.5 **Additives and adhesives**

Additives modify material properties, improve the performance of composite and manufacturing process and are used in low quantities in comparison with other constituents. When put to the composites, additives usually increase the cost of the material system as well as the usefulness and durability of the product. The type of additives available:

- Catalysts, promoters, inhibitors – accelerated the speed of the curing
- Colorants – provide colour
- Release agents – facilitate the removal of the moulds
- Thixotropic agents – reduces the flow or drain of the resin from the surfaces

Adhesives are used to bind composites to themselves as well to the other surfaces. In order to get a proper connection, surface must be carefully treated to ensure the bond strength. The most common adhesives are epoxy, acryl and urethane [26].

2.3.6 Gel coats

Gel coats provide an environmental and impact resistant surface finishing [25]. The thickness is determined depending on the intended application of the composite product. Gel coats provide no additional structural capacity, therefore they should be resilient; sustain deformations from the structure and do not crack due to temperature changes, be impenetrable and UV light proof, provide a colour scheme. They should enhance chemical, abrasion, fire and moisture resistance.

2.4 FRP sandwich panels

2.4.1 Composition of FRP sandwich panels

The composition of FRP laminates and core materials is defined as a sandwich structure. FRP sandwich panels with requisite mechanical properties can be designed depending on the intended use. The manufacturing process, type, distribution/orientation, bonding, of the materials, geometry, quantity/volume, orientation of the reinforcement and cost of products will influence the mechanical properties, quality and structural performance [28]. Figure 2.30 represents a typical sandwich composite construction and its components.

Figure 2.30 Principal illustration of a sandwich element [29]

The structural performance of the sandwich is analogous to I-beam (Figure 2.31); two top skins act as flanges taking tensile and compressive stresses, whereas the core act as web, providing shear resistance. The interfaces are bonded with adhesives to achieve a composite action and transfer shear forces between the constituents.
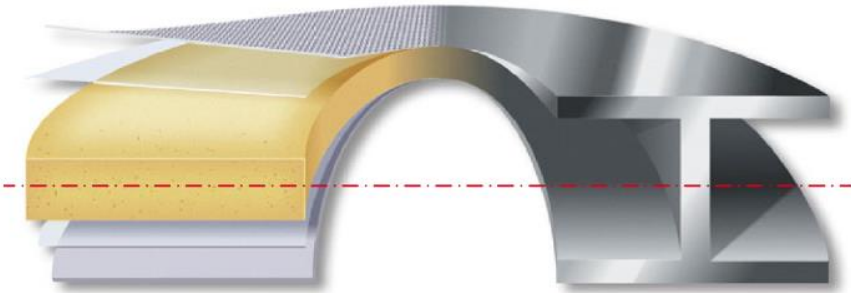

Figure 2.31 Analogy between FRP sandwich and steel I beam [30]

Core materials can be both load bearing or simply used for shaping the FRP sections. The baring cores should be designed for the efficient usage of sandwich construction. There are a variety of core materials currently in use, but the most common for structural applications are foam, balsa wood (Figure 2.32), honeycomb and corrugated cores (Figure 2.33).

Honeycomb as well as corrugated cores should be considered when the light-weight structure is substantial. The properties of these cores depend on the thickness of comb, cell geometry and size. The advantages of using polymer cores are an absence of internal corrosion and impact resilience. Moreover, the corrugation can be conformed to achieve required mechanical properties, making the structure more efficient. The problem of corrugated and honeycomb cores are that the area of surface for bonding is very limited, unlike foam cores. Foams are also light-weight, exhibit non-linear behaviour and can be reinforced with glass or other short fibres. Mechanical and physical properties depend on density, amount, type and distribution of fibres. Balsa wood is a light-weight, natural and renewable core material from balsa trees and is advantageous to foams in compression and shear loadings.

Figure 2.32 Foam and balsa wood cores [30]
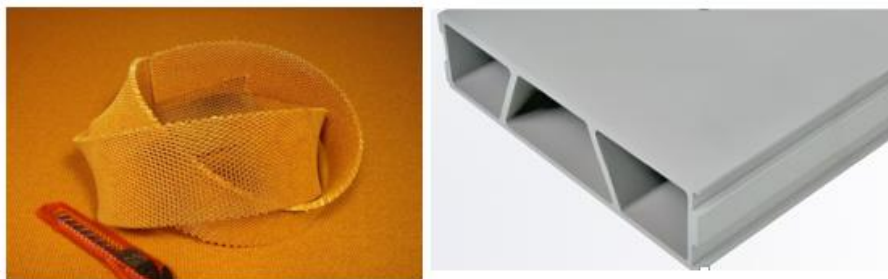
Figure 2.33 Honeycomb [31] and corrugated cores [14]

Typically, the core materials are not rigid, therefore shear deflection inwards the core is negligible in most cases, but if the core is weak, the efficiency of the whole sandwich structure is significantly decreased. Moreover, structural core are required to have high shear modulus and strength, satisfactory strength in the through-thickness direction, thermal and dimensional stability, fatigue, impact and moisture resistance, thermal and dimensional stability and geometrical diversity. In order to obtain a required utilization of the sandwich the core also should:

- Be stiff enough to maintain a constant distance between FRP laminates
- Be rigid enough to take shear stresses and the sliding of laminates should be prevented (Figure 2.34) in order to guarantee the interaction between layers, otherwise the sandwich action will be completely lost, having only separate structures
- Be rigid enough to prevent laminates for in-plane buckling under compressive stresses
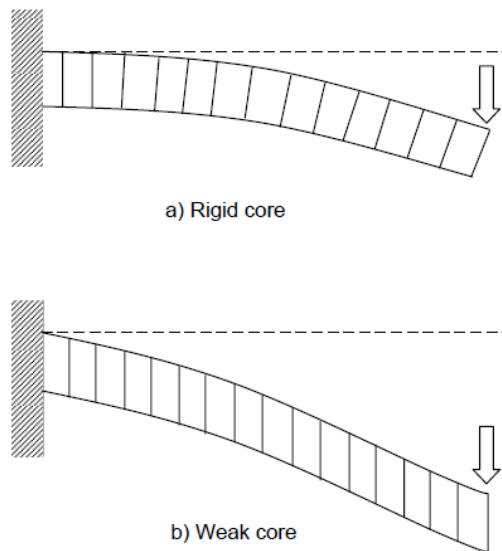
Figure 2.34 Effect of rigid and weak core [29]

The FRP laminates should be placed with a certain distance from the neutral axis of the structure, hereby increasing moment of inertia and flexural rigidity. Moreover, when it comes to design, the shear deflection in the laminates can be neglected and local flexural rigidity of each laminate is inconsiderable therefore disregarded. The through-thickness fibres increase the shear stiffness and retards delamination between layers of the laminate. The greatest stiffness is in the direction of the fibres in tension. The properties influencing an elastic modulus of the FRP are fibre modulus, matrix modulus and fibre volume ratio. The ultimate stress of a laminate is a function of ultimate fibre strength, ultimate matrix strength fibre volume ratio and relative failure strains [23].

2.4.2 Composition of the study-case FRP sandwich panel

The sandwich structure analysed in this thesis consists of glass fibre, epoxy resin, and foam core, bonded with epoxy adhesives. The promotion for choosing glass fibre from the variety of fibres is that they are cheap and provide high strength. Moreover, structures containing glass fibres are stiff, corrosion and impact resistant which is greatly important in the application for culverts, due to constant exposition to severe environment and abrasion sensibility. For the examined sandwich "E" type glass fibres were tailored, because of their high tensile strength and durability.

The epoxy resins suggest high workability and durability (Section Matrix constituents). Foam core provides a well-performing structure due to greater interface between laminas and core (Figure 2.35). In order to obtain a high-strength bond, sandwich is compounded with epoxy adhesives.
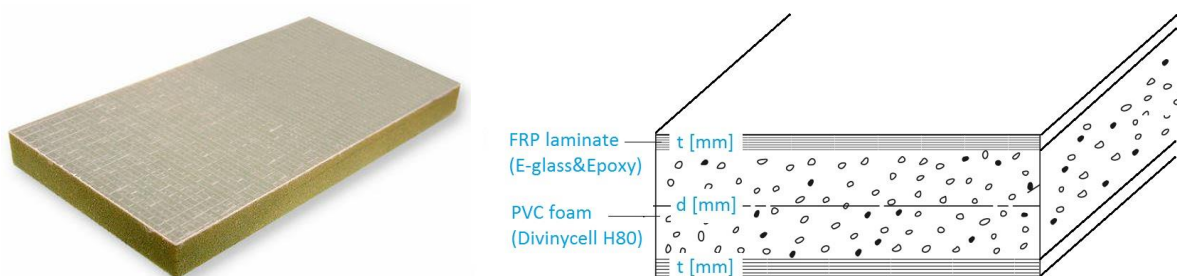
Figure 2.35 Example of FRP sandwich with foam core [32]

2.4.3 Advantages of FRP sandwiches

FRP sandwiches have a superior performance and serviceability when comparing with steel. In Figure 2.36 the general comparison of CFRP, GFRP and steel is introduced; showing linear elastic behaviour to failure, exhibiting no yielding, higher ultimate strength, lower strain at failure. The quantitative comparison [23] is illustrated in Figure 2.37 shows that FRP has higher ultimate strength, lower failure strain, however lower elastic modulus. The deflection criteria comparison between steel panel and FRP sandwich is presented in Figure 2.38Figure 2.38. The results show that for the same loading, geometrical and stiffness conditions, the weight of composite sandwich can be approximately 90% less.
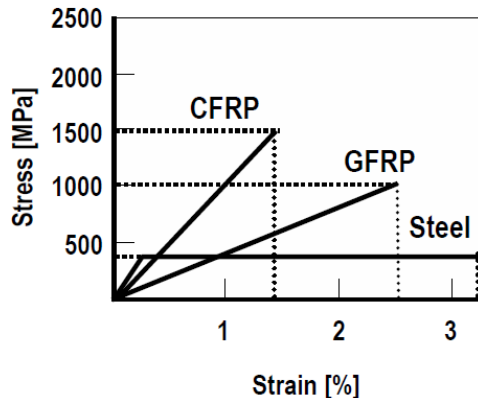
*Figure 2.36 The comparison of carbon/glass FRP and steel **[23]***

Material	Ultimate Strength	Elastic Modulus	Failure Strain
Glass FRP	517-1207 MPa	30-55 GPa	2-4.5 %
Carbon FRP	1200-2410 MPa	147-165 GPa	1-1.5 %
Aramid FRP	1200-2068 MPa	50-74 GPa	2-2.6 %
Steel	483-690 MPa	200 GPa	>10 %

*Figure 2.37 Quantitative comparison of GFRP and steel **[23]***
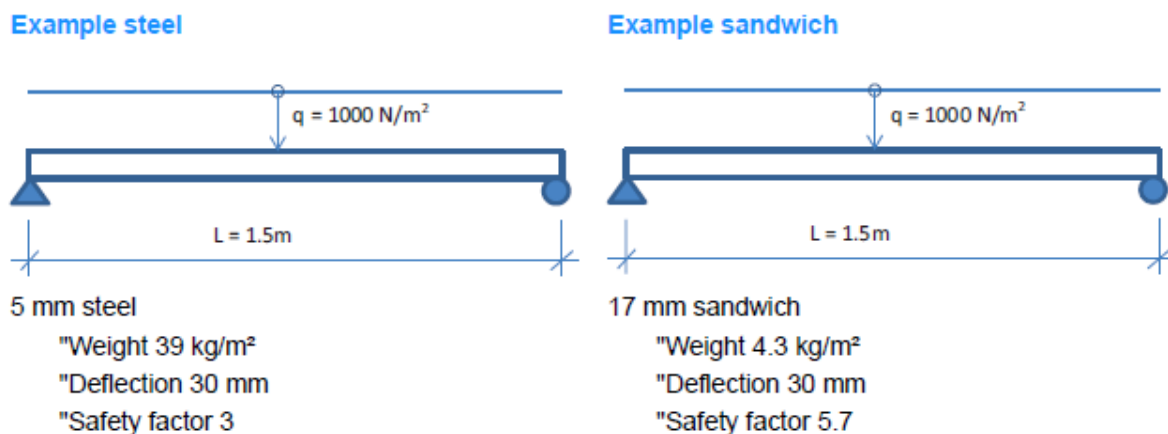
*Figure 2.38 Comparison between steel panel and composite sandwich **[30]***

The considerable benefits of composite sandwiches are [33], [34]:

- **High stiffness/strength-to-weight ratio.** These material characteristics enhances the flexural rigidity of a structure, facilitates transportation and installation, decreased the need for foundations, resulting in material and cost saving.
- **Corrosion resistance.** One of the most prevailing steel problem is corrosion, thus FRP composites exhibits very high resistance against this material deterioration as well as to chemical agents. Since culverts are constantly exposed to poor environment, the application of FRP would provide longer service life and lower maintenance, therefore having a lower life-cycle cost and durable construction.
- **Fatigue resistance.** Most of the composites are considered to possess higher fatigue resistance than traditional materials, which might be neglected in a certain structures, increasing design versatility. Due to varying moment, this parameter sometimes can be dominant when considering the design of the culvert and its cover height. As distinct from metals, FRP composites subjected to cyclic loading softens gradually or loses stiffness in a microscopic level before any visible cracks appear [35]
- **Rapid and easy installation.** This property makes the material very applicable for constructions where short installation time is prerequisite, e.g. bridges, allowing mounting the structures without users inconvenience and traffic interruption.
- **Geometrical possibilities and tailored properties.** The diversity of geometrical shapes can be offered because of the way FRP composites are manufactured. Using relevant cross-sections in the most exposed regions makes the structure cost and material effective. In addition to this, properties can be tailored due to material anisotropy where is a need for additional strength in any direction desired, hereby utilizing the material optimally and improving economy.

2.5 Future outlook of the application of FRP materials

There has been a great deal of development of FRP composite technology in tremendous amount of applications. However, to utilise the full advantages of the FRP composites further research is required in several fields [36], [33], [34]. Potential areas of investigation include:

- Design code specification, standardization of test methods, design practices and acceptance criteria
- Durability, including the performance of FRP under elevated temperatures, behaviour under realistic fatigue loadings, actual environmental consequences on the material and the combination of fatigue and degradation effects on the material in practical applications. More effort should be put into long-time performance investigation of the rates of the material degradation over time
- Development of both mechanical and adhesive connections; designs are adopted from metallic analogues rather than developed from a real-case studies and performance of FRP structures due to failure. This lead to overestimation of safety margins resulting in inefficient design or premature failure. Moreover, joints should be structurally efficient, durable and ensure rapid installation. Adhesive connection should provide stability when exposed to fire, chemicals and aggressive environment.
- Wearing surfaces; some bridges exhibit cracking or de-bonding of the wearing surfaces, therefore a research of the efficient re-surfacing of worn coatings and the feasibility of wearing surfaces in specific applications is required
- Due to relatively low elastic modulus and elastic-brittle behaviour, deflection control is a critical part of the design of the FRP. Low stiffness lead to deflection driven

design that inhibits to fully utilize the strength of FRP, resulting in inadequate safety factor application for strength.

- The high initial cost and uncertain long-term cost of FRP is intimidating in comparison with conventional materials, therefore a precise life-cycle cost and life-cycle assessment should be obtained

- Some manufacturing methods might be not economically suitable for structural applications of FRP, so a relevant technique should be applied in order to minimise labour and construction cost

- Fire resistance. In general FRP materials are susceptible to fire, sometimes producing toxic gases. Deeper studies are required to get a knowledge about the loss of strength during fire. There is a need to utilize constructional (fire protection) or structural (redundant systems) measures.

3 Design of Steel Culverts

3.1 Introduction

In this section culverts using corrugated steel plates are design for a collection of representative cases. An analysis of the design results is performed to investigate the governing issue that involved in the design of steel culverts, which helps to obtain a clear picture about the primary problems that limit the application of steel culverts in practice.

The design reports of steel culverts can be found in the Appendix A.2. The Swedish Design Method (SDM) [37]developed by Lars Pettersson and Håkan Sundquist is applied in the design reports. Since it's a design method that independent of codes [38], both Swedish standards and European codes can be used in the verification. In this thesis relevant Eurocodes are applied to the design process (see Table 3.1).

Table 3.1 Eurocodes used for the design of steel culverts

Issues	Eurocodes
Loads and Materials	EN 1990, EN 1991-2, EN 1993-1-1, EN 1993-2
Fatigue	EN 1993-1-8, EN 1993-1-9

3.2 Design cases
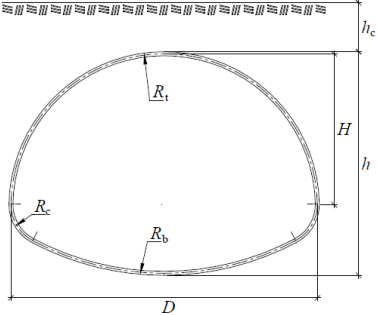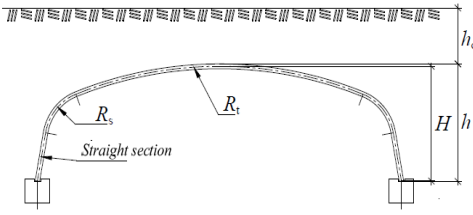
In order to have a comprehensive understanding of steel culverts regarding mechanical performance the primary task is to determine a reasonable and representative collection of the design cases that culvert structures can be designed for. The conditions that control the choice of design models includes: 1) culvert profile, 2) dimension of span and 3) height of the soil cover.

In the SDM manual seven types of culverts are introduced. The Profile E (Pipe-arch culvert) and Profile G (Box culvert) are chosen for study. The Pipe-arch profile, also known as low-rise profile, is one of the most commonly used types for the culvert bridges, while the box culverts are preferred in long-span cases. The proper dimensions of span corresponding to these two culvert profiles are determined (see Table 3.2).

The height of soil cover has substantial influence on the culvert structure. Four values—0.5 meter, 0.75 meter, 1.0 meter and 3.0 meter—are selected for the design cases. As introduced in the SDM manual the minimum height of soil cover is 0.5 meter. A soil cover of 0.75-meter- or 1.0-meter-height is commonly applied in the bridge culvert projects, and the 3-meter soil represents the upper limit condition.

Based on the variables discussed 16 design cases in total are determined to carry on the design of steel culverts (see Table 3.2).

Table 3.2 A collection of representative 16 cases for steel culvert design

Culvert Profile	Span [meter]	Height of Soil Cover [meter]	Case No.
Pipe-arch 	3	0,50	01
		0,75	02
		1,00	03
		3,00	04
	6	0,50	05
		0,75	06
		1,00	07
		3,00	08
Box 	6	0,50	09
		0,75	10
		1,00	11
		3,00	12
	12	0,50	13
		0,75	14
		1,00	15
		3,00	16

3.3 Materials

The steel culvert bridges is also called as soil steel composite bridges, which shows that the design includes both soil and steel culvert structure. The design of backfilling soil and steel plates for culverts are introduced individually.

3.3.1 Backfilling soil material

In Sweden two types of soil are commonly used for backfilling in the bridge projects—crushed rock and base course material [4]. Soil parameters are provided in SDM manual. In this thesis the base course material is chosen as the backfilling soil surrounding the culvert structure (see Table 3.3).
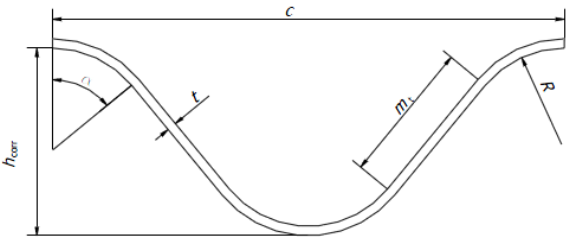
Table 3.3 Soil parameters for base course backfilling material (Reference [37], Table B.2.1)

Fill material	Optimum density	Density	Angel of friction	Static soil pressure	C_u	d_{50}
	kN/m^3	kN/m^3	^{o}	K_0	d_{60}/d_{10}	mm
Base course material	20.6	20	40	0.36	10	20

3.3.2 **Corrugated steel plates**

Corrugations available on the market are normally given in such dimensions as shown in the Table 3.4 below[37]. Steel plates of type 200*55 and type 380*140 are used for Pipe-arch culverts and Box culvert respectively. In the design of box culverts, the crown and corner sections usually become the most exposed regions. It is an economical way to apply the reinforcing plate to increase the load-bearing capacity in certain sections (see Figure 3.1).

Table 3.4 Dimension of corrugated steel plates

Profile	Type [mm*mm]	c [mm]	h.corr [mm]	t [mm]
	125*26	125	26	1.5 – 4
	150*50	150	50	2 – 7
	200*55	200	55	2 – 7
	380*140	380	140	4 – 7
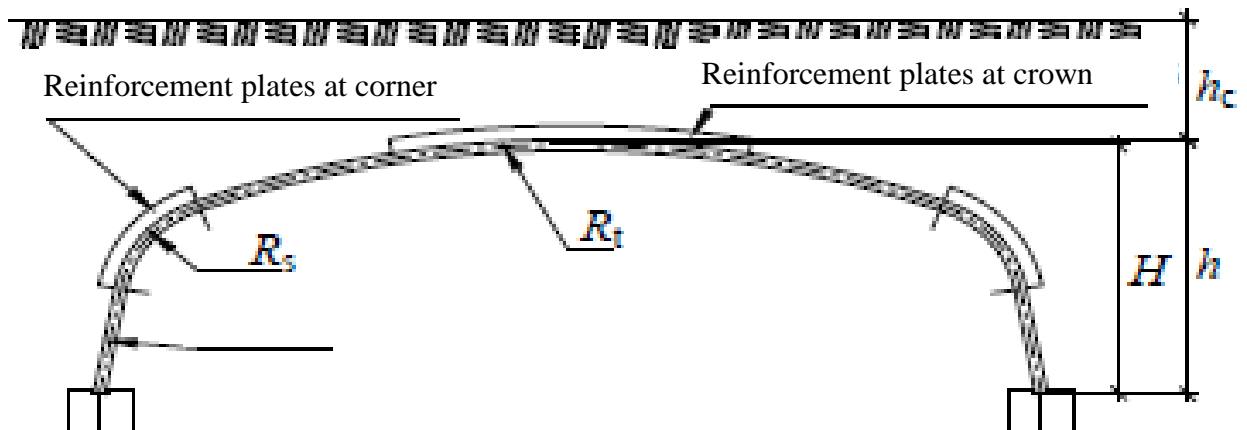
Figure 3.1 Box culverts with reinforcement plates in crown and corner region

3.4 Loads

3.4.1 Load effects from the surrounding soil
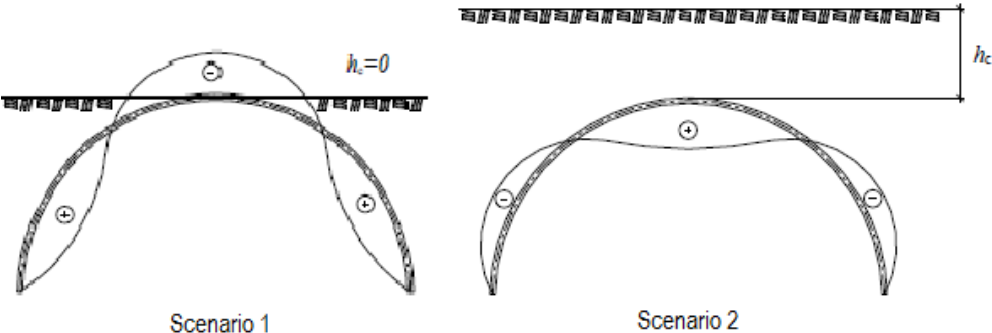
Figure 3.2 Moment distribution in a culvert during backfilling. Scenario 1: Backfilling till the crown level. Scenario 2: Backfilling till the soil cover height

In terms of different load effect, the soil body is treated separately as two parts. The first part is the surrounding soil, which refers to the backfilling material till the crown level of the culvert. The second part is the soil cover with varying design heights. See Figure 3.2.

3.4.2 Load effects from live traffic

Four types of load group are considered in the design, including LM1, LM2, LM3 from European codes EN 1991-2 and Typfordon from Swedish standard TRVK Bro 11 (2011:085).

According to the SDM, the traffic load is converted into an equivalent line load based on the Boussinesq's semi-infinite body method. In order to obtain the value of equivalent line loads corresponding to different load groups, a numerical method is used to find the most unfavorable load position where the live traffic load gives the highest vertical pressure on the culvert's crown region. This maximum vertical pressure will be used to calculate the corresponding equivalent line load, which is conservatively assumed acting along the longitudinal direction.

The result of equivalent line loads corresponding to the four load groups is shown in the Figure 3.3. The traffic load due to LM2 is used when the soil cover height is no more than 1 meter, while LM1 is applied for cases with 3-meter-height soil cover.
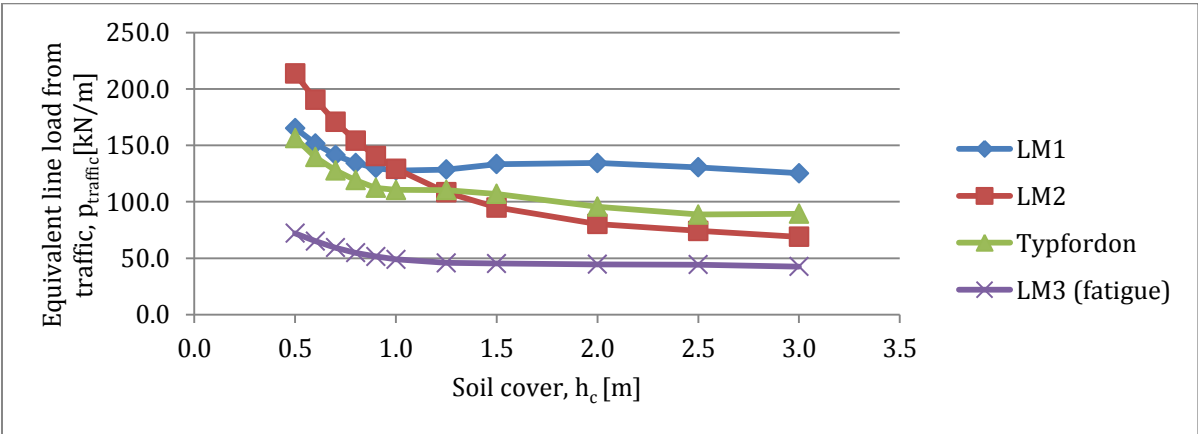
Figure 3.3 Four types of load group are converted into equivalent line load regarding different soil cover height (The data is provided by the consultant company WSP, office in Gothenburg)

3.5 Verification and results

The capacity checks of the pipe-arch culvert have some minor difference with those of box culverts. So, the verification list and final design results will be described separately. The capacity of steel culverts are checked in the ultimate limit state (ULS) and the serviceability state (SLS). Checks concerning fatigue are also performed, which can be regarded as a part of the ultimate limit state checks. It is worthy to mention that the design cases with numbers in red mean that the designed culvert structures cannot satisfy the requirements even though the design parameters reach maximum values.

3.5.1 Case 01-08: Pipe-arch culvert

Verification

Table 3.5 Checks included in the verification of pipe-arch culverts

Culvert Profile	Verification	
Pipe-arch Culvert	SLS	Check 1: yielding in the upper section when backfilling till crown
		Check 2: yielding in the upper section when soil cover completed
		Check 3: Local buckling
	ULS	Check 4: Plastic hinge in the crown, N & M
		Check 5: Plastic hinge in the crown, N (M=0)
		Check 6: Capacity in the bottom section
		Check 7: Capacity of Bolts, shear stress
		Check 8: Capacity of bolts, tensile stress
		Check 9: Capacity of bolts, interaction
	Fatigue	Check 10: Fatigue of the plate
		Check 11: fatigue of Bolts, shear stress
		Check 12: fatigue of Bolts, tensile stress
		Check 13: fatigue of Bolts, interaction

Results

Table 3.6 Verification results of pipe-arch culverts

	No	Span	[1]h_c	Corrugated Plates	Bolts	Verification												
				Thickness	[2]Number of Bolts	SLS		ULS						Fatigue			
						Check 1	Check 2	Check 4	Check 5	Check 6	Check 7	Check 8	Check 9	Check 10	Check 11	Check 12	Check 13
		[m]	[m]	2-7mm	[1/m]												
Pipe-arch	1	3	0,5	200*55	7	20	0,04	1,07	1,01	0,36	0,17	0,13	0,17	0,25	2,39	0,21	1,27	2,07
	2		0,75		7	15	0,04	0,63	0,67	0,12	0,14	0,14	0,13	0,23	1,37	0,22	0,98	0,95
	3		1		6	9	0,05	0,44	0,52	0,07	0,14	0,21	0,12	0,29	0,95	0,29	1	0,99
	4		3		3	6	0,08	0,42	0,67	0,12	0,27	0,65	0,07	0,35	0,38	0,21	0,34	0,03
	5	6	0,5		7	20	0,2	1,08	1,2	0,85	0,22	0,16	0,18	0,28	2,63	0,21	1,4	2,75
	6		0,75		7	19	0,2	0,7	0,93	0,56	0,2	0,15	0,12	0,23	1,75	0,17	0,98	0,94
	7		1		7	14	0,2	0,48	0,73	0,35	0,19	0,19	0,1	0,27	1,26	0,2	0,96	0,9
	8		3		4	7	0,33	0,52	1	0,3	0,46	0,88	0,09	0,61	0,39	0,27	0,39	0,06

[1]h_c—Height of the soil cover
[2]The maximum number of bolts that can be used in the steel plates with corrugation 200*55 is 20 per meter.

3.5.2 **Case 09-16: Box culvert**

Verification

Table 3.7 Checks included in the verification of box culverts

Culvert Profile	Verification	
Box Culvert	SLS	Check 1: yielding in the upper section when backfilling till crown
		Check 2: yielding in the upper section when soil cover completed
		Check 3: Local buckling
	ULS	Check 4: Plastic hinge in the crown, N & M
		Check 5: Plastic hinge in the crown, N (M=0)
		Check 6: Plastic hinge in the corner, N & M
		Check 7: Plastic hinge in the corner, N (M=0)
		Check 8: Capacity of Bolts, shear stress
		Check 9: Capacity of bolts, tensile stress
		Check 10: Capacity of bolts, interaction
	Fatigue	Check 11: Fatigue of the plate
		Check 12: fatigue of Bolts, shear stress
		Check 13: fatigue of Bolts, tensile stress
		Check 14: fatigue of Bolts, interaction

Result

Table 3.8 Verification results of box culverts

	No Span	[1]h_c	Corrugated Plates			Bolts	Verification												
			Thickness	[2]Reinf. Top	Reinf. Corner	[3]Number of Bolts	SLS		ULS							Fatigue			
	[m]	[m]	4-7mm			[1/m]	Check 1	Check 2	Check 4	Check 5	Check 6	Check 7	Check 8	Check 9	Check 10	Check 11	Check 12	Check 13	Check 14
Box	9	0,50	380* 140	7	Yes	No	15	0,05	0,51	0,99	0,74	0,73	0,13	0,21	0,55	0,61	1,11	0,28	3,95	61,47
	10 6	0,75		5	Yes	No	15	0,07	0,46	0,83	0,52	0,79	0,12	0,25	0,33	0,43	0,92	0,22	2,32	12,54
	11	1,00		4	Yes	No	15	0,08	0,42	0,73	0,41	0,86	0,13	0,29	0,23	0,34	0,76	0,19	1,55	3,69
	12	3,00		7	No	No	10	0,15	0,87	0,99	0,21	0,74	0,09	0,38	0,40	0,67	0,52	0,19	0,85	0,61
	13	0,50		7	Yes	No	15	0,04	0,56	1,59	1,16	0,87	0,19	0,28	0,57	0,69	1,05	0,28	3,74	52,38
	14 12	0,75		7	Yes	No	15	0,04	0,47	1,22	0,80	0,83	0,14	0,28	0,46	0,61	0,76	0,22	2,70	19,73
	15	1,00		7	Yes	No	15	0,04	0,43	1,02	0,63	0,84	0,12	0,29	0,41	0,58	0,59	0,19	2,12	9,51
	16	3,00		7	Yes	Yes	15	0,04	0,70	0,95	0,28	0,68	0,10	0,53	0,64	0,99	0,26	0,16	0,95	0,85

[1]h_c—Height of the soil cover
[2]Reinf.—Reinforcement plates in the top region or corner region
[3]The maximum number of bolts that can be used in the steel plates with corrugation 380*140 is 15 per meter.

3.6 Summary and conclusions

The verification checks highlight the governing issue and limitations that involved with steel culverts. In terms of the mechanical performance two major conclusions are worthy to be mentioned:

1) Fatigue is the governing issue of steel culvert design. When the soil cover is no more than one meter, the fatigue checks are dominant. In order to satisfy the fatigue requirements the material utilization ratio is quite low.

2) Steel culverts are facing more challenges in the condition with large span. As shown in the Box culvert design (Case 13-Case 15) not only fatigue but also capacity of steel plates in ULS cannot be satisfied when the span increases to 12 meters.

The performance of steel culverts in terms of fatigue and strength gives high interest to study the alternative using FRP materials, since the high fatigue-resistance and strength are features of the FRP material.

3.7 Limitations and assumptions

As defined in the SDM manual in the section 3.3[37], the analysis of culvert is based on the assumption that no special measures are applied during backfilling process. For instance, adding soil on the pipe's crown region during backfill is one method used to reduce the crown rise. If this measure is applied, the calculation for forces and moments need to be adapted.

4 Design of FRP Culverts

4.1 Introduction

According to the analysis of design results of steel culverts, it reveals that the most challenging cases for steel culverts feature a large span with a shallow soil cover, for instance the Case 13 with 12-meter-span and 0.5-meter-soil cover. Since the soil cover of 0.5-meter height is an extreme condition, a more representative and practical design model—Case 14 with 0.75-meter-soil cover—is chosen to be design with FRP sandwich panels instead of corrugated steel plates.

By the study of applying FRP sandwich panels to the box culvert structure instead of steel plates, this section aims to 1) investigate the feasibility of FRP culvert structure under the challenging conditions; 2) propose a practical approach to the design of FRP culverts. In the former design for Case 14 with steel plates, the load-bearing capacity in ULS and fatigue problems are the governing issues. Since the fatigue is no longer a problem for the FRP material, the design of FRP culverts focuses on the load-bearing capacity of FRP material in ULS and deflection in SLS.

4.2 Methodology

Since the design of FRP sandwich includes not only the geometry of face and core but also the construction of FRP laminate for the face section, it results in more design parameters than the steel plates. To carry out the design in an efficient way, the design is decided to be conducted in two phases (see Figure 4.1):

Preliminary design

The first phrase is the preliminary design, which aims to determine 1) FRP material for sandwich face, 2) core material and 3) the geometric parameters of FRP sandwich panel. A practical approach to the design calculation of FRP culverts is proposed. The calculation that programed in a Mathcad file can fast verify the design, in order to narrow the scope of feasible initial geometry.

Optimization design

The second phrase is the optimization design, which deals with the construction of a multidirectional FRP laminate—multiple FRP plies stack up in different fiber orientation angles.

In order to carry out this two-phase-design, the program—Mathcad is used to develop the tools for calculation. Three Mathcad files developed for the FRP culvert design are shown in the Table 4.1. Figure 4.2 shows how the Mathcad tools are applied to the design process. More details will be discussed in the following Section 4.4, Section 4.5 and Section 4.6.1. One Mathcad sample of design report is included in the Appendix B.2.
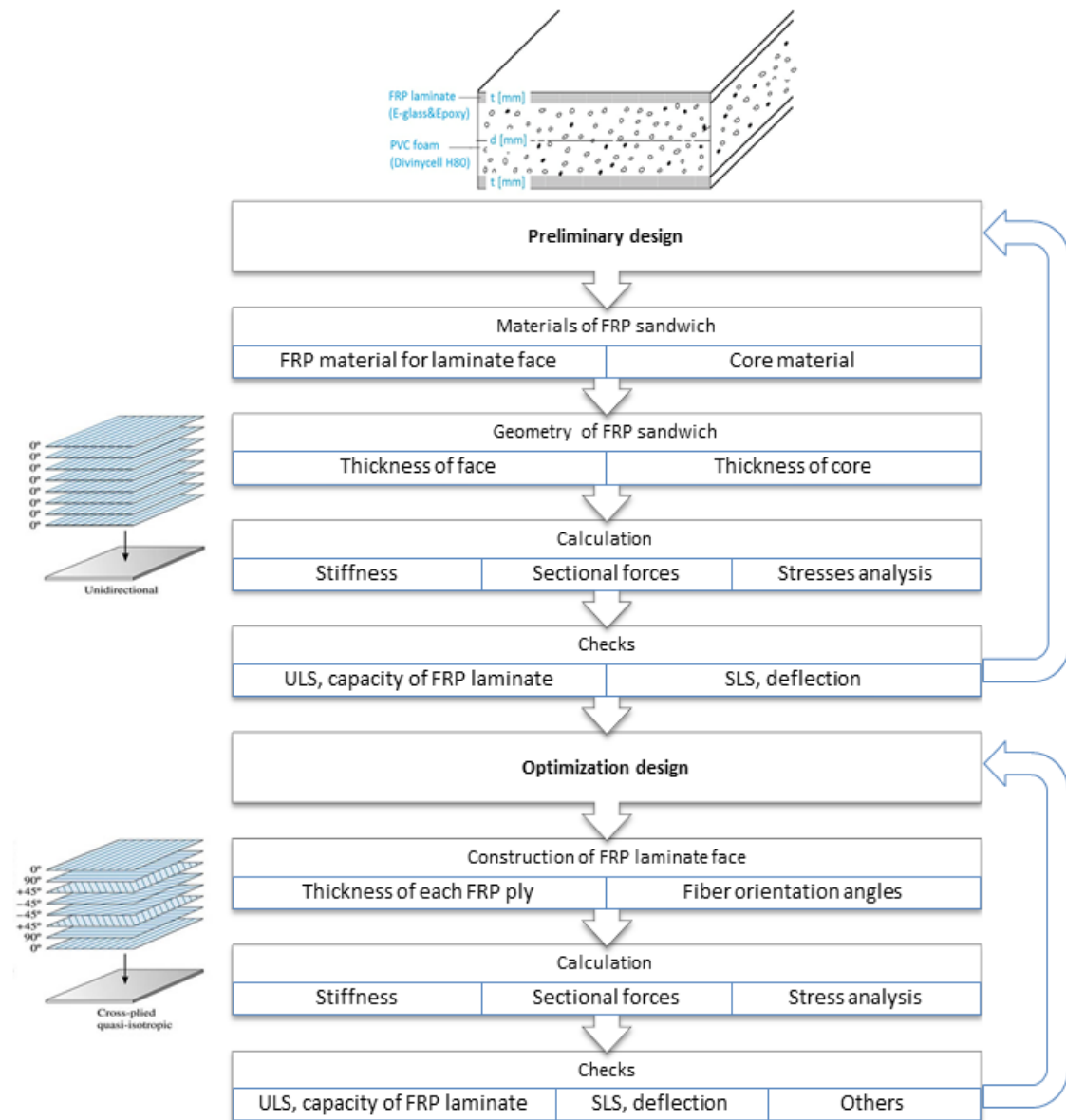
Figure 4.1 Proposed methodology for the design of FRP culvert structures

Table 4.1 Mathcad files developed for the FRP culvert design

Title	Function	More details
Mathcad No.1	Stiffness calculation and stresses analysis of the designed FRP sandwich	Section 4.4
Mathcad No.2	Sectional forces in the FRP culvert under design conditions	Section 4.6.1
Mathcad No.3	Failure prediction of FRP laminate	Section 4.5
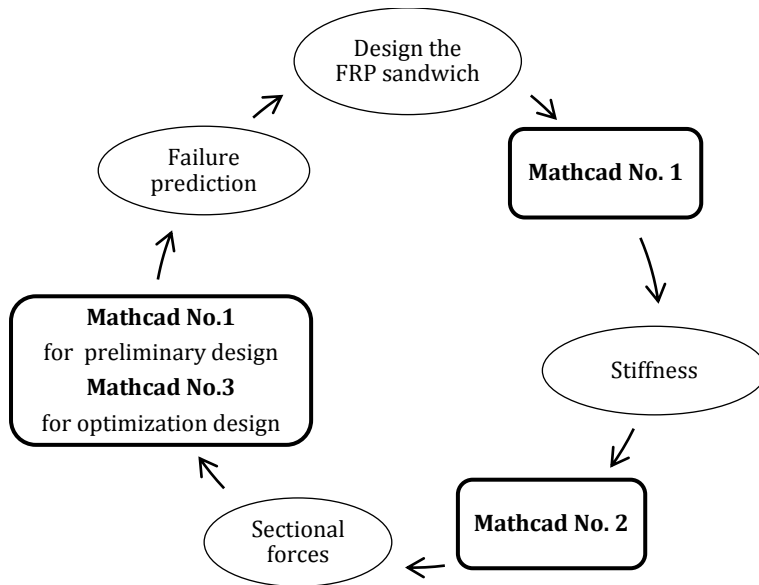
Figure 4.2 Mathcad tools applied in the design process

4.3 **Materials of the FRP sandwich panel**

4.3.1 **FRP laminate face**

Ten commercial composites are listed in Reference [39] (Table A4-1). The fiber reinforced composite E-glass—epoxy is chosen to construct the FRP laminate face of sandwich panel. The physical and mechanical properties are shown in the Table 4.2. Partial factors for FRP material are according to EUROCOMP Design Code [40] shown in Table 4.3. In the preliminary design, all the FRP plies are stacking in the same fiber orientation angle, which constructs a unidirectional FRP laminate with the longitudinal direction parallel to the loading direction. In the optimization design, the combinations of different fiber orientation angles are studied.

Table 4.2 Mechanical properties of chosen FRP material for initial design [39]

Material	Fiber Volume Fraction	Elastic Constants				Strengths				
		E_{11} GPa	E_{22} GPa	v_{12}	G_{12} GPa	σ_{11}^t MPa	σ_{11}^c MPa	σ_{22}^t MPa	σ_{22}^c MPa	τ_{12} MPa
E-glass & Epoxy	45%	38.6	8.27	0.26	4.41	1062	610	31	118	72

Table 4.3 Partial factors for FRP material according to EUROCOMP Design Code [40]

	Partial Factors for FRP material			
	γ_{M1}	γ_{M2}	γ_{M3}	$\gamma_M = \gamma_{M1} * \gamma_{M2} * \gamma_{M3}$
SLS	1,50	1,20	1,00	1,80
ULS	1,50	1,20	2,50	4,50

CHALMERS, *Civil and Environmental Engineering*, Master's Thesis 2014:123

4.3.2 Core material

Both foam and honeycomb are commonly used material for sandwich panels. In the FRP culvert design, PVC foam—Divinycell H80 from producer DIAB—is chosen as core material for the FRP sandwich panel. Since the elastic modulus ratio between foam and FRP material is about 0.2%, the mechanical contribution from foam material is neglected.

4.4 Stiffness and stress analysis of the FRP sandwich

After an initial geometry of the FRP sandwich is assumed, the cross-sectional stiffness becomes essential to continue the design calculation. Compared with isotropic steel material, the orthotropic FRP lamina has more independent elastic constants and the stress-strain characteristic. When the FRP laminas stack into a FRP laminate face of the sandwich, it takes more effort to obtain the stiffness properties of the designed sandwich cross-section. When a set of sectional forces are applied, the analysis of stresses in each FRP lamina needs to consider not only the position of the FRP lamina but also its fiber orientation angle.

A Mathcad file (Mathcad No.1) is developed to carry out the stiffness calculation and stresses analysis of the designed FRP sandwich. The program in Mathcad file is based on the methodology in Reference [41].The flow chart (Figure 4.3) shows how the Mathcad file works. This Mathcad file can be found in Appendix B.1.
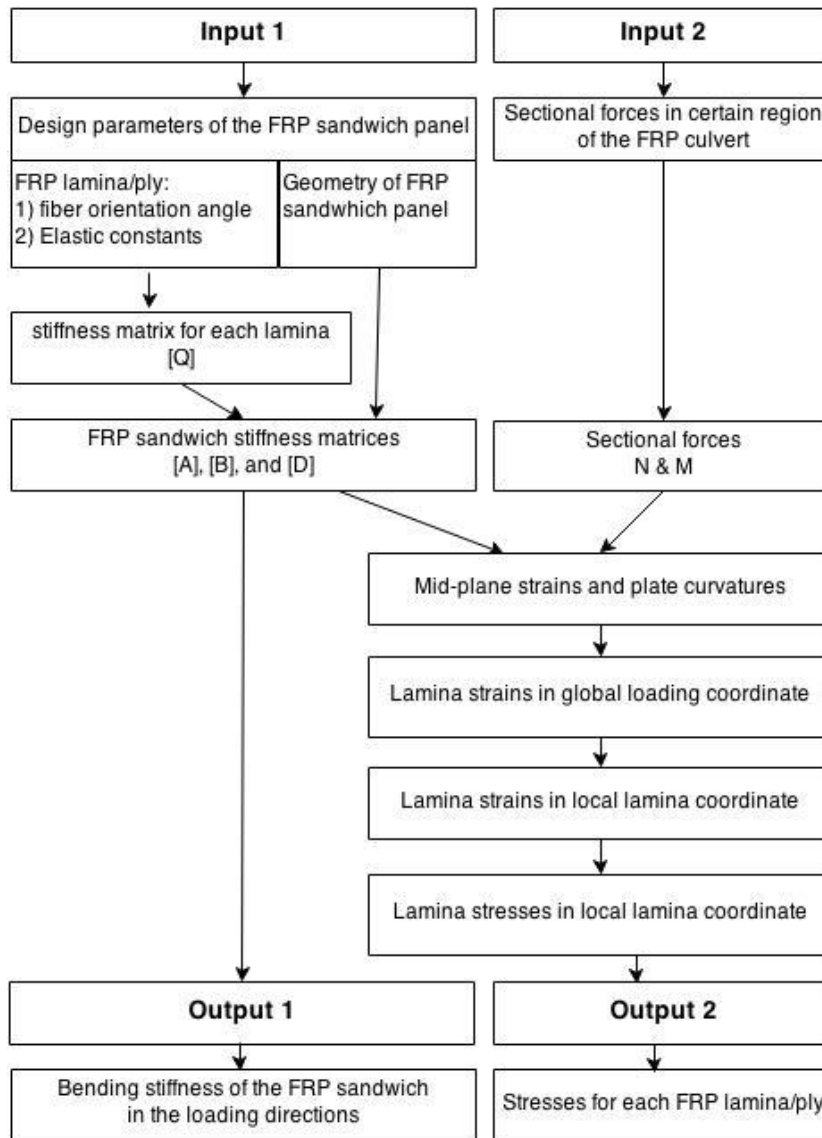
Figure 4.3 The flow chart shows how the Mathcad file functions to obtain the stiffness of designed FRP sandwich and stresses for each FRP lamina

4.5 Failure prediction of FRP laminates

In the preliminary design phrase, the FRP laminate is constructed in a unidirectional way. The stresses are linearly distributed according to the ply's position. In these cases, the first-ply-failure is applied, which means that the FRP laminate lose capacity when the ply with maximum stresses fails. It can be performed in the Mathcad No.1 as shown in the Figure 4.2.

However, the first-ply-failure is too conservative to be used when it comes to the optimization design with multi-directional FRP laminate. For a FRP laminate with a combination of different fiber orientation angles, one ply fails does not necessarily mean the laminate loses the load-bearing capacity. In order to predict the failure of a FRP laminate in general, a Mathcad file (Mathcad No.3) is developed to perform the prediction. The flow chart (Figure 4.4) below shows how the Mathcad program works. The Mathcad No.3 can be found in Appendix B.3.
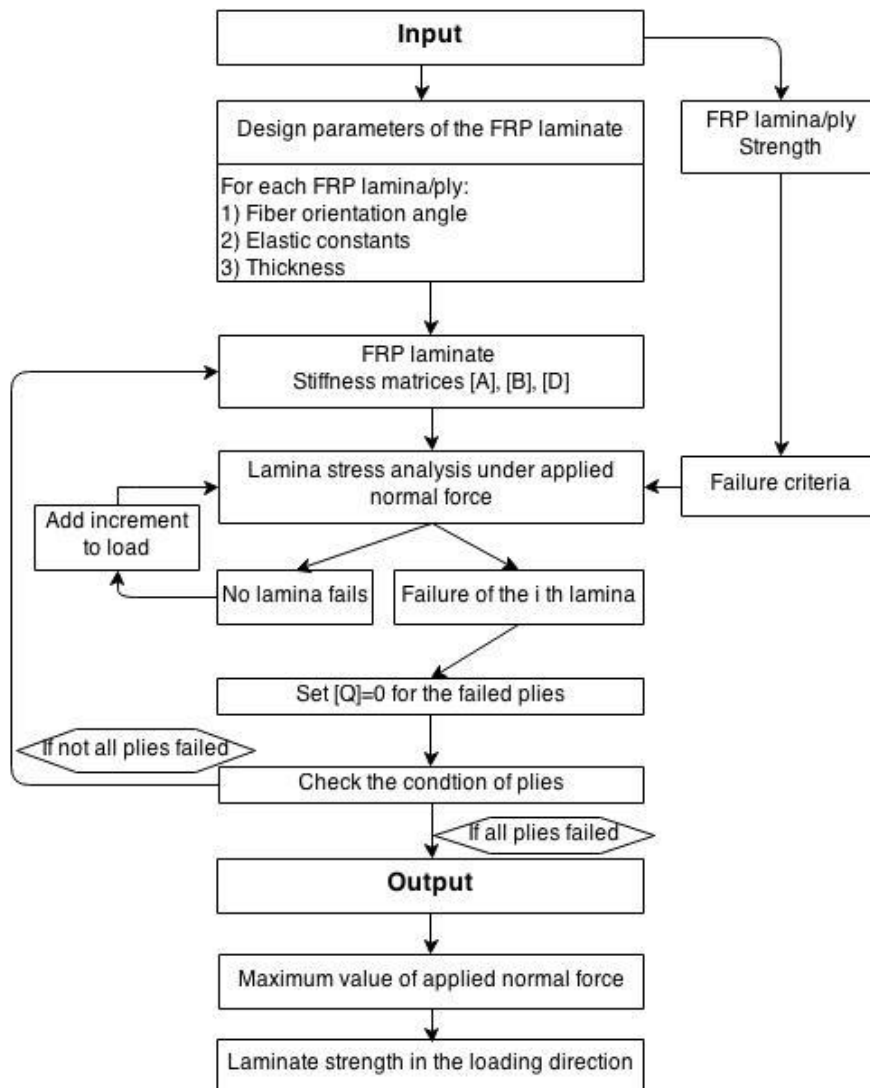
Figure 4.4 The flow chart shows how the Mathcad file functions to predict the failure of multi-directional FRP laminate and obtain the equivalent strength

4.6 Sectional forces in FRP culverts

Besides the challenges discussed due to the orthotropic FRP material, the main task of FRP culvert design is obtain the sectional forces in the FRP culvert structure. Since the application of FRP material to the culvert structure is a newly proposed study branch, no experience and design manual are available for guiding the FRP culvert design. It becomes critical to figure out a practical approach to obtain the sectional forces.

In the Swedish Design Method (SDM) for the steel culvert design, the original Soil Culvert Interaction (SCI) method developed by Duncan (1977) is amended for the calculation of sectional forces[4]. Inspired by the SDM, the calculation of FRP culvert is determined to follow the amended SCI method in the SDM. The reliability of hand-calculation results using SCI method will be discussed and then verified by FE-modeling with Abaqus. A comparison of hand-calculation and FE-modeling results is conducted to obtain the constructive suggestions for refining the hand-calculation process.

4.6.1 **Hand-calculation based on the SCI method**

The Figure 4.5 shows the parameters used to calculate sectional forces by the modified SCI method in the SDM manual. When FRP sandwich panels are used for the culvert structure instead of steel plates, only the factor that represents the stiffness of culvert wall needs to be modified to obtain normal forces and bending moments. A Mathcad file (Mathcad No.2) is developed. A sample will be included in the Appendix B.2.

Stiffness of soil: E_s	**Stiffness of culvert wall**: EI	Design span of culvert: D	Geometry of culvert structure	Geometry of surrounding soil

Flexibility number	Geometry parameters

Sectional forces: N & M
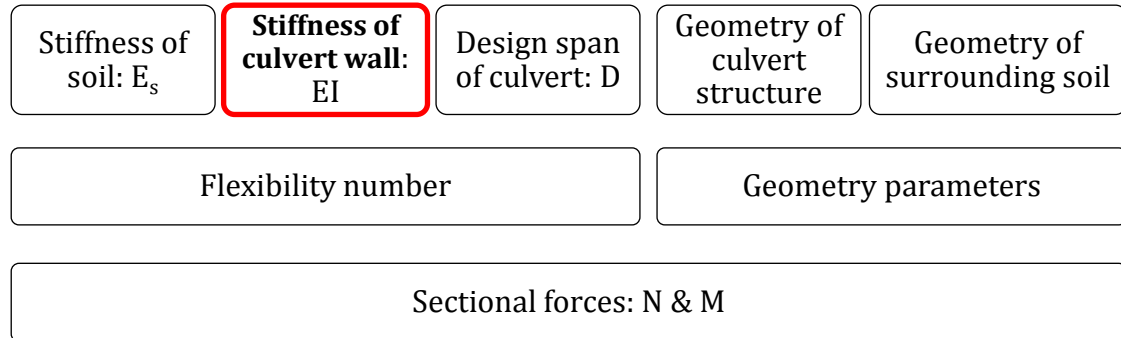
Figure 4.5 Factors used to calculate sectional forces by the SCI method in the SDM manual

The Table 4.4 below shows the sectional forces in the FRP culvert by using SCI method in the SDM. Case 14 is the design model, while case 15 is introduced as a control design, which helps offer more data for comparison between hand-calculation and FE-modeling results in the following sections. It reveals that the sectional forces at the crown region in ULS get the maximum value when the backfilling till the soil cover height.

Table 4.4 Sectional forces for the design case 14 and control case 15 calculated according to the SCI method in the SDM

Results	Senario 1		Senario 2				
	Backfilling till the crown		Backfilling till the soil cover height				
	SLS		SLS		ULS		
	N	M_crown	N	M_crown	**N**	**M_crown**	M_corner
	kN/m	kN*m/m	kN/m	kN*m/m	**kN/m**	**kN*m/m**	kN*m/m
Case 14	-134,6	-3,7	-404,9	86,6	**-546,6**	**118,3**	48,4
Case 15	-134,6	-3,7	-418,5	78,0	**-565,0**	**106,7**	49,0

4.6.2 **Reliability of hand-calculation**

The SCI method in the SDM is amended for the steel culvert design and verified by the in-site experiments. When it's applied for the FRP culvert calculation, the reliability of results needs to be analyzed and verified.

Since the calculation model in the SDM is two dimensional considering a unit strip of the culvert, the stiffness of culvert wall as discussed in the Figure 4.5 is the stiffness along the span direction. It means that the stiffness in the culvert's longitudinal direction is neglected. It's acceptable for the steel culvert since the longitudinal

stiffness of corrugated steel plates is slight compared with the stiffness in the span direction (Figure 4.6). However, it's not the same case for the FRP culvert. For instance, the longitudinal stiffness of the unidirectional FRP laminate used in the preliminary design is about 20% of the stiffness in the span direction (Figure 4.6). If the longitudinal stiffness of FRP culvert is not considered, as done in the SDM, the results become conservative compared with the real situation where the load is taken in two directions. The Table 4.5 shows the conceptual analysis of results using the SCI method in the SDM for steel culverts and FRP culverts design.
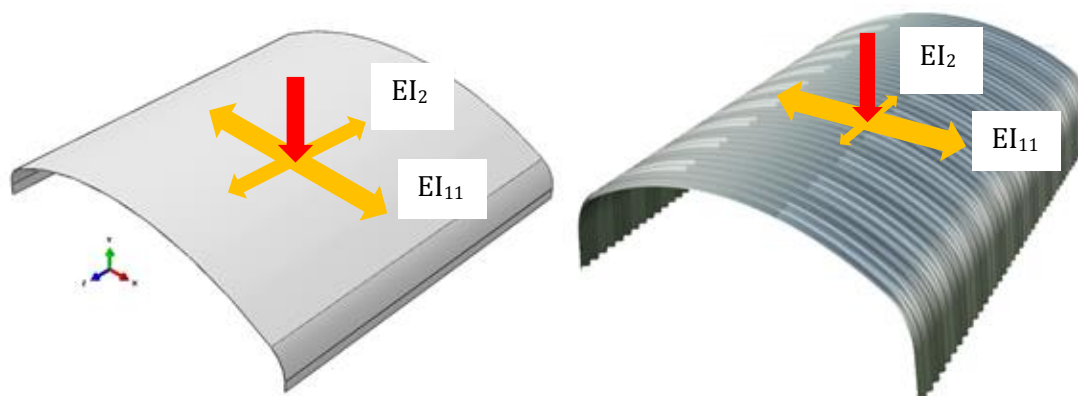
Figure 4.6 On the left, for the FRP culvert the load is taken down in two directions. For the steel culvert on the right, the load is almost supported in the span direction. (EI_{11}--Stiffness in the span direction; EI_{22}--Stiffness in the longitudinal direction)

Table 4.5 The difference of stiffness ratio between FRP culvert and steel culvert results in the conservative results for FRP culverts when the SCI method in the SDM is applied

	FRP Culvert	**Steel Culvert**
EI_{22}/EI_{11} (Longitudinal/Transveral)	$\approx 20\%$	$\approx 0\%$
Hand-calculation* Results	Conservative	Acceptable
*The hand-calculation is performed by the Mathcad No.2 according to the modified SCI method in the SDM, which neglects the longitudinal stiffness of the culvert structure and regards it as plain strain problem.		

4.6.3 **Verification by FE-modeling**

Models in Abaqus

The FE-modeling using program Abaqus is conducted in this section in order to verify the hand-calculation results by Mathcad. Considering the load effects due to surrounding soil and live traffic, two models are built in Abaqus with the traffic load applied in different ways.

In the first FE-model, referred as Abaqus Model 1, the traffic load LM2 is applied directly on the soil cover over the crown region, which represents the real situation (see Figure 4.7). Abaqus Model 1 is used to verify whether the hand-calculation results in Mathcad file is on the conservative side.
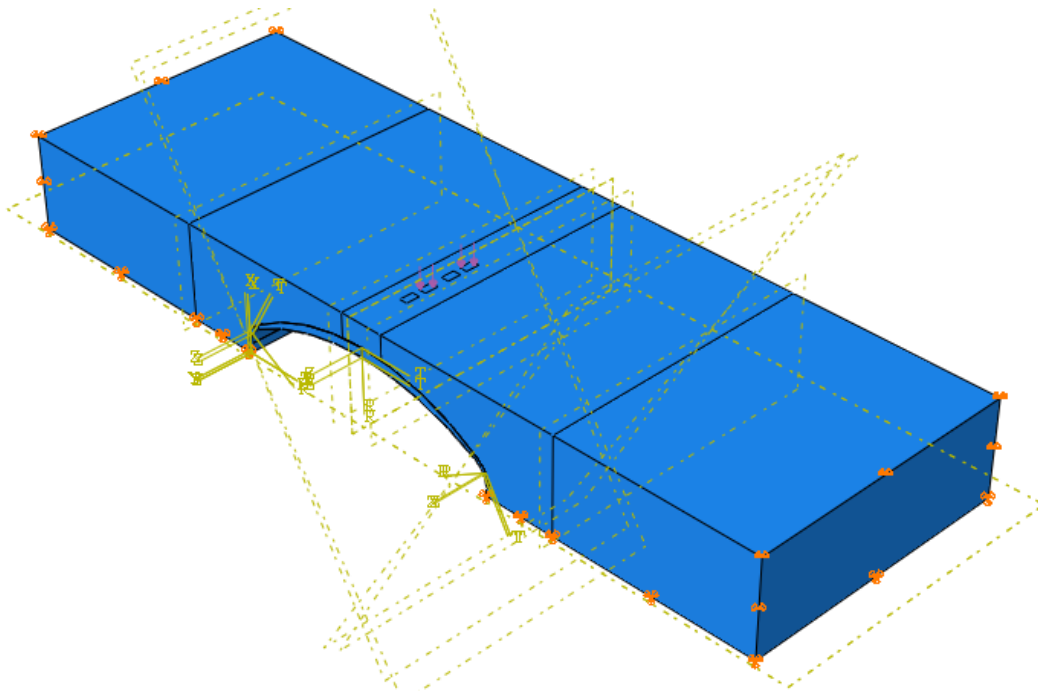
Figure 4.7 Abaqus model 1 of the culvert bridge with real traffic load LM2

In the second FE-model, referred as Abaqus Model 2, the traffic load is applied as an equivalent line load corresponding to the LM2 in a conservative way (see Figure 4.8). Abaqus Model 2 is supposed to set an upper limit for the result in the hand-calculation. It gives a general idea about whether the conservative result from hand-calculation is still in an acceptable range.
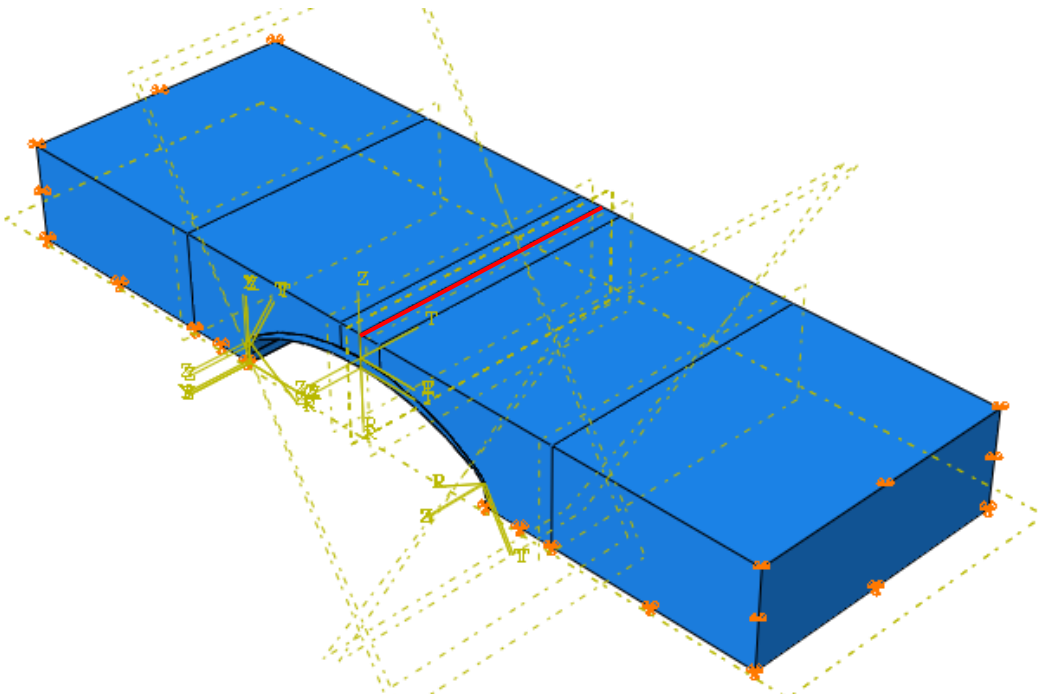
Figure 4.8 Abaqus model 2 of the culvert bridge with an equivalent line load converted from LM2 and applied in the longitudinal direction (The line load is applied along the highlighted red line)

More details about FE-modeling of the culvert bridge can be found in Appendix B.4.

CHALMERS, *Civil and Environmental Engineering*, Master's Thesis 2014:123

Comparison of hand-calculation with FE-modeling results

The verification of hand-calculation by FE-modeling focuses on the sectional forces in the crown region. Since the sectional forces are due to the surrounding soil and live traffic, the results are analyzed separately, as shown in the Table 4.6Table 4.6 Both the hand-calculation and FE-modeling are conducted for the control case 15, which is used to see whether the difference of results varies in different conditions, for instance, the soil cover height increases from 0.75 meter to 1.0 meter.

Table 4.6 Sectional forces for case 14 and case 15

| Sectional forces	Case 14				Case 15				Comment
Crown	Soil		Traffic		Soil		Traffic		
	N	M	N	M	N	M	N	M	
Abaqus Model 1	188,8	14,5	109,8	50,5	223,2	22	96,3	41	LM2
Hand-calculation	327,3	27,1	219,4	91,3	390,6	40,4	174,4	69,3	SCI & SDM
Abaqus Model 2	188,8	14,5	270	162,4	223,2	22	207	121	Equivalent LM2

The Figure 4.9 derived from the Table 4.6 shows the result ratio between hand-calculation and FE-modeling. Based on the comparison, the following conclusion can be drawn:

1) The hand-calculation is conservative. When the SCI method in the SDM is applied directly to the FRP culvert design, the results from hand-calculation are greater than those from Abaqus Model 1 which represents the real situation. It is valid no matter when it comes to normal force or bending moment, soil load or traffic load, and case 14 or case 15.

2) The hand-calculation doesn't exceed the upper limit. The sectional forces due to traffic load in the hand-calculation are lower than the results from Abaqus Model 2. Even though the initial hand-calculation results are on the conservative side, they are still in an acceptable range. For preliminary design phrase, reduction factors can be introduced to refine the initial hand-calculation.

3) Considering the sectional forces due to soil, the difference between hand-calculation and FE-modeling keeps stable by comparing case 14 with case 15. As discussed in the last section, the difference of results comes from the neglect of longitudinal stiffness of FRP culvert in the SCI method.

4) Considering the sectional forces due to traffic, the ratio between Abaqus Model 1 and Hand-calculation varies from case 14 to case 15. The ratio increases from 50% to 55% for the normal force, and from 55% to 59% for the bending moment. Since the different condition between case 14 and case 15 is the height of soil cover, it means that not only the longitudinal stiffness but also the height of soil cover has influence on the reliability of sectional forces due to traffic in the hand-calculation.
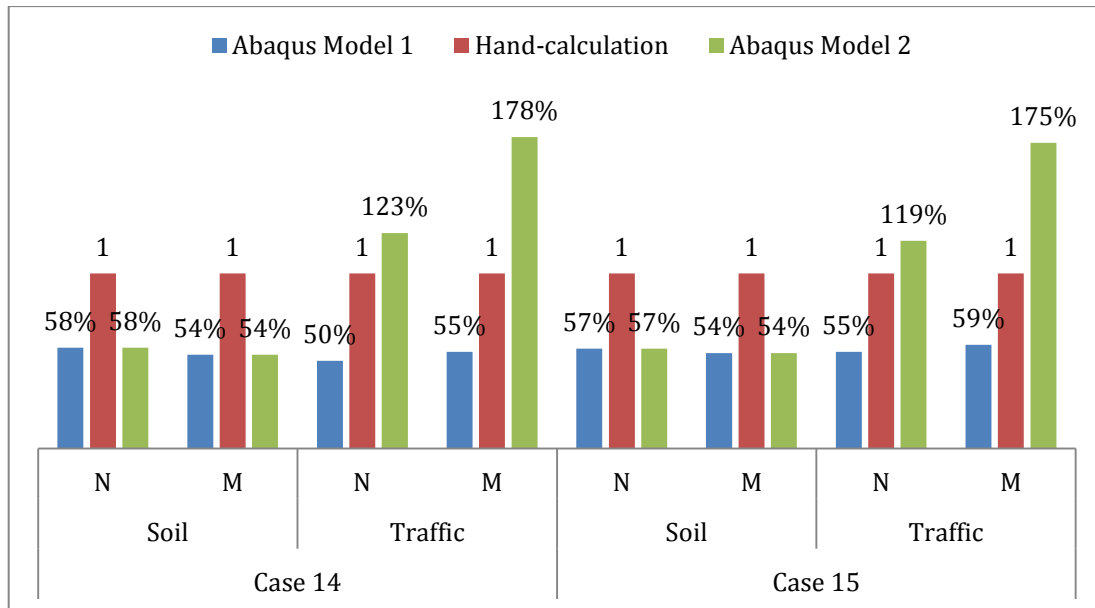
Figure 4.9 Results of ratio between Abaqus modeling and hand-calculation in design case 14 and control case 15 (N—normal force; M—bending moment)

4.7 Checks and results

The checks in the verification of FRP culvert includes 1) the load-bearing capacity of FRP laminate in the ULS, which is shown as material utilization ratio in the Table 4.7; 2) the deflection in the SLS, which should not exceed the span dimension divided by 400 (12 meter/400) [42].

Table 4.7 Verification of the FRP culvert design in terms of ULS and SLS

Abaqus Results	ULS	SLS	Cross-section of the FRP sandwich	
	Utilization ratio of FRP Laminate	**Deflection** [Max. 30 mm]	FRP laminate face [Unidirectional]	Core
Case 14	25,5%	**-25,3**	E-glass & Epoxy	PVC foam
Case 15	26,0%	**-34,0**	9 mm	400 mm

It's worthy to mention that the verification results in the Table 4.7 correspond to the design of FRP sandwich in the preliminary phrase. Due to the limited schedule, the optimization design is not conducted.

The verification clearly shows that the FRP culvert has sufficient load-bearing capacity in the case 14 with 12-meter-span. However, the deflection control becomes the governing issue for the FRP culvert. Since the flexibility of constructing a multi-directional FRP laminate, it is promising to achieve a better deflection performance by the optimization design.

4.8 Summary and conclusions

4.8.1 Structural feasibility of FRP culverts

The design of FRP culvert in this chapter shows that issues of fatigue and load-bearing capacity are not problems when FRP sandwich panels are applied to the culvert structure instead of steel plates. In terms of the checks of FRP strength and deflection, the verification shows that FRP culvert can succeed the challenges from the design case 14. Since the deflection of FRP culverts becomes dominant, the design of multi-directional FRP laminate in the optimization phrase is promising to have good control of deflection.

4.8.2 Refine the proposed design method for FRP culverts

Based on the analysis of results and comparison, the hand-calculation of sectional forces (performed by Mathcad No.2) is worthy to be refined. It will be further discussed in the Section 6.2.1.

5 Life-cycle Cost Analysis

5.1 Introduction

Life cycle cost analysis is a technique to estimate the comparative cost of the assets over the whole service-life or specific period of time by applying economic factors [43]. Life-cycle cost phases which considerably influence the total LCC of the system are represented in Figure 5.1. The life-cycle stages show that the total investment in the project has a number of components that includes monetary means by the consumption of material and energy.
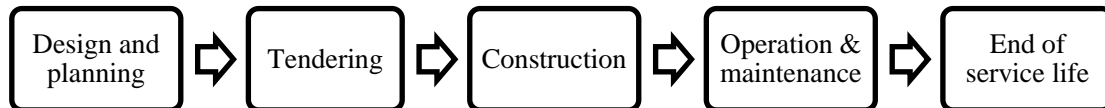
Design and planning ⇒ Tendering ⇒ Construction ⇒ Operation & maintenance ⇒ End of service life

*Figure 5.1 Life-cycle cost phases **[34]***

Generally, life-cycle costs are divided into agency and social costs (Figure 5.2). Agency costs include initial construction, operation and maintenance and disposal costs, basically consisting of the analogous elements: material, transportation, equipment and labour costs. The price for maintenance activities for inspection and repair should be accounted for long-term issues, which might become even more complex due to upraise of modern technologies and uncertainties for future maintenance actions. Disposal costs appear at the end of service life of the asset. One of the cost elements waste disposal can be even profitable, due to recyclable materials such as steel or FRP. Social costs are mostly related to traffic and people, and are divided into user and society costs. The cost units of user delay, vehicle operating and accident are calculated by respective equations (Social costs). Environmental costs are often taken into account by performing life-cycle assessment [2], [34].

Total life-cycle cost

- Agency costs
  - Initial construction costs
    - Material costs
    - Transportation costs
    - Equipment costs
    - Labour costs
  - Operation & maintenance costs
    - Material costs
    - Transportation costs
    - Equipment costs
    - Labour costs
  - Disposal costs
    - Waster disposal
    - Transportation costs
    - Equipment costs
    - Labour costs
- Social costs
  - User costs
    - User delay costs
    - Vehicle operating costs
  - Society costs
    - Environmental costs
    - Accident costs

*Figure 5.2 Cost phases of life-cycle cost analysis **[34]***

CHALMERS, *Civil and Environmental Engineering*, Master's Thesis 2014:123

5.2 LCC analysis of the study-case

5.2.1 Purpose of LCC analysis

In this thesis life-cycle cost analysis is performed in order to show that FRP sandwich is an economical solution for a culvert structure. The aim of the case study is not to obtain the total investment, but to acquire the prices of the materials, structural members itself and maintenance in order to show the monetary differences of two alternatives.

5.2.2 Assumptions

To be consistent with the study, case 14 is chosen for further analysis, considering the fact that this case can be applicable in reality, moreover having a big span of 12 meter, therefore being challenging for steel. Additionally, two culverts are assumed to be newly built as a road bridges and water passage under it. For the cost analysis the following assumptions are made:

- The costs in the design phase are excluded
- Due to the scope of the thesis, construction site preparation, earthwork (excavation, backfill), pavement and guard railing costs are omitted
- Environmental issues are not considered in this thesis.
- Accidental costs are disregarded due to lack of data.

5.2.3 Limitations

The life-span of the FRP culvert is assumed to be 100 years, while steel culvert has 80 years. In order to make a comparison the assumption of obsolescence is made, therefore both culverts are demolished. The analysis assumed to be confined to such boundaries:

- The period of analysis is assumed to be from the manufacturing of the culvert structural members until demolition
- The costs that are included in the analysis: materials, manufacturing, transportation, installation & construction, users, maintenance and demolition.

5.3 Agency costs

5.3.1 Initial construction costs

Initial costs include material, manufacturing, transportation and installation costs. Aside user costs are considered due to road works during culvert erection and since it is assumed a water passage via conduit, there is neither vehicle nor passenger traffic interruption during maintenance.

Material costs

Steel culvert price include:

- SuperCor SC-54 B corrugated panels
- Crown and corner reinforcement plates
- M 20 class 8.8 class
- Protective layers: hot-dip galvanizing (according to EN ISO 1461) with an average coat thickness 85 μm and extra epoxy painting with a thickness of 200 μm, covered from both sides 100 % perimeter

The steel conduit panels are transported in the typical widths of 836 mm and lengths of 2664 mm [44]. Overall, 90 panels of box and 60 reinforcement panels with specific dimensions are needed to be transported to the construction site using 24 tons truck.

Fibre reinforced polymer sandwich consists of E-glass fibres, epoxy matrix and foam Divinycell H 80.

FRP conduit is transported with 12 tons truck, in panels in a half of structure with a width of 3 meters, overall, 8 sandwich panels are needed. Since there are no culverts from FRP material it is assumed that the installation time for both materials are the same. The fastening of this type of structure is not solved thoroughly, but due to durability of FRP, same material fasteners are preferred. The mold price is assumed to be used in 10 more typical projects hereby being a future investment. Table 5.1 and Table 5.2 represents initial prices for both materials

Table 5.1 Initial costs of steel

Steel	Value	Unit
Culvert structure[1] (panels, reinforcement, bolts)	800000	SEK
Transportation and installation		
Transportation (24 ton truck)	12	SEK/km per ton
Men power[2]	160	SEK/h
Number of workers	7	
Number of working hours on site	64	H
[1]Giedrius Alekna, ViaCon Baltic, e-mail 2014-05-29 [2]byggnads.se		

Table 5.2 Initial costs of FRP

FRP sandwich materials	Price	Unit
Epoxy matrix	100	SEK/l
E-glass fibers	12	SEK/m^2
[1]Foam Divinycell H 80	4800	SEK/m^3
Moulds for laminas	4000	SEK/m^2
FRP fastening[2]	130	SEK/unit
Transportation and installation		
Transportation (12 ton truck)	6	SEK/km per ton
Men power[3]	160	SEK/h
Number of workers	7	
Number of working hours on site	64	h
Number of working hours for laminas production	56	H

5.3.2 Operation and maintenance costs

In order to find the total price of LCC the phase of operation and maintenance should be thoroughly done. Due to deficiency of accurate data of specific maintenance activities, an annual steel culvert maintenance price was adopter according to Safi, 2012. However, the maintenance activities that are done during the service life of steel culvert usually are [45]:

- Foundations. Check for erosion, cleavage, corrosion of reinforcement, flushing, settlements, cracks, displacement
- Slopes
- Walls (inlets and outlets). Check for erosion, cleavage, corrosion of reinforcement, cracks, deformation, displacement
- Main bearing structure (conduit). Check for corrosion, cracks, protective layer, change of conduit shape, displacement of the structure
- Bolts. Check for corrosion, degradation, dissolve
- Entire bridge. Check for vegetation, damping, scouring, debris, siltation

The major concern about the exploitation of steel culvert arise when maintaining a sufficient protective layer against corrosion, therefore the culvert is assumed to be repainted every 15 years.

The service life of FRP culvert can be taken as almost no maintenance, due to resistance to the aggressive environment, which in study-case is water passing under the culvert. Despite the durability of FRP the same general checks for obstruction or maintaining other parts of the whole system are required, therefore the service-life cost is taken into account as 10 % of steel maintenance cost.

In order to evaluate future investment a Net Present Value method (NPV) is used [2]. In this method a discount rate is used; the basic principle of discounting is that the sum of money at hand at the present has a higher value than the same amount of money in the future (Langdon, 2007). Discount rate computes future amount of money into present value, taking into consideration inflation and the actual earning power of money. All these future investments should be converted to the present value with a discount rate of 3.5 % [46]. This can be done by using equation:

$$NPV = \sum_{n=0}^{L} \frac{C_n}{(1+r)^n}$$

Where:

NPV=the life-cycle cost expressed as a present value;

n=the year considered;

C_n=sum of all cash flows in year n;

r=discount rate.

5.3.3 **Disposal costs**

Disposal costs are at the end of the service life of the structures. In this study case the costs of transportation and demounting are assumed to be the same as in initial phase. Demounted steel structures are recycled with a profit of 452 SEK/ton [34] and FRP recycled with a profit of 1130 SEK/ton [Mika Lange, Zajons Zerkleinerungs GmbH, e-mail 2014-06-05].

5.4 **Social costs**

Social costs are related to traffic disruptions that take place during construction as well as maintenance. As it is indicated in the Section Assumptions, society costs, that includes environment and accident costs are not considered. Social costs that include user delay and vehicle operating costs are dependent on additional time that bridge users consume on detours and can be calculated by equations [47]:

$$\text{User delay costs} = \left(\frac{L}{S_a} - \frac{L}{S_n}\right) \cdot \text{ADT} \cdot N \cdot w$$

$$\text{Vehicle operating costs} = \left(\frac{L}{S_a} - \frac{L}{S_n}\right) \cdot \text{ADT} \cdot N \cdot r$$

Where:

    L = length of affected roadway the cars are driving;

    S_a = traffic speed during bridge work activity;

    S_n = normal traffic speed;

    ADT = average daily traffic;

    N = number of days of roadwork

    w = hourly time value of drivers;

    r = hourly vehicle operating cost;

The social costs might be omitted during the bridge exploitation, because it is assumed that there is no traffic under the culvert, therefore no traffic interruption occur during the maintenance. To conclude, social costs in this study-case are related only with the inconvenience for drivers in construction phase, hence user delay and vehicle operation costs are only included in the analysis of the initial price.

5.4.1 **User costs**

With the reference to the data earlier, user costs in this study-case can be calculated based on equations:

$$\text{User delay costs} = \Delta t \cdot \text{ADT} \cdot N \cdot w$$

$$\text{Vehicle operating costs} = \Delta t \cdot \text{ADT} \cdot N \cdot r$$

Where:

    Δt = driver delay time due to detouring.

With a reference of [44] and Lars Hansing, ViaCon Sverige AB, e-mail 2014-06-02 8 days of road works to erect conduit are anticipated. Table 5.3 represents the same input data of user costs for steel and FRP. Input data is adopted from [34] as a diverse ADT, w, r or Δt do not influence the comparative price. Both alternatives are assumed

to have the same number of day of roadwork due to unknown installation time of FRP culvert, even though it might be shorter considering the fact that it is only 8 panels to be installed.

Table 5.3 User costs input data

Item	Value	Unit
Average daily traffic ADT[1]	796	Vehicle/day
Hourly time value of drivers[1] w	254	SEK/h
Hourly vehicle operating cost[1] r	187	SEK/h
Driver delay time due to detouring[1] Δt, 15 min	0,25	h
Number of days of roadwork[2] N	8	Days
[1]Mara V., 2014 [34]		
[2]Lars Hansing, ViaCon Sverige AB, e-mail 2014-06-02, ViaCon brochure [44]		

5.5 **Results**

Figure 5.3 represents the prices of all components that are considered in the analysis, showing that material price for steel is about 30 % higher as well as 90 % more for maintenance. Other elements prices such as installation, transportation, maintenance and disposal are equal or nearly equal. The cost distribution in the initial phase is shown in Figure 5.4 representing lower material cost of FRP in culvert structure.
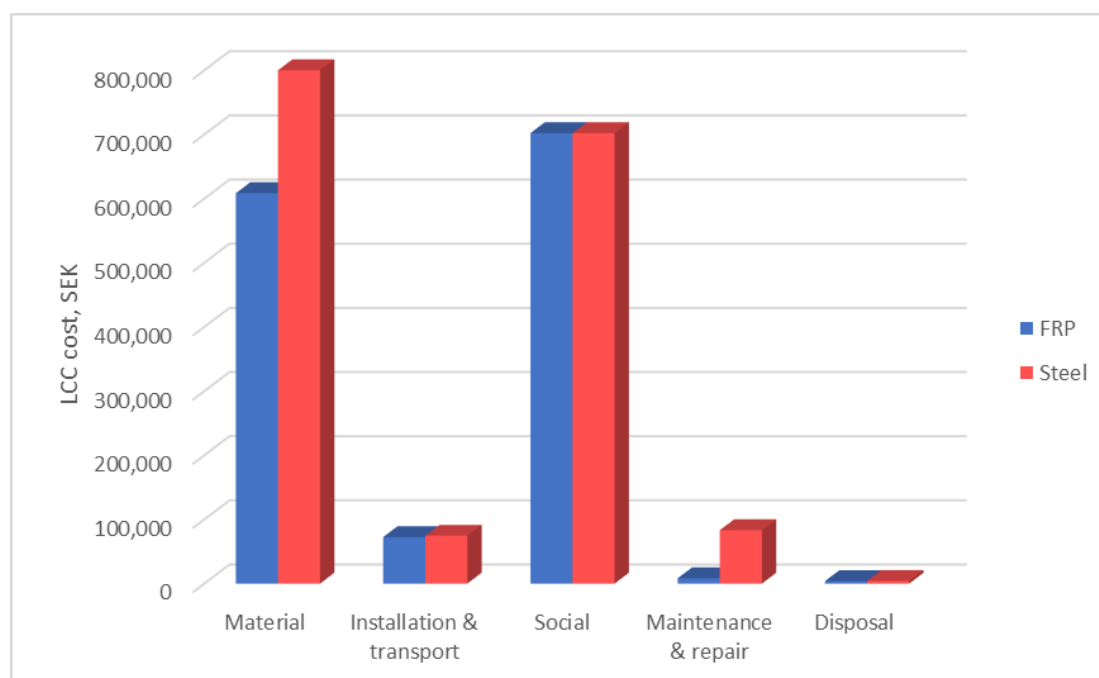

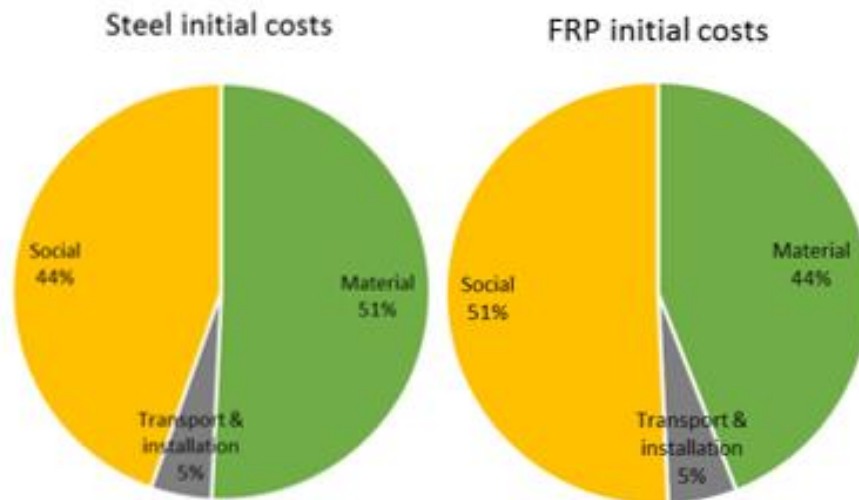*Figure 5.3 Life-cycle cost comparison between steel and FRP*

Figure 5.4 Initial cost distribution

The estimated costs for two alternatives are presented in Table 5.4. The cost category 1 represents the prices in each life-cycle phase of the bridges, and the cost category 2 shows the cost by entity. Agency cost includes material, installation, transportation, maintenance and end-of-life stages. The major differences occur in initial and maintenance expenses. Initial steel price is 14 % more than FRP as well as maintenance price is 90 % higher for steel culvert. End-of-life costs are almost equal mainly because both materials are recyclable. In general, it can be saved around 20 % of total steel price if choosing FRP proposal.

Obtained results show (see Table 5.4) that vast majority of investment for FRP culvert are in the initial phase, considering the fact that it requires almost no maintenance on the contrary to steel culvert. It can be observed that agency costs contribute 58 % for steel and 50 % for FRP of the total investment (Figure 5.6). This amount of money is greatly dependent on the location of the bridge and construction time. Since it is assumed that the bridge location in the same, the only element that can influence these costs is construction time. Note: a detailed input data that life-cycle comprise can be found in Appendix C.

Table 5.4 Life-cycle costs in SEK

Cost category	Steel	FRP
1 - By life-cycle phase		
Initial costs	1,576,728	1,383,032
Maintenance and repair costs	83,223	8,322
End-of-life costs	4,200	3,900
Total	**1,664,151**	**1,395,254**
2 - By cost entity		
Agency costs	961,983	693,182
Social costs	702,168	702,072
Total	**1,664,151**	**1,395,254**
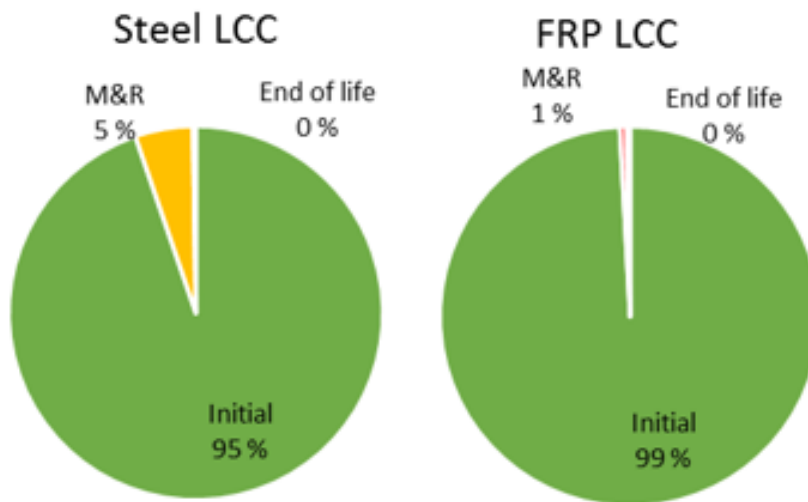
Figure 5.5 Total life-cycle cost by life-cycle phase
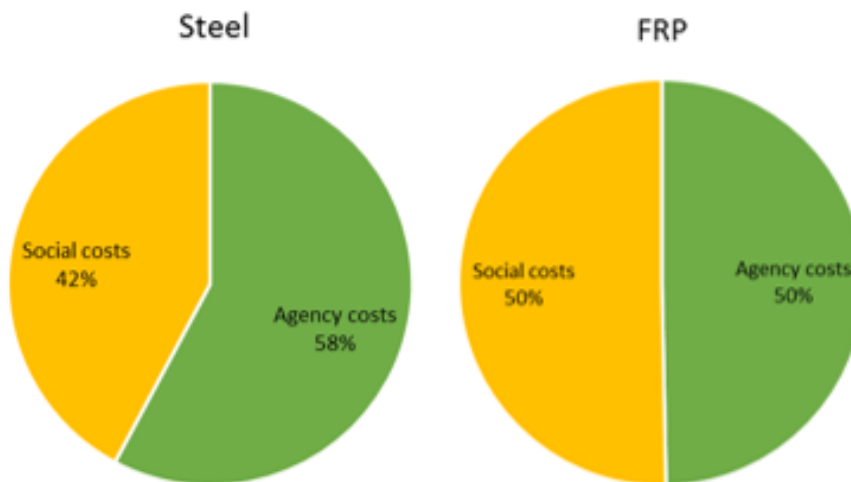
Figure 5.6 Life-cycle cost by cost entity

5.6 **Summary**

As a summary of the life-cycle cost analysis it can be concluded that FRP culvert is more economical alternative due to lower initial material and maintenance costs. It is durable solution as well, regarding FRP material as not susceptible to aggressive environment as distinct from steel material. In addition to this, the possibility to recycle FRP makes it considerably sustainable material. Lastly, in the particular study-case 14, an estimated FRP culvert is approximately 50 % lighter than steel culvert, possessing cheaper transportation and installation price as well as faster erection.

6 Conclusions

6.1 About FRP culvert structure

The study of applying FRP material in the culvert structure shows that the FRP culvert is a promising alternative to the traditional steel culvert in the design of challenging case.

Mechanical performance

The FRP culvert has better mechanical performance than the steel one in terms of load-bearing capacity and fatigue issues. The study of case 14 shows that the FRP culvert succeeds the challenges of large span and shallow soil cover, which cannot be satisfied by using steel plates.

LCC analysis

The LCC analysis shows that the FRP culvert is also an economical alternative. The application of FRP material gives culvert structure more durable and sustainable performance in the service life.

6.2 Suggestions for future study

6.2.1 Proposed design method for FRP culvert

The proposed methodology for FRP culvert design as discussed in the chapter 4 needs to be improved in the future study.

Calculation of sectional forces

In the preliminary design, the calculation of sectional forces for the FRP culvert follows the amended SCI method in the SDM for steel culvert design. The verification by FE-modeling proves that the results are conservative, and it's valuable to refine the hand-calculation method by introducing reduction factors. Based on the comparison in the section 4.6, the following comments about reduction factors can be made.

- The reduction factor for sectional forces due to soil is highly dependent on the stiffness ratio between longitudinal and transversal.
- The reduction factor for sectional forces due to traffic load is a function of both stiffness ratio and height of soil cover.

In order to obtain the functions for determining the value of reduction factors in different design conditions, more study cases by FE-modeling are required.

Verification of the FRP culvert structure

The verification of FRP culverts in this thesis includes the checks for load-bearing capacity of FRP laminate in the ultimate limit state and deflection in the serviceability limit state. In the future study more issues need to be considered in the design of FRP culverts.

- Capacity of core material
- Capacity of the interfacial connection between core and FRP face
- Design of connection details for FRP sandwich panels
- Creep of FRP material

6.2.2 **Applicability of FRP culverts**

In this thesis, the FRP culvert is designed and compared with steel culverts only for the selected challenging case 14 with 12-meter-span and 0.75-meter-soil cover. It's important to know whether the FRP culvert is still a competitive alternative when it comes to smaller spans, for instance. In order to investigate the applicability of FRP culverts, more comprehensive comparisons between steel and FRP culverts in different conditions are needed in the future research.

6.2.3 **Other materials for FRP culverts**

The design of FRP sandwich chooses PVC foam as core material. Since the elastic modulus of FRP material is much smaller than that of steel, it requires a large thickness of core section in order to get a proper stiffness. The fact motivates the study of honeycomb as core material instead of PVC foam in the future.

For the FRP laminate face, the epoxy matrix reinforced by E-glass fibers is chosen as the FRP material in the FRP culvert design. Other types of FRP material, for example, reinforced by G-glass or carbon fibers can also be applied if higher mechanical properties are required.

6.2.4 **Life-cycle assessment in the LCC analysis**

In order to get more precise service life costs of culverts, maintenance activities for both structures should be thoroughly analysed. Extraordinary attention should be paid to long-term behaviour of FRP material, due to lack of practical examples of underground structures. Moreover, since environmental issues nowadays becomes more and more important, an influence of exhaust fumes during material manufacturing, transportation, installation, maintenance and demolition should be taken into account. One of the ways to do that is to perform life-cycle assessment. After the evaluation of environmental impacts, a more evident conclusion could be drawn about life-cycle cost of the structures.

7 References

[1] L. Pettersson and H. Sundquist, "Design of Soil Steel Composite Bridges," Stockholm, 2010.

[2] M. Safi, "LCC Applications for Bridges and Integration with BMS," KTH Royal Institute of Technology, Stockholm, 2012.

[3] H. Sundquist, "Soil-Steel Structures. State-of-the-art. Swedish Research. Presentation in NordBalt Seminar," 2007.

[4] L. Petterson, "Full Scale Tests and Structural Evaluation of Soil Steel Flexible Culverts with Low Height of Cover," KTH, 2007.

[5] "Components of the Culvert." [Online]. Available: http://www.cjntech.co.nz/manuals/Find the Answer/#2864.htm.

[6] "Culverts." [Online]. Available: http://water.epa.gov/polwaste/nps/urban/upload/2003_07_24_NPS_unpavedroads_ch3.pdf.

[7] J. F. Levine, C. B. Eads, W. G. Cope, L. F. Humphries, R. B. Bringolf, P. R. Lazaro, D. Shea, J. Vander Pluym, D. Eggleston, M. A. Merril, J. Gregory, and A. E. Bogan, "Final Report Submitted To: North Carolina Department of Transportation (Project Number : HWY-2004-08) January 2007 Prepared By : Technical Report Documentation Page," 2007.

[8] U. University, "Culvert Rehabilitation Practices," Utah.

[9] "Snap-Tite Large Diameter Culvert Lining Systems." [Online]. Available: http://www.culvert-rehab.com/pdfs/big-idea.pdf.

[10] "Culvert Rehabilitation Systems." [Online]. Available: http://www.kenway.com/products/culvert-rehabilitation-systems/.

[11] "Steel Culvert Re-lining." [Online]. Available: http://www.eng.buffalo.edu/.

[12] "Fiberglass Digester Domes." [Online]. Available: http://www.mekco.com/fiberglass_digester.htm.

[13] "Mondial House." [Online]. Available: http://www.lightstraw.co.uk/ate/main/mondial/.

[14] "Fiberline Composites." [Online]. Available: http://www.fiberline.com/.

[15] "Dawlish Railway station." [Online]. Available: http://www.reinforcedplastics.com/view/29001/steel-footbridge-replaced-with-composite-at-uk-railway-station/.

[16]   "Dawlish FRP Railway Station." [Online]. Available:
        http://www.tech.plym.ac.uk/sme/composites/bridges.htm#dawlish.

[17]   "Corrosion Fluid Products Corp." [Online]. Available:
        http://corrosionfluid.com/.

[18]   "Plastics Pipe Institute." [Online]. Available: https://plasticpipe.org/about-
        ppi.html.

[19]   "Fiberglass pipe." [Online]. Available: http://www.gwhaley.com/FRPPipe.htm.

[20]   "Composites." [Online]. Available:
        http://www.plasticoncomposites.com/en/composites.

[21]   "FRP composites." [Online]. Available: http://reichhold.com/.

[22]   M. Zoghi, *The International Handbook of FRP Composites in Civil
        Engineering*. CRC Press, 2013, p. 706.

[23]   I. E. Comittee, "An Introduction to FRP Composites for Construction," 2006.

[24]   "FRP Pipe Technologies." [Online]. Available: http://www.pipemedic.com/.

[25]   "ABC's of FRP Materials." [Online]. Available:
        http://www.autocomposites.org/composites101/abc.cfm.

[26]   R. G. Weatherhead, *FRP Technology: Fibre Reinforced Resin Systems*. Applied
        Science, 1980, p. 462.

[27]   M. F. G. Companies, "Technical Design Guide for FRP Composite Products
        And Parts."

[28]   M. V. Hosur, M. Abdullah, and S. Jeelani, "Manufacturing and Low-Velocity
        Impact Characterization of Foam Filled 3-D Integrated Core Sandwich
        Composites with Hybrid Face Sheets," *Compos. Struct.*, vol. 69, no. 2, pp. 167–
        181, Jul. 2005.

[29]   E. M. Reis, "Characteristics of Innovative 3-D FRP Sandwich Panels," 2005.

[30]   "DIAB guide to core and sandwich," Laholm, 2012.

[31]   "Core Materials: Nomex Honeycomb." [Online]. Available:
        http://www.fibermaxcomposites.com/shop/nomex-aramid-
        honeycombbrthickness-mmbrcell-size-32-mm-p-647.html?cPath=77.

[32]   "Core materials: XPS foam." [Online]. Available: http://www.cs-
        jy.com/en/News/products-show.asp?cataid=000200020003.

[33]   "Current Practices in FRP Composites Technology." [Online]. Available:
        http://www.fhwa.dot.gov/bridge/frp/deckprac.cfm.

[34] V. Mara, "Fibre reinforced polymer bridge decks : Sustainability and a novel panel-level connection," Chalmers University of Technology, 2014.

[35] P. B. Potyrala, "Use of Fiber Reinforced Polymer Composites in Bridge Construction. State of the Art in Hybrid and All-Composite Structures," Technical University of Catalonia, 2011.

[36] T. A. Hoffard and L. J. Malvar, "Fiber-Reinforced Polymer Composites in Bridges: A State-of-the-Art Report," 2005.

[37] L. Pettersson and H. Sundquist, "Design of soil steel composite bridges," 2009.

[38] A. H. H. Wadi, *Soil steel composite bridges*. 2012.

[39] B. D. Agarwal, L. J. Broutman, and K. Chandrashekhara, *Analysis and Performance of Fiber Composites*. Wiley, 2006.

[40] J. L. Clarke, *Structural Design of Polymer Composites: Eurocomp Design Code and Background Document*. Taylor & Francis, 2003.

[41] P. K. Mallick, *Fiber-reinforced composites: materials, manufacturing, and design*. CRC Press, 2008.

[42] *Guide Specifications for Design of FRP Pedestrian Bridges, 1st Edition*. American Association of State Highway and Transportation Officials, 2008.

[43] "ETSI Project. Bridge Life Cycle Optimisation. Stage 3," 2013.

[44] ViaCon, "Burried Flexible Steel Structures SuperCor."

[45] Vägverket, "BaTMan – Mätning och bedömning av broars tillstånd," 2008.

[46] Trafikverket, "Samhällsekonomiska principer och kalkylvärden för transportsektorn: ASEK 5.1. Kapitel 3 Kalkylprinciper och generella kalkylvärden," 2014.

[47] M. A. EHLEN, "Life-Cycle Costs of Fiber-Reinforced-Polymer Bridge Decks," *J. Mater. Civ. Eng.*, vol. 11, pp. 224–230, 1999.

8 Appendices

The appendices are list below:

Appendix A.1   **Equivalent traffic line loads**

Appendix A.2   **Mathcad routine for design of corrugated steel culverts**
Mathcad sample of Case 14

Appendix B.1   **Mathcad routine for design of FRP culverts—Mathcad No.1**
Stiffness calculation and stress analysis

Appendix B.2   **Mathcad routine for design of FRP culverts—Mathcad No.2**
Calculation of sectional forces

Appendix B.3   **Mathcad routine for design of FRP culverts—Mathcad No.3**
Failure prediction of the FRP laminate

Appendix B.4   **Data for the FE analysis of FRP culverts in ABAQUS**

Appendix C   **Data for LCC analysis**

Appendix A.1 Equivalent line load due to live traffic

The data of equivalent line load converted from four traffic groups in different soil cover conditions are provided by the supervisor Kristoffer Karlssen from the consultant company WSP at Gothenburg.

Table A.1-1 Equivalent line load converted from traffic groups in varying soil cover conditions

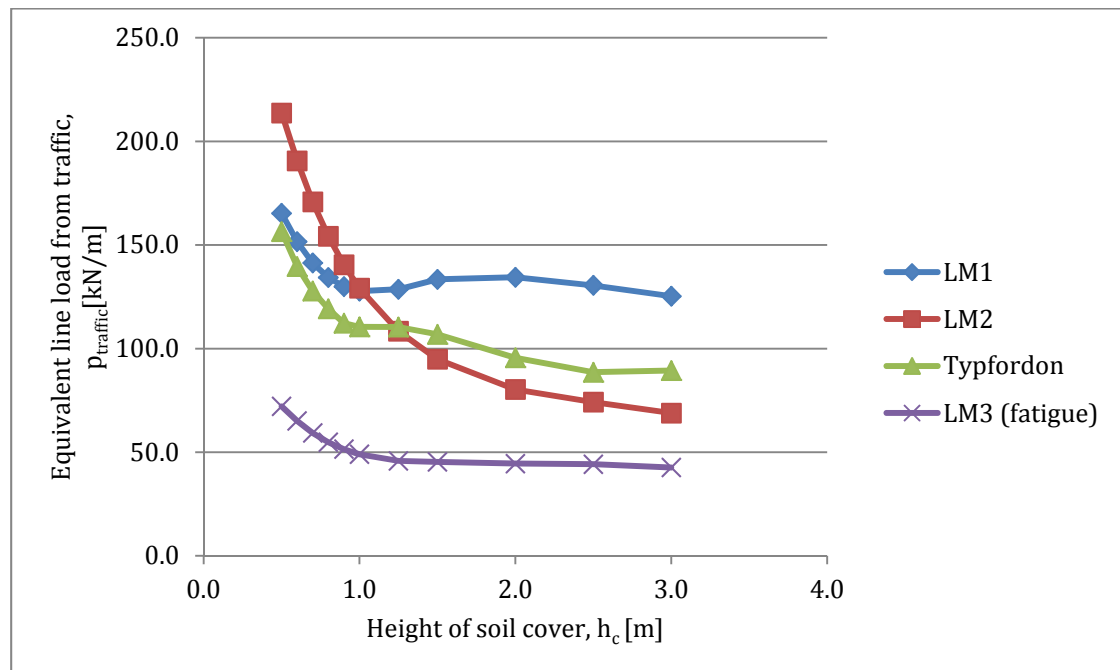| Equivalent line load due to live traffic											
Height of Soil Cover	0,5	0,6	0,7	0,8	0,9	1,0	1,3	1,5	2,0	2,5	3,0
LM1	165,3	151,6	141,3	134,3	129,9	127,7	128,6	133,4	134,4	130,5	125,3
LM2	213,7	190,6	170,8	154,2	140,5	129,2	108,4	94,9	80,3	74,2	68,9
Typfordon	156,5	139,6	127,8	119,2	112,3	110,5	110,4	106,9	95,6	88,6	89,4
LM3 (fatigue)	72,1	65,1	59,3	54,8	51,5	49,0	45,8	45,3	44,5	44,2	42,6

Figure A.1-1 Equivalent line load converted from traffic groups in varying soil cover conditions

Appendix A.2 Mathcad Routine for Design of Corrugated Steel Culverts

According to the Swedish Design Method developed by Pettersson & Sundquist

1. Input data

1.1. Geometry of the culvert bridge

Culvert profile: *Possible profiles are A, B, C, …, G, according to Handbook*

$profile := \text{"G: Box Culvert"}$ *SC-54B, Viacon*

$D := 12.270\,m$ *Span*

$H := 2.745\,m$ *Height*

$R_t := 11.430\,m$ *Top radius*

$R_s := 1.016\,m$ *Side/Corner radius*

Height of the soil cover

$h_c := 750\,mm$

1.2. Properties of the corrugated steel plates

Type of plate:

$type_{steel} := 2$ *Profile 200*55 gives 1, Profile 381*140 gives 2*

$t_s := 7\,mm$ *Plate thickness*

$Reinforce_{top} := \text{"yes"}$ *Use reinforcement plates in the top section*

$Reinforce_{cor} := \text{"yes"}$ *Use reinforcement plates in the corner section*

$$h_{corr} := \begin{vmatrix} (55mm) & \text{if } type_{steel} = 1 \\ (140mm) & \text{if } type_{steel} = 2 \\ \text{"Error"} & \text{otherwise} \end{vmatrix}$$ *Profile height*

$h_{corr} = 140\,mm$

$$c_{sp} := \begin{vmatrix} (200mm) & \text{if } type_{steel} = 1 \\ (380mm) & \text{if } type_{steel} = 2 \\ \text{"Error"} & \text{otherwise} \end{vmatrix}$$ *Wave length*

$c_{sp} = 380\,mm$

$$R_{sp} := \begin{vmatrix} (53mm) & \text{if } type_{steel} = 1 \\ (76.2mm) & \text{if } type_{steel} = 2 \\ \text{"Error"} & \text{otherwise} \end{vmatrix}$$ *Radius of curvature*

$R_{sp} = 76.2 \, \text{mm}$

Steel grade S 315MC

The SuperCor produced by Viacon conforms to EN 10149-2 or EN 10025-2

$f_{yk} := 315 \text{MPa}$

$f_{uk} := 470 \text{MPa}$

$E_s := 210 \text{GPa}$

1.3. Parameters of the bolted connection

Bolts

M20 class 8.8, EN ISO 898-1

$f_{ub} := 800 \text{MPa}$

$f_{yb} := 640 \text{MPa}$

$d_{bolt} := 20 \text{mm}$

$A_{bolt} := \dfrac{\pi}{4} \cdot d_{bolt}^2 = 314.159 \, \text{mm}^2$

$n_{bolt} := \dfrac{15}{\text{m}}$

$a_{bolt} := \begin{vmatrix} (100\text{mm}) & \text{if } \text{type}_{steel} = 1 \\ (190\text{mm}) & \text{if } \text{type}_{steel} = 2 \\ \text{"Error"} & \text{otherwise} \end{vmatrix}$

Distance between parallel rows (center to center)

1.4. Parameters of the backfilling soil

Type of the backfilling soil:

Base course material

Parameters of soil taken from Appendix 2 of Handbook

$\rho_{opt} := 20.6 \, \dfrac{\text{kN}}{\text{m}^3}$

Optium density

$RP := 97$

Degree of compaction (%), standard proctor method

$\rho_{cv} := \dfrac{RP}{100} \cdot \rho_{opt}$

$\rho_{cv} = 19.982 \cdot \dfrac{\text{kN}}{\text{m}^3}$

$\rho_1 := \rho_{cv}$

Density of the soil up to the height of the crown

$\rho_2 := \rho_{cv}$

Mean density of the soil material with the region (hc+H/2)

Partical size distribution

$d_{50} := 20 \text{mm}$ $\qquad$ $d_{60} := 30 \text{mm}$ $\qquad$ $d_{10} := 3 \text{mm}$

$\nu := 0.29$ *Poisson Ratio*

1.5. Partial coefficients

$\gamma_n := 1.1$ *The safety class recommended for structures with a span less than 15 meters is 2, according to the natation section in Handbook.*

Partial coefficients for material strength

$\gamma_{m.steel} := 1.1$

$\gamma_{m.soil} := 1.3$ *According to the Handbook 2010, Appendix 2, Table B2.1*

$\gamma_{M1} := 1.0$ *According to the Handbook 2010, Section 5.3 (3)*

$\gamma_{Mf} := 1.35$ *For fatigue strength: Safe life, high consequence, Table 3.1, EN 1993-1-9*

Partial coefficients for loads

Ultimate limit state: *Table A 2.4(B), EN 1990*

$\gamma_{G.u} := \begin{pmatrix} 1.35 \\ 1.00 \end{pmatrix}$ $\gamma_{Q.u} := \begin{pmatrix} 1.35 \\ 0 \end{pmatrix}$ *Upper: Unfavorable*
Lower: Favorable

Serviceability limit state: *Table A 2.6, EN 1990*

$\gamma_{G.s} := \begin{pmatrix} 1.00 \\ 1.00 \end{pmatrix}$ $\gamma_{Q.s} := \begin{pmatrix} 1.00 \\ 0 \end{pmatrix}$ *Upper: Unfavorable*
Lower: Favorable

Fatigue limit state:

$\gamma_{Ff} := 1.0$ *Section 9.3 (1), EN 1993-2*
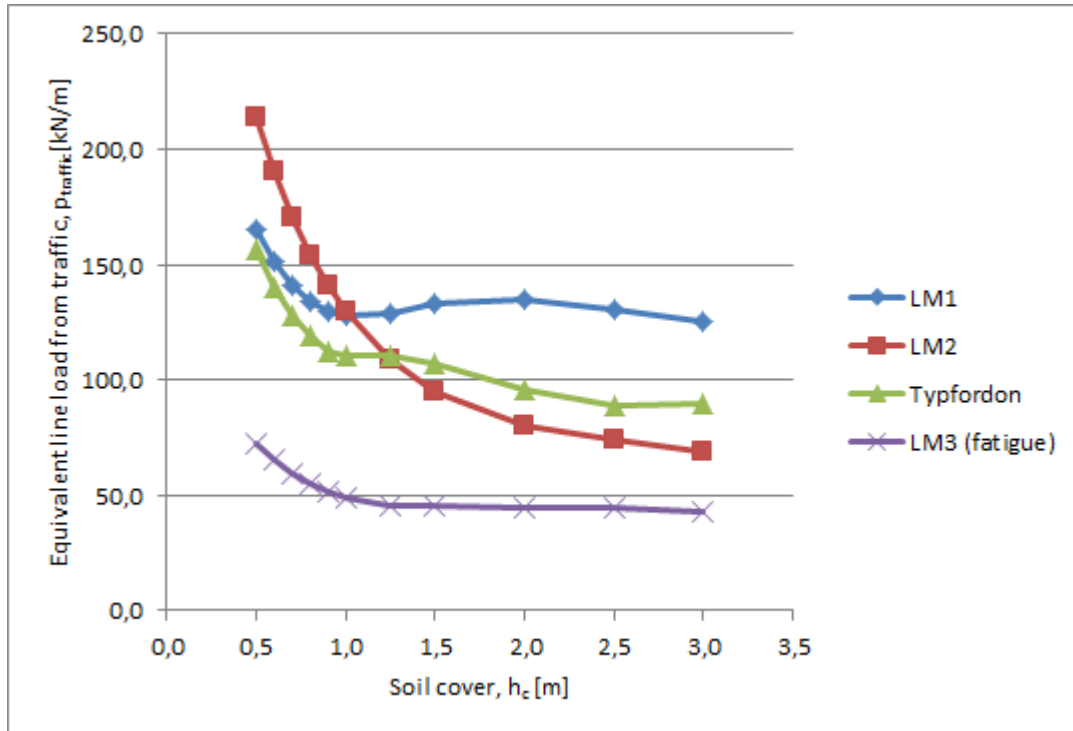
1.6. Live traffic load

Four load group types are considered:
(1) LM1 from EN 1991-2;
(2) LM2 from EN 1991-2;
(3) LM3 from EN 1991-2
(4) Typfordon from TRVK BRO 11, Publ nr 2011:085

The characteristic value of the equivalent line load for each of these 4 load types is obtained with the boussinesq method according to the Handbook, considering the most unfavorable loading position. The results of the equivalent line loads with different height of soil cover are shown in the figure below.

Figure*A.1-1 The equivalent line load converterd from traffic group at different soil cover height

*Note: The Calculation and results of the equivalent line load are provided by the supervisor from the consultant company WSP in Gothenburg

The equivalent traffic line load for SLS and ULS

$$
p_{traffic} := \begin{vmatrix} \left(213.7 \, \dfrac{kN}{m} \right) & \text{if } h_c = 0.5m \\[2mm] \left(162.5 \, \dfrac{kN}{m} \right) & \text{if } h_c = 0.75m \\[2mm] \left(129.2 \, \dfrac{kN}{m} \right) & \text{if } h_c = 1m \\[2mm] \left(125.3 \, \dfrac{kN}{m} \right) & \text{if } h_c = 3m \\[2mm] \text{"Error"} & \text{otherwise} \end{vmatrix}
$$

$$
p_{traffic} = 162.5 \cdot \frac{kN}{m}
$$

The equivalent traffic line load due to LM3 for fatigue

$$p_{traffic.fatigue} := \begin{Vmatrix} \left(72.1\,\dfrac{kN}{m}\right) & \text{if } h_c = 0.5m \\[2mm] \left(57.1\,\dfrac{kN}{m}\right) & \text{if } h_c = 0.75m \\[2mm] \left(49.0\,\dfrac{kN}{m}\right) & \text{if } h_c = 1m \\[2mm] \left(42.6\,\dfrac{kN}{m}\right) & \text{if } h_c = 3m \\[2mm] \text{"Error"} & \text{otherwise} \end{Vmatrix}$$

$$p_{traffic.fatigue} = 57.1 \cdot \frac{kN}{m}$$

2. Calculation

2.1. Soil tangent modulus

- **Determination of relevant factors**

$$\rho_s := 26\,\frac{kN}{m^3}$$

True density of the soil material, Appendix 2, Handbook

$$e_1 := \frac{\rho_s}{\rho_1} - 1 = 0.301$$

Void ratio

$$C_u := \frac{d_{60}}{d_{10}} = 10$$

Uniformity coefficient

$$m_1 := 282 \cdot C_u^{-0.77} \cdot e_1^{-2.83} = 1.43 \times 10^3$$

Modulus ratio

$$\beta := 0.29 \cdot \log\left(\frac{d_{50}}{0.01mm}\right) - 0.065 \cdot \log(C_u) = 0.892$$

Stress exponent

$$\phi_k := 26deg + 10deg \cdot \frac{(RP - 75)}{25} + 0.4deg \cdot C_u + 1.6deg \cdot \log\left(\frac{d_{50}}{1mm}\right)$$

$$\phi_k = 40.882 \cdot deg$$

Characteristic angle of internal friction of the backfill material

$$\phi_{k.d} := atan\left(\frac{tan(\phi_k)}{\gamma_n \cdot \gamma_{m.soil}}\right) = 31.189 \cdot deg$$

Design value of friction angle

- **Arching effect**

$$S_{v1} := \frac{0.8 \cdot tan(\phi_{k.d})}{\left(\sqrt{1 + tan(\phi_{k.d})^2} + 0.45 \cdot tan(\phi_{k.d})\right)^2} = 0.233$$

$$\kappa := 2 \cdot S_{v1} \cdot \frac{h_c}{D} = 0.028$$

$$S_{ar} := \frac{1 - e^{-\kappa}}{\kappa} = 0.986$$

- **Tangent modulus of soil material**

$$k_v := \frac{\sin(\phi_k) \cdot (3 - 2 \cdot \sin(\phi_k))}{2 - \sin(\phi_k)} = 0.823$$

$$E_{soil.k} := 0.42 \cdot m_1 \cdot 100 \text{kPa} \cdot k_v \cdot \left[\frac{(1 - \sin(\phi_k)) \cdot \rho_2 \cdot S_{ar} \cdot \left(h_c + \frac{H}{2} \right)}{100 \text{kPa}} \right]^{1 - \beta}$$

$$E_{soil.k} = 40.099 \cdot \text{MPa}$$

Characteristic value of the tangent modulus

$$E_{soil.d} := \frac{E_{soil.k}}{\gamma_n \cdot \gamma_{m.soil}} = 28.041 \cdot \text{MPa}$$

Design value of the tangent modulus

2.2. Cross-sectional parameters

$$r := R_{sp} + \frac{t_s}{2} = 79.7 \cdot \text{mm}$$

$$\alpha := \left| \begin{array}{l} \left(0.759 + 0.01 \cdot \dfrac{t_s}{\text{mm}} \right) \text{ if } type_{steel} = 1 \\[2ex] \left(0.859 + 0.003 \dfrac{t_s}{\text{mm}} \right) \text{ if } type_{steel} = 2 \end{array} \right.$$

Corrugation angle

$$\alpha = 50.42 \cdot \text{deg}$$

$$m_{tt} := \left| \begin{array}{l} (37.5\text{mm} - 1.83 \cdot t_s) \text{ if } type_{steel} = 1 \\ (115.1\text{mm} - 1.273 \cdot t_s) \text{ if } type_{steel} = 2 \end{array} \right.$$

$$m_{tt} = 106.189 \text{ mm}$$

Tangential length

$$e_{sp} := r \cdot \left(1 - \frac{\sin(\alpha)}{\alpha} \right) = 9.896 \text{ mm}$$

Area of steel profile

$$A_s := \frac{4 \cdot \alpha \cdot r \cdot t_s + 2 \cdot m_{tt} \cdot t_s}{c_{sp}} = 9.08 \cdot \frac{\text{mm}^2}{\text{mm}}$$

Moment of inertia

$$I_s := \frac{r^3 \cdot t_s \cdot \left(\alpha + \dfrac{\sin(2 \cdot \alpha)}{2} - \dfrac{2 \cdot \sin(\alpha)^2}{\alpha} \right) + 4 \cdot \alpha \cdot r \cdot t_s \cdot \left(\dfrac{h_{corr}}{2} - e_{sp} \right)^2 + \dfrac{t_s \cdot (m_{tt} \cdot \sin(\alpha))^3}{6 \cdot \sin(\alpha)}}{c_{sp}}$$

$$I_s = 2.105 \times 10^4 \cdot \frac{\text{mm}^4}{\text{mm}}$$

Elastic section modulus

$$W_s := \frac{2 \cdot I_s}{h_{corr} + t_s} = 286.379 \cdot \frac{mm^3}{mm}$$

Plastic section modulus

$$Z_s := \frac{4 \cdot \alpha \cdot r \cdot t_s \cdot \left(\frac{h_{corr}}{2} - e_{sp}\right) + \frac{t_s}{2 \cdot \sin(\alpha)} \cdot \left(m_{tt} \cdot \sin(\alpha)\right)^2}{c_{sp}} = 390.663 \ mm^2$$

$$Z_{s.rein} := 2 \frac{2 \cdot \alpha \cdot r \cdot t_s \cdot \left[\left(h_{corr} + t_s - e_{sp}\right) + e_{sp}\right] + 2t_s \cdot m_{tt} \cdot \frac{\left(h_{corr} + t_s\right)}{2}}{c_{sp}}$$ *With one more reinforcement plate*

In the crown section

$$A_{s.top} := \begin{vmatrix} \left(2 \cdot A_s\right) & \text{if } Reinforce_{top} = \text{"yes"} \\ A_s & \text{otherwise} \end{vmatrix}$$

$$I_{s.top} := \begin{vmatrix} \left[2 \cdot \left[I_s + A_s \cdot \left(\frac{h_{corr} + t_s}{2}\right)^2\right]\right] & \text{if } Reinforce_{top} = \text{"yes"} \\ I_s & \text{otherwise} \end{vmatrix}$$

$$W_{s.top} := \begin{vmatrix} \frac{I_{s.top}}{h_{corr} + t_s} & \text{if } Reinforce_{top} = \text{"yes"} \\ W_s & \text{otherwise} \end{vmatrix}$$

$$Z_{s.top} := \begin{vmatrix} Z_{s.rein} & \text{if } Reinforce_{top} = \text{"yes"} \\ Z_s & \text{otherwise} \end{vmatrix}$$

In the corner section

$$A_{s.cor} := \begin{vmatrix} \left(2 \cdot A_s\right) & \text{if } Reinforce_{cor} = \text{"yes"} \\ A_s & \text{otherwise} \end{vmatrix}$$

$$I_{s.cor} := \begin{vmatrix} \left[2 \cdot \left[I_s + A_s \cdot \left(\frac{h_{corr} + t_s}{2}\right)^2\right]\right] & \text{if } Reinforce_{cor} = \text{"yes"} \\ I_s & \text{otherwise} \end{vmatrix}$$

$$W_{s.cor} := \begin{vmatrix} \frac{I_{s.cor}}{h_{corr} + t_s} & \text{if } Reinforce_{cor} = \text{"yes"} \\ W_s & \text{otherwise} \end{vmatrix}$$

$$Z_{s.cor} := \begin{vmatrix} Z_{s.rein} & \text{if } Reinforce_{cor} = \text{"yes"} \\ Z_s & \text{otherwise} \end{vmatrix}$$

- **Summary of chosen cross-section properties**

$$A_s = 9.08 \cdot \frac{mm^2}{mm} \qquad I_s = 2.105 \times 10^4 \cdot \frac{mm^4}{mm}$$

$$W_s = 286.379 \cdot \frac{mm^3}{mm} \qquad Z_s = 390.663 \cdot \frac{mm^3}{mm}$$

Considering the reinforcement plate in the top section

$$A_{s.top} = 18.16 \cdot \frac{mm^2}{mm} \qquad I_{s.top} = 1.402 \times 10^5 \cdot \frac{mm^4}{mm}$$

$$W_{s.top} = 953.77 \cdot \frac{mm^3}{mm} \qquad Z_{s.top} = 1.335 \times 10^3 \cdot \frac{mm^3}{mm}$$

Considering the reinforcement plate in the corner section

$$A_{s.cor} = 18.16 \cdot \frac{mm^2}{mm} \qquad I_{s.cor} = 1.402 \times 10^5 \cdot \frac{mm^4}{mm}$$

$$W_{s.cor} = 953.77 \cdot \frac{mm^3}{mm} \qquad Z_{s.cor} = 1.335 \times 10^3 \cdot \frac{mm^3}{mm}$$

2.3. Relative stiffness between the culvert and the surrounding soil

$$Stiff_{soil} := E_{soil.d} \cdot D^3 = 5.18 \times 10^{10} \, J$$

$$Stiff_{steel} := E_s \cdot I_s = 4.42 \times 10^6 \, J$$

$$\lambda_f := \frac{Stiff_{soil}}{Stiff_{steel}} = 11718.7 \qquad \qquad \textit{The main limitation of stiffness number is:}$$
$$\textit{100} < \lambda_f < \textit{100,000}$$

2.4. Reduction of the effective height of soil cover

$$h_{c.red} := h_c - 0.015 \cdot D = 565.95 \, mm$$

2.5. Dynamic amplification factor

If loads from Swedish bridge code Bro 2004 are applied, a reduction is introduced provided that the cover depth is high.

$$r_d := \begin{array}{|ll} 1 & \text{if } h_{c.red} \le 2m \\ \left(1.1 - 0.05 \cdot \dfrac{h_{c.red}}{m}\right) & \text{if } 2m < h_{c.red} \le 6m \\ 0.8 & \text{if } 6m < h_{c.red} \end{array}$$

$$r_d = 1$$

For loads from Eurocode, the consideration about reduction factor is not needed.

2.6. Determination of normal forces

- **Normal force due to the surrounding soil**

$$N_{surr} := 0.2 \frac{H}{D} \cdot \rho_1 \cdot D^2 = 134.603 \cdot \frac{kN}{m}$$ *When the backfilling reaches the crown level*

$$N_{cover} := S_{ar} \cdot \left(0.9 \cdot \frac{h_{c.red}}{D} - 0.5 \cdot \frac{h_{c.red}}{D} \cdot \frac{H}{D}\right) \cdot \rho_{cv} \cdot D^2$$ *Due to the soil cover only*

$$N_{cover} = 107.818 \cdot \frac{kN}{m}$$

- **Normal force due to live traffic loads**

Since the distributed live load q in the equation below is taken into consideration in the calculation of equivalent line load with the Boussinesq method, so

$$q := 0 \frac{kN}{m}$$

$$N_t := \begin{array}{|ll} \left[p_{traffic} + \left(\dfrac{D}{2}\right) \cdot q\right] & \text{if } \dfrac{h_{c.red}}{D} \le 0.25 \\ \left[\left(1.25 - \dfrac{h_{c.red}}{D}\right) \cdot p_{traffic} + \left(\dfrac{D}{2}\right) \cdot q\right] & \text{if } 0.25 < \dfrac{h_{c.red}}{D} \le 0.75 \\ \left[0.5 \cdot p_{traffic} + \left(\dfrac{D}{2}\right) \cdot q\right] & \text{otherwise} \end{array}$$

$$N_t = 162.5 \cdot \frac{kN}{m}$$

$$N_{t.fatigue} := \begin{array}{|ll} \left[p_{traffic.fatigue} + \left(\dfrac{D}{2}\right) \cdot q\right] & \text{if } \dfrac{h_{c.red}}{D} \le 0.25 \\ \left[\left(1.25 - \dfrac{h_{c.red}}{D}\right) \cdot p_{traffic.fatigue} + \left(\dfrac{D}{2}\right) \cdot q\right] & \text{if } 0.25 < \dfrac{h_{c.red}}{D} \le 0.75 \\ \left[0.5 \cdot p_{traffic.fatigue} + \left(\dfrac{D}{2}\right) \cdot q\right] & \text{otherwise} \end{array}$$

$$N_{t.fatigue} = 57.1 \cdot \frac{kN}{m}$$

2.7. Determination of bending moments

- **Bending moment due to the surrounding soil**

$$f_1 := \begin{vmatrix} \left[0.67 + 0.87\left(\dfrac{H}{D} - 0.2 \right) \right] & \text{if } 0.2 < \dfrac{H}{D} \le 0.35 \\[2mm] \left[0.8 + 1.33\cdot\left(\dfrac{H}{D} - 0.35 \right) \right] & \text{if } 0.35 < \dfrac{H}{D} \le 0.5 \\[2mm] \left(2\cdot\dfrac{H}{D} \right) & \text{if } 0.5 < \dfrac{H}{D} \le 0.6 \end{vmatrix}$$

$$f_1 = 0.691$$

$$f_{2.surr} := \begin{vmatrix} \left(0.0046 - 0.001\cdot\log\left(\lambda_f \right) \right) & \text{if } \lambda_f \le 5000 \\[2mm] 0.0009 & \text{otherwise} \end{vmatrix}$$

$$f_{2.surr} = 9 \times 10^{-4}$$

$$f_3 := 6.67\cdot\frac{H}{D} - 1.33 = 0.162$$

$$M_{s.surr} := -\rho_1 \cdot f_1 \cdot f_3 \cdot f_{2.surr} \cdot D^3 = -3.721 \cdot \frac{kN\cdot m}{m}$$

When the backfilling reaches the crown level

$$f_{2.cover} := \begin{vmatrix} \left(0.018 - 0.004\cdot\log\left(\lambda_f \right) \right) & \text{if } \lambda_f \le 5000 \\[2mm] 0.0032 & \text{otherwise} \end{vmatrix}$$

$$f_{2.cover} = 0.003$$

$$M_{s.cover} := S_{ar}\cdot\rho_{cv}\cdot\frac{h_{c.red}}{D}\cdot\left(\frac{R_t}{R_s} \right)^{0.75}\cdot f_1 \cdot f_{2.cover} \cdot D^3$$

$$M_{s.cover} = 22.787 \cdot \frac{kN\cdot m}{m}$$

Moment value due to soil cover only

- **Bending moment due to live traffic**

$$f_{4'} := 0.65\cdot\left(1 - 0.2\log\left(\lambda_f \right) \right) = 0.121$$

$$f_{4''} := \begin{vmatrix} \left[0.12\cdot\left(1 - 0.15\cdot\log\left(\lambda_f \right) \right) \right] & \text{if } \lambda_f \le 100000 \\[2mm] 0.03 & \text{otherwise} \end{vmatrix}$$

$$f_{4''} = 0.047$$

$$f_{4'''} := 4\cdot 0.01^{\left(\frac{h_{c.red}}{D} \right)} + 0.4 = 3.635$$

$$\text{check} := \begin{array}{|ll} \text{"OK"} & \text{if } f_4 \cdot f_{4'''} < 1 \\ \text{"ERROR"} & \text{otherwise} \end{array}$$

$$\text{check} = \text{"OK"}$$

$$f_{4.IV} := \left(\frac{R_t}{R_s}\right)^{0.25} = 1.831$$

Moment value due to traffic only

$$M_t := f_4 \cdot f_{4''} \cdot f_{4'''} \cdot f_{4.IV} \cdot D \cdot p_{traffic} + S_{ar} \cdot \left(\frac{R_t}{R_s}\right)^{0.75} \cdot f_1 \cdot f_{2.cover} \cdot q \cdot D^2 = 75.12 \cdot \frac{kN \cdot m}{m}$$

$$M_{t.fatigue} := f_4 \cdot f_{4''} \cdot f_{4'''} \cdot f_{4.IV} \cdot D \cdot p_{traffic.fatigue} + S_{ar} \cdot \left(\frac{R_t}{R_s}\right)^{0.75} \cdot f_1 \cdot f_{2.cover} \cdot q \cdot D^2 = 26.396 \cdot \frac{kN \cdot m}{m}$$

3. Design value of normal forces and bending moments

3.1. Normal forces

Regarding normal forces, the loads due to both the soil and the live traffic are unfavorable.

- **Scenario 1: Backfilling reaches the crown level**

The load due to surrounding soil is considered as a live load in this stage.

$$N_{d.SLS.1} := \max(\gamma_{Q.s}) \cdot N_{surr} = 134.603 \cdot \frac{kN}{m}$$

- **Scenario 2: Backfilling completed**

SLS

$$N_{d.SLS.2} := \max(\gamma_{G.s}) \cdot (N_{surr} + N_{cover}) + \max(\gamma_{Q.s}) \cdot N_t$$

$$N_{d.SLS.2} = 404.922 \cdot \frac{kN}{m}$$

ULS

$$N_{d.ULS.2} := \max(\gamma_{G.u}) \cdot (N_{surr} + N_{cover}) + \max(\gamma_{Q.u}) \cdot N_t$$

$$N_{d.ULS.2} = 546.644 \cdot \frac{kN}{m}$$

3.2. Bending moment

Definition:
Negative bending moments at the crown are due to surrounding soil till crown level;
Positive bending moments at the crown are due to cover soil and live traffic load.

Thus, for the calculation of each bending moment, there are two possible load

combinations:
1) when the negative bending moment is dominant
: the load due to **surrounding soil** is **unfavorable**
: the load effects due to **cover soil** and **live traffic** are **favorable**
2) when the positive bending moment is dominant
: the load due to **surrounding soil** is **favorable**
: the load effects due to **cover soil** and **live traffic** are **unfavorable**;

- **Scenario 1: Backfilling reaches the crown level**

The load due to surrounding soil is considered as a live load in SLS:

$$M_{d.SLS.1} := \max(\gamma_{Q.s}) \cdot M_{s.surr} = -3.721 \cdot \frac{kN \cdot m}{m}$$

- **Scenario 2: Backfilling completed**

SLS

$$M_{d.SLS.2} := \begin{bmatrix} \max(\gamma_{G.s}) \cdot M_{s.surr} + \min(\gamma_{G.s}) \cdot M_{s.cover} + \min(\gamma_{Q.s}) \cdot \left(\frac{-M_t}{2}\right) \\ \min(\gamma_{G.s}) \cdot M_{s.surr} + \max(\gamma_{G.s}) \cdot M_{s.cover} + \max(\gamma_{Q.s}) \cdot M_t \end{bmatrix}$$

$$M_{d.SLS.2} = \begin{pmatrix} 19.066 \\ 94.187 \end{pmatrix} \cdot \frac{kN \cdot m}{m} \qquad \textit{Upper: Negative bending moment is dominant} \\ \textit{Lower: Positive bending moment is dominant}$$

ULS

$$M_{d.ULS.2} := \begin{pmatrix} \max(\gamma_{G.u}) \cdot M_{s.surr} + \min(\gamma_{G.u}) \cdot M_{s.cover} + \min(\gamma_{Q.u}) \cdot M_t \\ \min(\gamma_{G.u}) \cdot M_{s.surr} + \max(\gamma_{G.u}) \cdot M_{s.cover} + \max(\gamma_{Q.u}) \cdot M_t \end{pmatrix}$$

$$M_{d.ULS.2} = \begin{pmatrix} 17.764 \\ 128.454 \end{pmatrix} \cdot \frac{kN \cdot m}{m} \qquad \textit{Upper: Negative bending moment is dominant} \\ \textit{Lower: Positive bending moment is dominant}$$

4. Verification of load bearing capacity

4.1. Serviceability limit state capacity checks

- **Stress when the backfill soil reaches the crow level**

Corresponding to the Scenario 1

$$\sigma_{SLS.1} := \frac{N_{d.SLS.1}}{A_{s.top}} + \frac{|M_{d.SLS.1}|}{W_{s.top}} = 11.314 \cdot MPa$$

$$f_{yd} := \frac{f_{yk}}{\gamma_{m.steel} \cdot \gamma_n} = 260.331 \cdot MPa$$

$$check_{1.stress.SLS} := \begin{vmatrix} \text{"OK!"} & \text{if } |\sigma_{SLS.1}| \leq f_{yd} \\ \text{"NOT OK!"} & \text{otherwise} \end{vmatrix}$$

$check_{1.stress.SLS} = \text{"OK!"}$

$factor_{1.stress.SLS} := \dfrac{\sigma_{SLS.1}}{f_{yd}} = 0.043$

- **Stress when the backfilling process is complete**

Corresponding to the Scenario 2

$$\sigma_{SLS.2} := \begin{pmatrix} \dfrac{N_{d.SLS.2}}{A_{s.top}} + \dfrac{\left|M_{d.SLS.2_0}\right|}{W_{s.top}} \\ \dfrac{N_{d.SLS.2}}{A_{s.top}} + \dfrac{\left|M_{d.SLS.2_1}\right|}{W_{s.top}} \end{pmatrix}$$

$$\sigma_{SLS.2} = \begin{pmatrix} 42.287 \\ 121.049 \end{pmatrix} \cdot MPa \qquad \begin{array}{l} \textit{Upper: Negative bending moment is dominant} \\ \textit{Lower: Positive bending moment is dominant} \end{array}$$

$\sigma_{SLS.max} := \max\left(\sigma_{SLS.2}\right)$

$\sigma_{SLS.max} = 121.049 \cdot MPa$

$$check_{2.stress.SLS} := \begin{vmatrix} \text{"OK!"} & \text{if } \sigma_{SLS.max} \le f_{yd} \\ \text{"NOT OK!"} & \text{otherwise} \end{vmatrix}$$

$check_{2.stress.SLS} = \text{"OK!"}$

$factor_{2.stress.SLS} := \dfrac{\sigma_{SLS.max}}{f_{yd}} = 0.465$

4.2. Ultimate limit state capacity checks

4.2.1. Local buckling

According to Appendix 1 in the Handbook, the chosen corrugated profile must be checked regarding the risk of local buckling.

$M_u := Z_s \cdot \dfrac{f_{yk}}{\gamma_{M1}} = 123.059 \cdot \dfrac{kN \cdot m}{m}$ *Plastic moment capacity*

$M_{ucr} := \left(1.429 - 0.156 \cdot \ln\left(\dfrac{m_{tt}}{t_s} \cdot \sqrt{\dfrac{f_{yk}}{227MPa}}\right)\right) \cdot M_u = 120.503 \cdot kN \cdot \dfrac{m}{m}$

$Risk_{of.local.buckling} := \dfrac{M_{ucr}}{M_u} = 0.979$

$$check_{3.local.buckling} := \begin{vmatrix} \text{"No risk of local buckling"} & \text{if } Risk_{of.local.buckling} \ge 1 \\ \text{"Risk of local buckling exists"} & \text{otherwise} \end{vmatrix}$$

$\text{check}_{3.\text{local.buckling}}$ = "Risk of local buckling exists"

$\text{factor}_{3.\text{local.buckling}} := \min\left(1, \text{Risk}_{\text{of.local.buckling}}\right)$

$\text{factor}_{3.\text{local.buckling}} = 0.979$ *This factor will be used to reduce the plastic moment capacity if risk of local buckling exists.*

▲

4.2.2. Check for the plastic hinge in the crown of the culvert

▼ According to Section 5.3 in Handbook, the check against flexural buckling of the upper part of the pipe capacity is adapted based on EN 1993-1-1.
The section properties of the plates used for the culverts can be assumed in cross-section class 1 or 2. Thus, reduciton due to local buckling can be omitted.

Two conditions to be verified:

- **Check the maximum loaded section**

$$\frac{N_{Ed}}{\left(\dfrac{\chi_y \cdot f_{yk} \cdot A_s}{\gamma_{M1}}\right)} + k_{yy} \cdot \frac{M_{y.Ed}}{\left(\dfrac{f_{yk} \cdot Z_s}{\gamma_{M1}}\right)} \le 1.0$$

When $M_{z.Ed} := 0$ $\Delta M_{z.Ed} := M_{z.Ed} = 0$

The plate is presumed not to deflect alony longitudinal direction (z-axis)

     $\chi_{LT} := 1.0$ $\chi_Z := 1.0$

Design forces and moments

     $N_{Ed} := N_{d.ULS.2}$ *Corresponding to the ULS in Scenario 2*

     $N_{Ed} = 546.644 \cdot \dfrac{kN}{m}$

     $M_{y.Ed} := \max\left(\left|M_{d.ULS.2_0}\right|, \left|M_{d.ULS.2_1}\right|\right)$ *The worst load combination case in Scenario 2*

     $M_{y.Ed} = 128.454 \cdot \dfrac{kN \cdot m}{m}$

N_{cr} for the crown section   *According to Appendix 5 in Handbook*

     $K := \dfrac{h_c}{R_t} = 0.066$

     $\xi := \min\left(\sqrt{K}, 1\right) = 0.256$

$$\eta_j := 1 - \left(\frac{1}{1+K}\right)^2 = 0.119$$

$$\mu := \left[1.22 + 1.95 \cdot \left(\frac{E_s \cdot I_{s.top}}{\eta_j \cdot E_{soil.d} \cdot R_t^3}\right)^{0.25}\right]^2 \cdot \frac{1}{\sqrt{\eta_j}} = 8.968$$

$$N_{cr.el} := \frac{3\xi}{\mu} \cdot \sqrt{\frac{E_{soil.d} \cdot E_s \cdot I_{s.top}}{R_t}} = 728.257 \cdot \frac{kN}{m}$$

$$N_u := f_{yd} \cdot A_{s.top} = 4.728 \times 10^3 \cdot \frac{kN}{m}$$

$$\omega := \begin{vmatrix} \left(\dfrac{N_{cr.el}}{N_u}\right) & \text{if } \dfrac{N_{cr.el}}{N_u} \leq 0.5 \\[2em] \left(1 - 0.25 \dfrac{N_u}{N_{cr.el}}\right) & \text{otherwise} \end{vmatrix}$$

$$\omega = 0.154$$

$$N_{cr} := \omega \cdot N_u = 728.257 \cdot \frac{kN}{m}$$

Reduction factor for flexuaral buckling -- χ_y

   The relative slenderness

$$\lambda_{buk} := \sqrt{\frac{A_{s.top} \cdot f_{yk}}{N_{cr}}} = 2.803$$

According to EN 1993-1-1, section 6.3.1

   Imperfection factor α_{bu}

$$\alpha_{bu} := 0.49$$

$$\phi := 0.5 \cdot \left[1 + \alpha_{bu} \cdot \left(\lambda_{buk} - 0.2\right) + \lambda_{buk}^2\right] = 5.065$$

$$\chi_y := \min\left(1, \frac{1}{\phi + \sqrt{\phi^2 - \lambda_{buk}^2}}\right)$$

$$\chi_y = 0.108$$

Evaluation of ineraction factor -- k_{yy}

According to Table A.1 & A.2 in Appendix A in EN 1993-1-1 and recommendation given in Handbook in Section 5.3

$$N_{cr.y} := N_{cr.el} = 728.257 \cdot \frac{kN}{m}$$

Buckling curve C, EN 1993-1-1 6.3.1

Maximum theoretical deflection according to Appendix 3 in Handbook

$$\delta_{max} := 0.013 \cdot \frac{\rho_1 \cdot D^2}{E_{soil.k}} \cdot \left(\frac{H}{D}\right)^{2.8} \cdot \lambda_f^{\left(0.56 - 0.2 \cdot \ln\left(\frac{H}{D}\right)\right)} = 46.28 \ mm$$

Equivalent uniform moment factor, Table A.2

$$C_{my.0} := 1 + \left(\frac{\pi^2 \cdot E_s \cdot I_{s.top} \cdot |\delta_{max}|}{D^2 \cdot |M_{y.Ed}|} - 1\right) \cdot \frac{N_{Ed}}{N_{cr.y}} = 0.771$$

$$C_{my} := |C_{my.0}| = 0.771$$

$$w_y := \min\left(1.5, \frac{Z_{s.top}}{W_{s.top}}\right)$$

$$w_y = 1.399$$

$$n_{pl} := \frac{N_{Ed}}{\left(\frac{f_{yk} \cdot A_{s.top}}{\gamma_{M1}}\right)} = 0.096$$

$$C_{yy} := 1 + \left(w_y - 1\right) \cdot \left[2 - \frac{1.6}{w_y} \cdot C_{my}^2 \cdot \lambda_{buk} \cdot \left(1 + \lambda_{buk}\right)\right] \cdot n_{pl}$$

$$C_{yy} := \max\left(C_{yy}, \frac{W_{s.top}}{Z_{s.top}}\right) = 0.8$$

$$k_{yy} := \frac{C_{my}}{\left(1 - \chi_y \cdot \frac{N_{Ed}}{N_{cr.y}}\right) \cdot C_{yy}} = 1.05$$

Check the condition

$$cond_1 := \frac{N_{Ed}}{\left(\frac{\chi_y \cdot f_{yk} \cdot A_{s.top}}{\gamma_{M1}}\right)} + k_{yy} \cdot \frac{M_{y.Ed}}{\left(\frac{Z_{s.top} \cdot f_{yk} \cdot factor_{3.local.buckling}}{\gamma_{M1}}\right)} = 1.215$$

$$check_{4.upper.part.pipe} := \begin{vmatrix} \text{"OK!"} & \text{if } cond_1 \leq 1 \\ \text{"NOT OK"} & \text{otherwise} \end{vmatrix}$$

$$check_{4.upper.part.pipe} = \text{"NOT OK"}$$

$$factor_{4.upper.part.pipe} := cond_1 = 1.215$$

- **Check the capacity against the maximum normal force when M.d.u = 0**

Condition to be verified:
$$\left[\frac{N_{d.u}}{\omega \cdot \left(f_{yd} \cdot A_{s.top}\right)}\right]^{\alpha_c} \le 1$$

$$\eta := \frac{Z_{s.top}}{W_{s.top}} = 1.399$$

$$\alpha_c := \max\left(0.8, \eta^2 \cdot \omega\right) = 0.8$$

$$N_{d.u} := N_{d.ULS.2}$$

$$cond_2 := \left[\frac{N_{d.u}}{\omega \cdot \left(f_{yd} \cdot A_{s.top}\right)}\right]^{\alpha_c}$$

$$check_{5.upper.part.pipe} := \begin{array}{ll} \text{"OK!"} & \text{if } cond_2 \le 1 \\ \text{"NOT OK"} & \text{otherwise} \end{array}$$

$$check_{5.upper.part.pipe} = \text{"OK!"}$$

$$factor_{5.upper.part.pipe} := cond_2 = 0.795$$

4.2.3. Check for the plastic hinge in the corner section of the box culvert

Two conditions to be verified:

- **Check the maximum loaded case**

$$\frac{N_{Ed}}{\left(\dfrac{\chi_y \cdot f_{yk} \cdot A_s}{\gamma_{M1}}\right)} + k_{yy} \cdot \frac{M_{y.Ed}}{\left(\dfrac{f_{yk} \cdot Z_s}{\gamma_{M1}}\right)} \le 1.0$$

Design forces and moments

Corresponding to the ULS in Scenario 2

$$N_{Ed.cor} := N_{d.ULS.2}$$

$$N_{Ed.cor} = 546.644 \cdot \frac{kN}{m}$$

$$M_{d.ULS.2.cor} := \begin{bmatrix} \frac{2}{3}\left(\max\left(\gamma_{G.u}\right) \cdot M_{s.surr} + \min\left(\gamma_{G.u}\right) \cdot M_{s.cover}\right) + \frac{1}{3} \min\left(\gamma_{Q.u}\right) \cdot M_t \\ \frac{2}{3}\left(\min\left(\gamma_{G.u}\right) \cdot M_{s.surr} + \max\left(\gamma_{G.u}\right) \cdot M_{s.cover}\right) + \frac{1}{3} \max\left(\gamma_{Q.u}\right) \cdot M_t \end{bmatrix}$$

$$M_{y.Ed.cor} := \max\left(\left|M_{d.ULS.2.cor_0}\right|, \left|M_{d.ULS.2.cor_1}\right|\right)$$

$$M_{y.Ed.cor} = 51.832 \cdot \frac{kN \cdot m}{m}$$

N_{cr} for the corner section

$$K_{cor} := \frac{h_c}{R_s} = 0.738$$

$$\xi_{cor} := \min\left(\sqrt{K_{cor}}, 1\right) = 0.859$$

$$\eta_{j.cor} := 1 - \left(\frac{1}{1 + K_{cor}}\right)^2 = 0.669$$

$$\mu_{cor} := \left[1.22 + 1.95 \cdot \left(\frac{E_s \cdot I_{s.cor}}{\eta_{j.cor} \cdot E_{soil.d} \cdot R_s^3}\right)^{0.25}\right]^2 \cdot \frac{1}{\sqrt{\eta_{j.cor}}} = 13.941$$

$$N_{cr.el.cor} := \frac{3\xi_{cor}}{\mu_{cor}} \cdot \sqrt{\frac{E_{soil.d} \cdot E_s \cdot I_{s.cor}}{R_s}} = 5.271 \times 10^3 \cdot \frac{kN}{m}$$

$$N_{u.cor} := f_{yd} \cdot A_{s.cor} = 4.728 \times 10^3 \cdot \frac{kN}{m}$$

$$\omega_{cor} := \left| \begin{array}{ll} \left(\dfrac{N_{cr.el.cor}}{N_{u.cor}}\right) & \text{if } \dfrac{N_{cr.el.cor}}{N_{u.cor}} \leq 0.5 \\ \\ \left(1 - 0.25 \dfrac{N_{u.cor}}{N_{cr.el.cor}}\right) & \text{otherwise} \end{array} \right.$$

$$\omega_{cor} = 0.776$$

$$N_{cr.cor} := \omega_{cor} \cdot N_{u.cor} = 3.668 \times 10^3 \cdot \frac{kN}{m}$$

Reduction factor for flexuaral buckling -- $\chi_{y.cor}$

According to EN 1993-1-1, section 6.3.1

$$\lambda_{bu.cor} := \sqrt{\frac{A_{s.cor} \cdot f_{yk}}{N_{cr.cor}}} = 1.249 \qquad \textit{The relative slenderness}$$

Imperfection factor α_{bu}

$$\alpha_{bu} := 0.49 \qquad \textit{Buckling curve C, EN 1993-1-1 6.3.1}$$

$$\phi := 0.5 \cdot \left[1 + \alpha_{bu} \cdot \left(\lambda_{buk} - 0.2 \right) + \lambda_{buk}^2 \right] = 1.537$$

$$\chi_{y.cor} := \min \left(1, \frac{1}{\phi + \sqrt{\phi^2 - \lambda_{buk}^2}} \right)$$

$$\chi_{y.cor} = 0.411$$

Evaluation of ineraction factor -- $k_{yy.cor}$

According to Table A.1 & A.2 in Appendix A in EN 1993-1-1 and recommendation given in Handbook in Section 5.3

$$N_{cr.y} := N_{cr.el.cor} = 5.271 \times 10^3 \cdot \frac{kN}{m}$$

Equivalent uniform moment factor, Table A.2

$$C_{my.0} := 1 + \left(\frac{\pi^2 \cdot E_s \cdot I_{s.cor} \cdot |\delta_{max}|}{D^2 \cdot |M_{y.Ed}|} - 1 \right) \cdot \frac{N_{Ed}}{N_{cr.y}} = 0.968$$

$$C_{my} := |C_{my.0}| = 0.968$$

$$w_y := \min \left(1.5, \frac{Z_{s.cor}}{W_{s.cor}} \right)$$

$$w_y = 1.399$$

$$n_{pl} := \frac{N_{Ed.cor}}{\left(\dfrac{f_{yk} \cdot A_{s.cor}}{\gamma_{M1}} \right)} = 0.096$$

$$C_{yy} := 1 + \left(w_y - 1 \right) \cdot \left[2 - \frac{1.6}{w_y} \cdot C_{my}^2 \cdot \lambda_{buk} \cdot \left(1 + \lambda_{buk} \right) \right] \cdot n_{pl} = 0.961$$

$$C_{yy} := \max \left(C_{yy}, \frac{W_{s.cor}}{Z_{s.cor}} \right) = 0.961$$

$$k_{yy.cor} := \frac{C_{my}}{\left(1 - \chi_y \cdot \dfrac{N_{Ed.cor}}{N_{cr.y}} \right) \cdot C_{yy}} = 1.019$$

Check the condition

$$\text{cond}_1 := \frac{N_{Ed.cor}}{\left(\dfrac{\chi_{y.cor} \cdot f_{yk} \cdot A_{s.cor}}{\gamma_{M1}}\right)} + k_{yy.cor} \cdot \frac{M_{y.Ed.cor}}{\left(\dfrac{Z_{s.cor} \cdot f_{yk} \cdot factor_{3.local.buckling}}{\gamma_{M1}}\right)} = 0.361$$

$$\text{check}_{6.corner.part.pipe} := \begin{vmatrix} \text{"OK!"} & \text{if } \text{cond}_1 \leq 1 \\ \text{"NOT OK"} & \text{otherwise} \end{vmatrix}$$

$$\text{check}_{6.corner.part.pipe} = \text{"OK!"}$$

$$\text{factor}_{6.corner.part.pipe} := \text{cond}_1 = 0.361$$

- **Check the capacity against the maximum normal force when M.d.u = 0**

Condition to be verified:
$$\left[\frac{N_{d.u}}{\omega_{cor} \cdot \left(f_{yd} \cdot A_{s.cor}\right)}\right]^{\alpha_c} \leq 1$$

$$\eta_{cor} := \frac{Z_{s.cor}}{W_{s.cor}} = 1.399$$

$$\alpha_c := \max\left(0.8, \eta_{cor}^2 \cdot \omega_{cor}\right) = 1.519$$

$$N_{d.u.cor} := N_{d.ULS.2}$$

$$\text{cond}_2 := \left[\frac{N_{d.u.cor}}{\omega_{cor} \cdot \left(f_{yd} \cdot A_{s.cor}\right)}\right]^{\alpha_c}$$

$$\text{check}_{7.corner.part.pipe} := \begin{vmatrix} \text{"OK!"} & \text{if } \text{cond}_2 \leq 1 \\ \text{"NOT OK"} & \text{otherwise} \end{vmatrix}$$

$$\text{check}_{7.corner.part.pipe} = \text{"OK!"}$$

$$\text{factor}_{7.corner.part.pipe} := \text{cond}_2 = 0.055$$

4.2.4. Check for capacity of the bolt connection

The ULS checks of bolted connections in this section are according to the Section 5.3 of Handbook, which is adapted to Eurocode.

- **Shear capacity**

$$F_{v.Rd} := 0.6 A_{bolt} \cdot \frac{f_{ub}}{1.05 \cdot \gamma_n} = 130.56 \cdot kN \qquad \qquad \textit{Shear resistence per bolt}$$

$$F_{b.Rd} := \frac{2.5 \cdot f_{uk} \cdot d_{bolt} \cdot t_s}{1.05 \cdot \gamma_n} = 142.424 \cdot kN \qquad \qquad \textit{Bearing resistence per bolt}$$

$$N_{d.ULS} := N_{d.ULS.2} = 546.644 \cdot \frac{kN}{m}$$

$$check_{8.bolt.shear} := \begin{array}{|l} \text{"OK!"} \quad \text{if } N_{d.ULS} \leq \min(n_{bolt} \cdot F_{v.Rd}, n_{bolt} \cdot F_{b.Rd}) \\ \text{"Not OK"} \quad \text{otherwise} \end{array}$$

$$check_{8.bolt.shear} = \text{"OK!"}$$

$$factor_{8.bolt.shear} := \frac{N_{d.ULS}}{\min(n_{bolt} \cdot F_{v.Rd}, n_{bolt} \cdot F_{b.Rd})} = 0.279$$

- **Tension capacity**
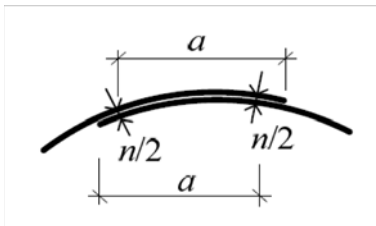
Figure: Notations used when determining the distance between bolts

$$F_{t.Rd} := 0.9 \cdot \frac{f_{ub} \cdot A_{bolt}}{1.05 \cdot \gamma_n} = 195.84 \cdot kN$$

$$M_{d.ULS} := \max(M_{d.ULS.2}) = 128.454 \cdot \frac{kN \cdot m}{m}$$

$$check_{9.bolt.tension} := \begin{array}{|l} \text{"OK!"} \quad \text{if } M_{d.ULS} \leq a_{bolt} \cdot \frac{n_{bolt} \cdot F_{t.Rd}}{2} \\ \text{"Not OK"} \quad \text{otherwise} \end{array}$$

$$check_{9.bolt.tension} = \text{"OK!"}$$

$$factor_{9.bolt.tension} := \frac{M_{d.ULS}}{\left(a_{bolt} \cdot \frac{n_{bolt} \cdot F_{t.Rd}}{2}\right)} = 0.46$$

- **Interaction**

$$F_{st} := 2 \cdot \frac{M_{d.ULS}}{a_{bolt} \cdot n_{bolt}} = 90.143 \cdot kN$$

$$F_{t.Ed} := F_{st}$$

$$F_{sv} := \frac{N_{d.ULS}}{n_{bolt}} = 36.443 \cdot kN$$

$$F_{v.Ed} := F_{sv}$$

$$\text{Interaction} := \frac{F_{v.Ed}}{F_{v.Rd}} + \frac{F_{t.Ed}}{1.4 \cdot F_{t.Rd}} = 0.608$$

$$\text{check}_{10.bolt.interaction} := \begin{vmatrix} \text{"OK!"} & \text{if Interaction} \leq 1 \\ \text{"Not OK"} & \text{otherwise} \end{vmatrix}$$

$$\text{factor}_{10.bolt.interaction} := \text{Interaction} = 0.608$$

4.3. Fatigue checks

4.3.1. Check the fatigue of the plate at the crown seciton

Range values of normal force and bending moment due to LM3

$$\Delta N_{t.f} := N_{t.fatigue} = 57.1 \cdot \frac{kN}{m}$$

$$\Delta M_{t.f} := M_{t.fatigue} \cdot 1.5 = 39.594 \cdot \frac{kN \cdot m}{m}$$

Equation 4.ab, Section 4.4.5 Handbook

Stresses in the plate material due to fatigue loading

According to section 4.4.5 in the handbook, the minimum moment due to traffic load is assumed to be half of the maxium moment bending in opposite direction.

Stress at top fiber

$$\sigma_{top.c} := \frac{-\Delta N_{t.f}}{A_{s.top}} + \frac{-\Delta M_{t.f}}{W_{s.top}} = -44.658 \cdot MPa \qquad \textit{Compression}$$

$$\sigma_{top.t} := \frac{-\Delta N_{t.f}}{A_{s.top}} + \frac{\frac{\Delta M_{t.f}}{2}}{W_{s.top}} = 17.612 \cdot MPa \qquad \textit{Tension}$$

Stress at bottom fiber

$$\sigma_{bott.t} := \frac{-\Delta N_{t.f}}{A_{s.top}} + \frac{\Delta M_{t.f}}{W_{s.top}} = 38.369 \cdot MPa \qquad \textit{Tension}$$

$$\sigma_{bott.c} := \frac{-\Delta N_{t.f}}{A_{s.top}} + \frac{\frac{-\Delta M_{t.f}}{2}}{W_{s.top}} = -23.901 \cdot MPa \qquad \textit{Compression}$$

The effective stress range at the crown section due to LM3

$$\Delta\sigma_{top} := 60\% \cdot |\sigma_{top.c}| + |\sigma_{top.t}| = 44.407 \cdot MPa \qquad \textit{Figure 7.4, Section 7.2.1, EN 1993-1-9}$$

$$\Delta\sigma_{bott} := 60\% \cdot |\sigma_{bott.c}| + |\sigma_{bott.t}| = 52.71 \cdot MPa$$

$$\Delta\sigma_p := \max(\Delta\sigma_{top}, \Delta\sigma_{bott}) = 52.71 \cdot MPa$$

The damage equivalent stress range related to 2 million cycles

$$\Delta\sigma_{E.2.p} := \lambda \ \phi_2 \cdot \Delta\sigma_p \qquad\qquad\qquad\text{*Section 9.4.1, EN 1993-2*}$$

Damage equivalent impact factor

$$\phi_2 := 1$$

Damage equivalence factor

$$\lambda := \lambda_1 \cdot \lambda_2 \cdot \lambda_3 \cdot \lambda_4 \text{ and } \quad \lambda < \lambda_{max}$$

λ_1--factor for damage effect of traffic, according to Figure 9.5 EN 1993-2

$$\lambda_1 := \begin{vmatrix} 2.25 & \text{if } D \le 10m \\ \left[2.25 - 0.7 \cdot \dfrac{(D - 10m)}{70m} \right] & \text{otherwise} \end{vmatrix}$$

$$\lambda_1 = 2.227$$

λ_2--factor for traffic volume according to Table 9.1 EN 1993-2

$$Q_0 := 480kN \qquad\qquad N_0 := 0.5 \cdot 10^6 \qquad\qquad \text{*Recommended in Section 9.5.2*}$$

Average gross weight of lorries in the slow lane

$$Q_{m1} := 300kN$$

Number of heavy vehicles per year per slow lane

$$N_{obs} := 0.5 \cdot 10^6$$

Category 2, table 4.5 (n), EN 1991-2 , which corresponding to 1500<ADT heavy traffic < 6000 in B3.2.1.3, TRAFIKVERKET TRVK BRO 11,Publ nr 2011:085

$$\lambda_2 := \frac{Q_{m1}}{Q_0} \cdot \left(\frac{N_{obs}}{N_0} \right)^{\frac{1}{5}}$$

$$\lambda_2 = 0.625$$

λ_3--factor for design life for the bridge according to Table 9.2 EN 1993-2

Assumption of design life span $t_{Ld} := 80$

$$\lambda_3 := \left(\frac{t_{Ld}}{100}\right)^{\frac{1}{5}} = 0.956$$

λ_4--factor for traffic in the other lanes

$$\lambda_4 := 1 \qquad\qquad \textit{According to the guidance from National Annex,}$$
$$\textit{VVFS 2009, Page 34}$$

$$\lambda_{max} := \begin{vmatrix} 2.5 & \text{if } D < 10m \\ \left(2.5 - 0.5 \cdot \dfrac{D - 10m}{15m}\right) & \text{otherwise} \end{vmatrix}$$

$$\lambda_{max} = 2.424$$

So,

$$\lambda := \min\left(\lambda_1 \cdot \lambda_2 \cdot \lambda_3 \cdot \lambda_4, \lambda_{max}\right) = 1.331$$

$$\Delta\sigma_{E.2.p} := \lambda \cdot \phi_2 \cdot \Delta\sigma_p = 70.173 \cdot MPa$$

Fatigue verification

The section category for the plate

$$\Delta\sigma_{c.p} := 125MPa \qquad\qquad \textit{Detail 5 in Table 8.1, EN 1993-1-9}$$

$$check_{11.fatigue.plate} := \begin{vmatrix} \text{"OK!"} & \text{if } \dfrac{\gamma_{Ff} \cdot \Delta\sigma_{E.2.p}}{\left(\dfrac{\Delta\sigma_{c.p}}{\gamma_{Mf}}\right)} \leq 1 \wedge \Delta\sigma_{E.2.p} \leq 1.5 \cdot f_{yk} \\ \\ \text{"Not OK, Plate Fatigue"} & \text{otherwise} \end{vmatrix}$$

$$check_{11.fatigue.plate} = \text{"OK!"}$$

$$factor_{11.fatigue.plate} := \dfrac{\gamma_{Ff} \cdot \Delta\sigma_{E.2.p}}{\left(\dfrac{\Delta\sigma_{c.p}}{\gamma_{Mf}}\right)} = 0.758$$

4.3.2 Check the fatigue of bolted connections
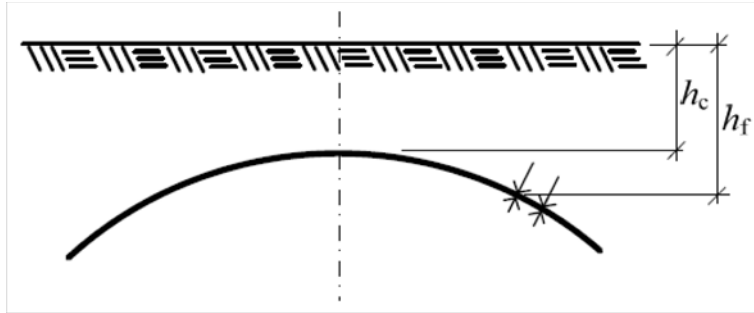
Figure When the joints are situated at positions with greater depth of cover than at the crown, the designing moment due to fatigue can be reduced

Assume the position of bolted connection at depth h_f

$$h_f := \frac{h_c}{0.85}$$

- **Fatigue of bolts**

Shear force on each bolt in the connection due to normal force

$$\Delta F_{d.v} := \frac{\Delta N_{t.f}}{n_{bolt}} = 3.807 \cdot kN$$

Shear stress

$$\Delta \tau_{E.2.b} := \lambda \cdot \phi_2 \cdot \frac{\Delta F_{d.v}}{A_{bolt}} = 16.131 \cdot MPa$$

$$\Delta \tau_c := 100 MPa \qquad \textit{Detail 15, Table 8.1, EN 1993-1-9}$$

Tensile force on each bolt in the connection due to bending moment

$$\Delta F_{d.t} := \frac{\dfrac{2\Delta M_{t.f}}{a_{bolt}} \dfrac{h_c}{h_f}}{n_{bolt}} = 23.618 \cdot kN$$

Tensile stress

$$\Delta \sigma_{E.2.b} := \lambda \cdot \phi_2 \cdot \frac{\Delta F_{d.t}}{A_{bolt}} = 100.084 \cdot MPa$$

$$\Delta \sigma_c := 50 MPa \qquad \textit{Detail 14, Table 8.1, EN 1993-1-9}$$

Fatigue verification

According to section 8 EN 1993-1-9

Shear stress

$$\text{check}_{12.\text{fatigue.shear}} := \begin{vmatrix} \text{"OK!"} & \text{if } \dfrac{\gamma_{Ff} \cdot \Delta\tau_{E.2.b}}{\dfrac{\Delta\tau_c}{\gamma_{Mf}}} \leq 1 \wedge \Delta\tau_{E.2.b} \leq 1.5 \cdot \dfrac{f_{uk}}{\sqrt{3}} \\ \\ \text{"Not OK, Shear stress fatigue in bolts"} & \text{otherwise} \end{vmatrix}$$

$$\text{check}_{12.\text{fatigue.shear}} = \text{"OK!"}$$

$$\text{factor}_{12.\text{fatigue.shear}} := \frac{\gamma_{Ff} \cdot \Delta\tau_{E.2.b}}{\dfrac{\Delta\tau_c}{\gamma_{Mf}}} = 0.218$$

Tensile stress

$$\text{check}_{13.\text{fatigue.tension}} := \begin{vmatrix} \text{"OK!"} & \text{if } \dfrac{\gamma_{Ff} \cdot \Delta\sigma_{E.2.b}}{\dfrac{\Delta\sigma_c}{\gamma_{Mf}}} \leq 1 \wedge \Delta\sigma_{E.2.b} \leq 1.5 \cdot f_{uk} \\ \\ \text{"Not OK, Shear stress fatigue in bolts"} & \text{otherwise} \end{vmatrix}$$

$$\text{check}_{13.\text{fatigue.tension}} = \text{"Not OK, Shear stress fatigue in bolts"}$$

$$\text{factor}_{13.\text{fatigue.tension}} := \frac{\gamma_{Ff} \cdot \Delta\sigma_{E.2.b}}{\dfrac{\Delta\sigma_c}{\gamma_{Mf}}} = 2.702$$

Interaction of shear and tension

$$\text{interaction}_{\text{fatigue}} := \left(\frac{\gamma_{Ff} \cdot \Delta\sigma_{E.2.b}}{\dfrac{\Delta\sigma_c}{\gamma_{Mf}}} \right)^3 + \left(\frac{\gamma_{Ff} \cdot \Delta\tau_{E.2.b}}{\dfrac{\Delta\tau_c}{\gamma_{Mf}}} \right)^5 = 19.733$$

$$\text{check}_{14.\text{fatigue.interaction}} := \begin{vmatrix} \text{"OK!"} & \text{if } \text{interaction}_{\text{fatigue}} \leq 1 \\ \text{"Not OK, Fatigue in bolts"} & \text{otherwise} \end{vmatrix}$$

$$\text{factor}_{14.\text{fatigue.interaction}} := \text{interaction}_{\text{fatigue}} = 19.733$$

4.4. Structural stiffness check

This check ensures that the culvert structure has adequate rigidity during installation and handling processs.

$$\text{stiffness} := \frac{D^2}{E_s \cdot I_s} = 0.034 \cdot \frac{m}{kN}$$

$$\eta_m := 0.2 \frac{m}{kN}$$

According to Section 5.2 Handbook,
0.2 m/kN--for arched and low-rise sections;
0.13 m/kN--for circular sections

$$\text{check}_{15.\text{stiff}} := \begin{vmatrix} \text{"OK!"} & \text{if stiffness} \leq \eta_m \\ \text{"Not OK"} & \text{otherwise} \end{vmatrix}$$

$$\text{check}_{15.\text{stiff}} = \text{"OK!"}$$

$$\text{stiffness} = 0.034 \cdot \frac{m}{kN}$$

◄

5. Summary

5.1. Input data

- **Geometry**

Culvert profile $\quad\quad$ profile = "G: Box Culvert"

Span $\quad\quad$ $D = 12.27 \cdot m$

Soil cover $\quad\quad$ $h_c = 750 \, mm$

- **Corrugated steel plates**

Type of plate $\quad\quad$ $\text{type}_{\text{steel}} = 2$ $\quad$ *Type 1: 200*55; Type 2: SuperCor*

Thickness of plate $\quad\quad$ $t_s = 7 \, mm$ $\quad$ $\text{Reinforce}_{\text{top}} = \text{"yes"}$ $\quad$ $\text{Reinforce}_{\text{cor}} = \text{"yes"}$

- **Bolts**

Diameter of bolts $\quad\quad$ $d_{\text{bolt}} = 20 \, mm$

Bolt class 8.8 $\quad\quad$ $f_{ub} = 800 \cdot MPa$

Number of bolts per meter $\quad\quad$ $n_{\text{bolt}} = 15 \cdot m^{-1}$

- **Loads**

Traffic load $\quad\quad$ $p_{\text{traffic}} = 162.5 \cdot \frac{kN}{m}$

Traffic load-fatigue $\quad\quad$ $p_{\text{traffic.fatigue}} = 57.1 \cdot \frac{kN}{m}$

5.2. Checks

- **Serviceability limit state capacity checks**

$\text{check}_{1.\text{stress.SLS}} = \text{"OK!"}$

Backfill till the crown level

$\text{factor}_{1.\text{stress.SLS}} = 0.043$

$\text{check}_{2.\text{stress.SLS}} = \text{"OK!"}$

After soil cover completed

$\text{factor}_{2.\text{stress.SLS}} = 0.465$

- **Ultimate limit state capacity checks**

Check for the plastic hinge in the upper part of the culvert

$\text{check}_{4.\text{upper.part.pipe}} = \text{"NOT OK"}$

Considering normal force and bending moment

$\text{factor}_{4.\text{upper.part.pipe}} = 1.215$

$\text{check}_{5.\text{upper.part.pipe}} = \text{"OK!"}$

Considering normal force only

$\text{factor}_{5.\text{upper.part.pipe}} = 0.795$

Check for capacity in the corner of the pipe

$\text{check}_{6.\text{corner.part.pipe}} = \text{"OK!"}$

Considering normal force and bending moment

$\text{factor}_{6.\text{corner.part.pipe}} = 0.361$

$\text{check}_{7.\text{corner.part.pipe}} = \text{"OK!"}$

Considering normal force only

$\text{factor}_{7.\text{corner.part.pipe}} = 0.055$

Check for capacity of bolts

$\text{check}_{8.\text{bolt.shear}} = \text{"OK!"}$

Considering shear stress only

$\text{factor}_{8.\text{bolt.shear}} = 0.279$

$\text{check}_{9.\text{bolt.tension}} = \text{"OK!"}$

Considering tensile stress only

$\text{factor}_{9.\text{bolt.tension}} = 0.46$

$\text{check}_{10.\text{bolt.interaction}} = \text{"OK!"}$

Considering interaction of shear and tension

$\text{factor}_{10.\text{bolt.interaction}} = 0.608$

- **fatigue checks**

Check the fatigue of the plate at the crown seciton

$\text{check}_{11.\text{fatigue.plate}} = \text{"OK!"}$

$\text{factor}_{11.\text{fatigue.plate}} = 0.758$

Check the fatigue of bolted connections

$\text{check}_{12.\text{fatigue.shear}}$ = "OK!"

$\text{factor}_{12.\text{fatigue.shear}}$ = 0.218

$\text{check}_{13.\text{fatigue.tension}}$ = "Not OK, Shear stress fatigue in bolts"

$\text{factor}_{13.\text{fatigue.tension}}$ = 2.702

$\text{check}_{14.\text{fatigue.interaction}}$ = "Not OK, Fatigue in bolts"

$\text{factor}_{14.\text{fatigue.interaction}}$ = 19.733

- **Other checks**

Local buckling

$\text{check}_{3.\text{local.buckling}}$ = "Risk of local buckling exists"

$\text{factor}_{3.\text{local.buckling}}$ = 0.979

Structural stiffness check

$\text{check}_{15.\text{stiff}}$ = "OK!"

Appendix B.1 Mathcad Routine for Design of FRP Culverts
-- *Mathcad No.1 Stiffness Calculation and Stresses Analysis*

ORIGIN := 1

Program 1: Stiffness matrices of the designed FRP sandwich panel

▼ Q matrix for each FRP ply

Total stiffness matrix of each lamina with a certain fiber orientation angle

$$
Q(E_{11}, E_{22}, v_{12}, G_{12}, \theta) := \left| \begin{array}{l}
v_{21} \leftarrow \dfrac{E_{22}}{E_{11}} \cdot v_{12} \\[2mm]
Q_{11} \leftarrow \dfrac{E_{11}}{1 - v_{12} \cdot v_{21}} \\[2mm]
Q_{22} \leftarrow \dfrac{E_{22}}{1 - v_{12} \cdot v_{21}} \\[2mm]
Q_{12} \leftarrow \dfrac{v_{12} \cdot E_{22}}{1 - v_{12} \cdot v_{21}} \\[2mm]
Q_{21} \leftarrow \dfrac{v_{21} \cdot E_{11}}{1 - v_{12} \cdot v_{21}} \\[2mm]
Q_{66} \leftarrow G_{12} \\[2mm]
U_1 \leftarrow \dfrac{1}{8} \cdot (3 \cdot Q_{11} + 3 \cdot Q_{22} + 2 \cdot Q_{12} + 4 Q_{66}) \\[2mm]
U_2 \leftarrow \dfrac{1}{2} \cdot (Q_{11} - Q_{22}) \\[2mm]
U_3 \leftarrow \dfrac{1}{8} \cdot (Q_{11} + Q_{22} - 2 \cdot Q_{12} - 4 Q_{66}) \\[2mm]
U_4 \leftarrow \dfrac{1}{8} \cdot (Q_{11} + Q_{22} + 6 \cdot Q_{12} - 4 Q_{66}) \\[2mm]
U_5 \leftarrow \dfrac{1}{2} \cdot (U_1 - U_4) \\[2mm]
\theta \leftarrow \text{stack}(\theta, \text{reverse}(\theta)) \\[2mm]
QQ_{11} \leftarrow U_1 + U_2 \cdot \cos(2 \cdot \theta) + U_3 \cdot \cos(4 \cdot \theta) \\[2mm]
QQ_{12} \leftarrow U_4 - U_3 \cdot \cos(4 \cdot \theta) \\[2mm]
QQ_{22} \leftarrow U_1 - U_2 \cdot \cos(2 \cdot \theta) + U_3 \cdot \cos(4 \cdot \theta) \\[2mm]
QQ_{16} \leftarrow \dfrac{1}{2} \cdot U_2 \cdot \sin(2 \cdot \theta) + U_3 \cdot \sin(4 \cdot \theta)
\end{array} \right.
$$

$$QQ_{26} \leftarrow \frac{1}{2} \cdot U_2 \cdot \sin(2 \cdot \theta) - U_3 \cdot \sin(4 \cdot \theta)$$

$$QQ_{66} \leftarrow U_5 - U_3 \cdot \cos(4 \cdot \theta)$$

$$QQ \leftarrow \begin{pmatrix} QQ_{11} & QQ_{12} & QQ_{16} \\ QQ_{12} & QQ_{22} & QQ_{26} \\ QQ_{16} & QQ_{26} & QQ_{66} \end{pmatrix}$$

▲ Q matrix for each FRP ply

▼ Coordinates of each FRP ply

h_i refers to the distance from the midplane to the top of the ith lamina.

$$h(t, no, d) := \begin{array}{|l} \text{for } i \in 1 .. (no + 1) \\ \qquad h_i \leftarrow \left[\dfrac{-(t \cdot no \cdot 2 + d)}{2} + (i - 1) \cdot t \right] \\ \text{for } i \in (no + 2) .. (2no + 2) \\ \qquad h_i \leftarrow \left[\dfrac{-(t \cdot no \cdot 2 + d)}{2} + d + (i - 2) \cdot t \right] \\ \text{return } h \end{array}$$

▲ Coordinates of each FRP ply

▼ Matrices A B D for the FRP Sandwich

Extensional stiffness matrix for the FRP sandwich (unite: N/m)

$$A\big(E_{11}, E_{22}, \upsilon_{12}, G_{12}, \theta, t, no, d\big) := \begin{array}{|l} \text{for } i \in 1 .. no \\ \qquad ha_i \leftarrow \left[h(t, no, d)_{(i+1)} - h(t, no, d)_i \right] \\ \text{for } i \in (no + 1) .. (2 \cdot no) \\ \qquad ha_i \leftarrow \left[h(t, no, d)_{(i+2)} - h(t, no, d)_{(i+1)} \right] \\ \text{for } i \in 1 .. 3 \\ \qquad \text{for } j \in 1 .. 3 \\ \qquad\qquad A_{i,j} \leftarrow Q\big(E_{11}, E_{22}, \upsilon_{12}, G_{12}, \theta\big)_{i,j} \, ha \\ A \end{array}$$

Coupling stiffness matrix for the FRP sandwich (unit: N)

$$B\left(E_{11}, E_{22}, \upsilon_{12}, G_{12}, \theta, t, no, d\right) := \begin{array}{|l} \text{for } i \in 1 \mathinner{\ldotp\ldotp} no \\ \quad hb_i \leftarrow \left[\left(h(t,no,d)_{i+1}\right)^2 - \left(h(t,no,d)_i\right)^2\right] \\ \text{for } i \in (no+1) \mathinner{\ldotp\ldotp} (2 \cdot no) \\ \quad hb_i \leftarrow \left[\left[h(t,no,d)_{(i+2)}\right]^2 - \left[h(t,no,d)_{(i+1)}\right]^2\right] \\ \text{for } i \in 1 \mathinner{\ldotp\ldotp} 3 \\ \quad \text{for } j \in 1 \mathinner{\ldotp\ldotp} 3 \\ \qquad B_{i,j} \leftarrow \left(Q\left(E_{11}, E_{22}, \upsilon_{12}, G_{12}, \theta\right)\right)_{i,j} hb \cdot \dfrac{1}{2} \\ B \end{array}$$

Bending stiffness matrix for the FRP sandwich (unit: N*m)

$$D\left(E_{11}, E_{22}, \upsilon_{12}, G_{12}, \theta, t, no, d\right) := \begin{array}{|l} \text{for } i \in 1 \mathinner{\ldotp\ldotp} no \\ \quad hd_i \leftarrow \left[\left(h(t,no,d)_{i+1}\right)^3 - \left(h(t,no,d)_i\right)^3\right] \\ \text{for } i \in (no+1) \mathinner{\ldotp\ldotp} (2 \cdot no) \\ \quad hd_i \leftarrow \left[\left[h(t,no,d)_{(i+2)}\right]^3 - \left[h(t,no,d)_{(i+1)}\right]^3\right] \\ \text{for } i \in 1 \mathinner{\ldotp\ldotp} 3 \\ \quad \text{for } j \in 1 \mathinner{\ldotp\ldotp} 3 \\ \qquad D_{i,j} \leftarrow \left(Q\left(E_{11}, E_{22}, \upsilon_{12}, G_{12}, \theta\right)\right)_{i,j} hd \cdot \dfrac{1}{3} \\ D \end{array}$$

▲ Matrices A B D for the FRP Sandwich

▼ Stiffness parameters derived from matrices

The equivalent membrane elastic constants

$$EA_{xx}\left(E_{11}, E_{22}, \upsilon_{12}, G_{12}, \theta, t, no, d\right) := \frac{1}{\left(A\left(E_{11}, E_{22}, \upsilon_{12}, G_{12}, \theta, t, no, d\right)^{-1}\right)_{1,1}}$$

$$EA_{yy}\left(E_{11}, E_{22}, \upsilon_{12}, G_{12}, \theta, t, no, d\right) := \frac{1}{\left(A\left(E_{11}, E_{22}, \upsilon_{12}, G_{12}, \theta, t, no, d\right)^{-1}\right)_{2,2}}$$

$$EA_{xy}\left(E_{11}, E_{22}, \upsilon_{12}, G_{12}, \theta, t, no, d\right) := \frac{1}{\left(A\left(E_{11}, E_{22}, \upsilon_{12}, G_{12}, \theta, t, no, d\right)^{-1}\right)_{3,3}}$$

The equivalent bending elastic constants

$$EI_{xx}\left(E_{11}, E_{22}, \upsilon_{12}, G_{12}, \theta, t, no, d\right) := \dfrac{1}{\left(D\left(E_{11}, E_{22}, \upsilon_{12}, G_{12}, \theta, t, no, d\right)^{-1}\right)_{1,1}}$$

$$EI_{yy}\left(E_{11}, E_{22}, \upsilon_{12}, G_{12}, \theta, t, no, d\right) := \dfrac{1}{\left(D\left(E_{11}, E_{22}, \upsilon_{12}, G_{12}, \theta, t, no, d\right)^{-1}\right)_{2,2}}$$

$$EI_{xy}\left(E_{11}, E_{22}, \upsilon_{12}, G_{12}, \theta, t, no, d\right) := \dfrac{1}{\left(D\left(E_{11}, E_{22}, \upsilon_{12}, G_{12}, \theta, t, no, d\right)^{-1}\right)_{3,3}}$$

▲ Stiffness parameters derived from matrices

Program 2: Stresses analysis of FRP sandwich panel in each FRP ply

▼ Midplane strains and curvatures due to sectional forces

$$D1\left(E_{11}, E_{22}, \upsilon_{12}, G_{12}, \theta, t, no, d\right) := \begin{array}{|l} D \leftarrow D\left(E_{11}, E_{22}, \upsilon_{12}, G_{12}, \theta, t, no, d\right) \\[4pt] Ainv \leftarrow A\left(E_{11}, E_{22}, \upsilon_{12}, G_{12}, \theta, t, no, d\right)^{-1} \\[4pt] B \leftarrow B\left(E_{11}, E_{22}, \upsilon_{12}, G_{12}, \theta, t, no, d\right) \\[4pt] D1 \leftarrow (D - B \cdot Ainv \cdot B)^{-1} \end{array}$$

$$A1\left(E_{11}, E_{22}, \upsilon_{12}, G_{12}, \theta, t, no, d\right) := \begin{array}{|l} D1 \leftarrow D1\left(E_{11}, E_{22}, \upsilon_{12}, G_{12}, \theta, t, no, d\right) \\[4pt] Ainv \leftarrow A\left(E_{11}, E_{22}, \upsilon_{12}, G_{12}, \theta, t, no, d\right)^{-1} \\[4pt] B \leftarrow B\left(E_{11}, E_{22}, \upsilon_{12}, G_{12}, \theta, t, no, d\right) \\[4pt] A1 \leftarrow Ainv + Ainv \cdot B \cdot D1 \cdot B \cdot Ainv \end{array}$$

$$B1\left(E_{11}, E_{22}, \upsilon_{12}, G_{12}, \theta, t, no, d\right) := \begin{array}{|l} D1 \leftarrow D1\left(E_{11}, E_{22}, \upsilon_{12}, G_{12}, \theta, t, no, d\right) \\[4pt] Ainv \leftarrow A\left(E_{11}, E_{22}, \upsilon_{12}, G_{12}, \theta, t, no, d\right)^{-1} \\[4pt] B \leftarrow B\left(E_{11}, E_{22}, \upsilon_{12}, G_{12}, \theta, t, no, d\right) \\[4pt] B1 \leftarrow -Ainv \cdot B \cdot D1 \end{array}$$

$$C1\left(E_{11}, E_{22}, \upsilon_{12}, G_{12}, \theta, t, no, d\right) := \begin{array}{|l} D1 \leftarrow D1\left(E_{11}, E_{22}, \upsilon_{12}, G_{12}, \theta, t, no, d\right) \\[4pt] Ainv \leftarrow A\left(E_{11}, E_{22}, \upsilon_{12}, G_{12}, \theta, t, no, d\right)^{-1} \\[4pt] B \leftarrow B\left(E_{11}, E_{22}, \upsilon_{12}, G_{12}, \theta, t, no, d\right) \\[4pt] C1 \leftarrow -D1 \cdot B \cdot Ainv \end{array}$$

For a symmetric laminate, [B]=[0], and therefore, [A1]=[A^{-1}], [B1]=[C1]=[0], and [D1]=[D^{-1}]

Midplane strains and curvatures

$$\varepsilon_{mid}(E_{11}, E_{22}, \upsilon_{12}, G_{12}, \theta, t, no, d, NF, M) := \begin{vmatrix} A1 \leftarrow A1(E_{11}, E_{22}, \upsilon_{12}, G_{12}, \theta, t, no, d) \\ B1 \leftarrow B1(E_{11}, E_{22}, \upsilon_{12}, G_{12}, \theta, t, no, d) \\ A1 \cdot NF + B1 \cdot M \end{vmatrix}$$

$$k_{mid}(E_{11}, E_{22}, \upsilon_{12}, G_{12}, \theta, t, no, d, NF, M) := \begin{vmatrix} C1 \leftarrow C1(E_{11}, E_{22}, \upsilon_{12}, G_{12}, \theta, t, no, d) \\ D1 \leftarrow D1(E_{11}, E_{22}, \upsilon_{12}, G_{12}, \theta, t, no, d) \\ C1 \cdot NF + D1 \cdot M \end{vmatrix}$$

▲ Midplane strains and curvatures due to sectional forces

▼ In-plane strains for each FRP ply

Lamina strains and stresses due to applied loads

Distance from the sandwich midplane to the midplane of each lamina

$$z(t, no, d) := \begin{vmatrix} \text{for } i \in 1 .. no \\ \quad z_i \leftarrow \left[\dfrac{-(t \cdot no \cdot 2 + d) - t}{2} + i \cdot t \right] \\ \text{for } i \in (no + 1) .. (2no) \\ \quad z_i \leftarrow \left[\dfrac{-(t \cdot no \cdot 2 + d) - t}{2} + d + i \cdot t \right] \\ \text{return } z \end{vmatrix}$$

$$\varepsilon_{ply}(E_{11}, E_{22}, \upsilon_{12}, G_{12}, \theta, t, no, d, NF, M) := \begin{vmatrix} \varepsilon_{mid} \leftarrow \varepsilon_{mid}(E_{11}, E_{22}, \upsilon_{12}, G_{12}, \theta, t, no, d, NF, M) \\ k_{mid} \leftarrow k_{mid}(E_{11}, E_{22}, \upsilon_{12}, G_{12}, \theta, t, no, d, NF, M) \\ z \leftarrow z(t, no, d) \\ \text{for } i \in 1 .. (2 \cdot no) \\ \quad \varepsilon_i \leftarrow \varepsilon_{mid} + z_i \cdot k_{mid} \\ \text{return } \varepsilon \end{vmatrix}$$

▲ In-plane strains for each FRP ply

▼ In-plane stresses for each FRP ply

Lamina strains and stresses due to applied loads

$$Q_{ply}\left(E_{11}, E_{22}, \upsilon_{12}, G_{12}, \theta, no\right) := \begin{vmatrix} Q \leftarrow Q\left(E_{11}, E_{22}, \upsilon_{12}, G_{12}, \theta\right) \\ \text{for } i \in 1 .. (2 \cdot no) \\ \quad \begin{vmatrix} QQ_i \leftarrow \begin{pmatrix} 0 & 0 & 0 \\ 0 & 0 & 0 \\ 0 & 0 & 0 \end{pmatrix} \\ \text{for } x \in 1 .. 3 \\ \quad \text{for } y \in 1 .. 3 \\ \qquad \left(QQ_i\right)_{x,y} \leftarrow \left(Q_{x,y}\right)_i \end{vmatrix} \\ \text{return } QQ \end{vmatrix}$$

$$\text{stress}\left(E_{11}, E_{22}, \upsilon_{12}, G_{12}, \theta, t, no, d, NF, M\right) := \begin{vmatrix} \varepsilon \leftarrow \varepsilon_{ply}\left(E_{11}, E_{22}, \upsilon_{12}, G_{12}, \theta, t, no, d, NF, M\right) \\ Q \leftarrow Q_{ply}\left(E_{11}, E_{22}, \upsilon_{12}, G_{12}, \theta, no\right) \\ \text{for } i \in 1 .. (2 \cdot no) \\ \quad \text{stress}_i \leftarrow Q_i \cdot \varepsilon_i \\ \text{return stress} \end{vmatrix}$$

🔺 In-plane stresses for each FRP ply

Design Process

Step 1: Choose the materials for the FRP sandwich panel

🔽 Face and Core

Face material   Fiber: E-glass   Matrix: Epoxy   Fiber/Matrix: 45%

$E_{k.11} := 38.6\text{GPa}$ $E_{k.22} := 8.27\text{GPa}$ $G_{k.12} := 4.14\text{GPa}$

$\upsilon_{12} := 0.26$

Strength

$\sigma_{k.11.c} := 610\text{MPa}$ $\sigma_{k.22.c} := 118\text{MPa}$ $\tau_{k.12} := 72\text{MPa}$

$\sigma_{k.11.t} := 1062\text{MPa}$ $\sigma_{k.22.t} := 31\text{MPa}$

Partial factor for FRP laminate

--according to Eurocomp Design Code and Handbook, Section 2.3.3.2

$\gamma_{M1} := 1.5$ Derivation of properties

$$\gamma_{M2} := 1.2$$ Method of manufacture: Resin transfer moulding

$$\gamma_{M3} := 2.5$$ 1.0 for long-term loading in ULS;
2.5 for short-term loading in SLS

$$\gamma_M := \gamma_{M1} \cdot \gamma_{M2} \cdot \gamma_{M3} = 4.5$$

Design value

$$E_{11} := \frac{E_{k.11}}{\gamma_M} \qquad\qquad E_{22} := \frac{E_{k.22}}{\gamma_M} \qquad\qquad G_{12} := \frac{G_{k.12}}{\gamma_M}$$

$$\sigma_{d.11.c} := \frac{\sigma_{k.11.c}}{\gamma_M} \quad \sigma_{d.22.c} := \frac{\sigma_{k.22.c}}{\gamma_M} \quad \tau_{d.12} := \frac{\tau_{k.12}}{\gamma_M}$$

$$\sigma_{d.11.t} := \frac{\sigma_{k.11.t}}{\gamma_M} \quad \sigma_{d.22.t} := \frac{\sigma_{k.22.t}}{\gamma_M}$$

Core Material   Divinycell H 80 from DIAB

▲ Face and Core
___

Step 2: Assume a geometry of the FRP sandwich panel and obtain the bending stiffness

▼ Design the thickness of face and core

Thicknesss of face $t_{face} := 9mm$

$t := 1mm$ Thickness of each ply

$no := \dfrac{t_{face}}{t} = 9$ Number of plies for one laminate face

Fiber orientation for each ply (0 degree in the preliminary design)

$\theta := stack(0deg, 0deg, 0deg, 0deg, 0deg, 0deg, 0deg, 0deg, 0deg)$

$$CheckInput := \begin{vmatrix} \text{"OK"} & \text{if } no = rows(\theta) \\ \text{"Error"} & \text{otherwise} \end{vmatrix}$$

$CheckInput = \text{"OK"}$

Initial bending stiffness

Thickness of core $d := 150mm$

$$EI_{xx}\left(E_{11}, E_{22}, \upsilon_{12}, G_{12}, \theta, t, no, d\right) = 0.977 \cdot 10^6 \frac{N \cdot m^2}{m}$$

Bending stiffness in the top

Thickness of core   d := 400mm

$$EI_{xx}\left(E_{11}, E_{22}, \upsilon_{12}, G_{12}, \theta, t, no, d\right) = 6.458 \cdot 10^6 \frac{N \cdot m^2}{m}$$

Bending stiffness in the corner

Thickness of core   d := 150mm

$$EI_{xx}\left(E_{11}, E_{22}, \upsilon_{12}, G_{12}, \theta, t, no, d\right) = 0.977 \cdot 10^6 \frac{N \cdot m^2}{m}$$

▲ Design the thickness of face and core

Step 3: Input the sectional forces calculated by the SCI method in the SDM (Mathcad No.2) and get the stresses

Crown region   d := 400mm

▼ Sectional forces and stresses due to soil

Normal forces

$$NF := \begin{pmatrix} -327.3 \\ 0 \\ 0 \end{pmatrix} \frac{kN}{m} \qquad \begin{matrix} N.xx \\ N.yy \\ N.xy \end{matrix} \qquad \begin{matrix} \text{Positive--tensile forces} \\ \text{Negative--compressive forces} \end{matrix}$$

Bending moments

$$M := \begin{pmatrix} 27.1 \\ 0 \\ 0 \end{pmatrix} \frac{kN \cdot m}{m} \qquad \begin{matrix} M.xx \\ M.yy \\ M.xy \end{matrix}$$

Top: from 1 to no

$$stress\left(E_{11}, E_{22}, \upsilon_{12}, G_{12}, \theta, t, no, d, NF, M\right)_1 = \begin{pmatrix} -25.688 \\ 0 \\ 0 \end{pmatrix} \cdot MPa$$

Bottom: from (no+1) to (2*no)

$$stress\left(E_{11}, E_{22}, \upsilon_{12}, G_{12}, \theta, t, no, d, NF, M\right)_{18} = \begin{pmatrix} -10.678 \\ 0 \\ 0 \end{pmatrix} \cdot MPa$$

▲ Sectional forces and stresses due to soil

▼ Sectional forces and stresses due to traffic

Normal forces

$$NF := \begin{pmatrix} -219.4 \\ 0 \\ 0 \end{pmatrix} \frac{kN}{m} \qquad \begin{matrix} N.xx \\ N.yy \\ N.xy \end{matrix}$$

Positive value for tensile forces;
Negative value for compressive forces

Bending moments

$$M := \begin{pmatrix} 91.3 \\ 0 \\ 0 \end{pmatrix} \frac{kN \cdot m}{m} \qquad \begin{matrix} M.xx \\ M.yy \\ M.xy \end{matrix}$$

Top: from 1 to no

$$stress\left(E_{11}, E_{22}, \upsilon_{12}, G_{12}, \theta, t, no, d, NF, M\right)_1 = \begin{pmatrix} -37.473 \\ 0 \\ 0 \end{pmatrix} \cdot MPa$$

Bottom: from (no+1) to (2*no)

$$stress\left(E_{11}, E_{22}, \upsilon_{12}, G_{12}, \theta, t, no, d, NF, M\right)_{18} = \begin{pmatrix} 13.095 \\ 0 \\ 0 \end{pmatrix} \cdot MPa$$

▲ Sectional forces and stresses due to traffic

Corner region $\quad d := 150mm$

▼ Sectional forces and stresses due to soil

Normal forces

$$NF := \begin{pmatrix} -219.4 \\ 0 \\ 0 \end{pmatrix} \frac{kN}{m} \qquad \begin{matrix} N.xx \\ N.yy \\ N.xy \end{matrix}$$

Positive--tensile forces
Negative--compressive forces

Bending moments

$$M := \begin{pmatrix} 11.8 \\ 0 \\ 0 \end{pmatrix} \frac{kN \cdot m}{m} \qquad \begin{matrix} M.xx \\ M.yy \\ M.xy \end{matrix}$$

Top: from 1 to no

$$\text{stress}\left(E_{11}, E_{22}, \upsilon_{12}, G_{12}, \theta, t, no, d, NF, M\right)_1 = \begin{pmatrix} -20.841 \\ 0 \\ 0 \end{pmatrix} \cdot MPa$$

Bottom: from (no+1) to (2*no)

$$\text{stress}\left(E_{11}, E_{22}, \upsilon_{12}, G_{12}, \theta, t, no, d, NF, M\right)_{18} = \begin{pmatrix} -3.537 \\ 0 \\ 0 \end{pmatrix} \cdot MPa$$

🔺 Sectional forces and stresses due to soil

🔻 Sectional forces and stresses due to traffic

Normal forces

$$NF := \begin{pmatrix} -219.4 \\ 0 \\ 0 \end{pmatrix} \frac{kN}{m} \qquad \begin{matrix} N.xx \\ N.yy \\ N.xy \end{matrix}$$

Positive value for tensile forces;
Negative value for compressive forces

Bending moments

$$M := \begin{pmatrix} 30.4 \\ 0 \\ 0 \end{pmatrix} \frac{kN \cdot m}{m} \qquad \begin{matrix} M.xx \\ M.yy \\ M.xy \end{matrix}$$

Top: from 1 to no

$$\text{stress}\left(E_{11}, E_{22}, \upsilon_{12}, G_{12}, \theta, t, no, d, NF, M\right)_1 = \begin{pmatrix} -34.478 \\ 0 \\ 0 \end{pmatrix} \cdot MPa$$

Bottom: from (no+1) to (2*no)

$$\text{stress}\left(E_{11}, E_{22}, \upsilon_{12}, G_{12}, \theta, t, no, d, NF, M\right)_{18} = \begin{pmatrix} 10.1 \\ 0 \\ 0 \end{pmatrix} \cdot MPa$$

🔺 Sectional forces and stresses due to traffic

Appendix B.2 Mathcad Routine for Design of FRP Culverts
-- Mathcad No.2 Calculation of Sectional forces

Based on the Soil Culvert Interaction (SCI) thoery in the Swedish design method developed by Pettersson & Sundquist

$\text{ORIGIN} := 1$

1. Input data

1.1. Stiffness of the designed FRP sandwhich panel

$EI_{FRP} := 3.762 \times 10^6 \, J$ *It refers to the stiffness in the span direction*

1.2. Geometry of the culvert bridge

Culvert profile: *Possible profiles are A, B, C, ..., G, according to Handbook*

$\text{profile} := \text{"G: Box Culvert"}$ *SC-54B, Viacon*

$\text{case} := 14$

$D := 12.270 \, m$ *Span*

$H := 2.745 \, m$ *Height*

$R_t := 11.430 \, m$ *Top radius*

$R_s := 1.016 \, m$ *Side/Corner radius*

Height of the soil cover

$h_c := 750 \, mm$

1.3. Parameters of the backfilling soil

Type of the backfilling soil:

Base course material   *Parameters of soil taken from Appendix 2 of Handbook*

$\rho_{opt} := 20.6 \, \dfrac{kN}{m^3}$ *Optium density*

$RP := 97$ *Degree of compaction (%), standard proctor method*

$\rho_{cv} := \dfrac{RP}{100} \cdot \rho_{opt}$ $\rho_{cv} = 19.982 \cdot \dfrac{kN}{m^3}$

$\rho_1 := \rho_{cv}$ *Density of the soil up to the height of the crown*

$\rho_2 := \rho_{cv}$ *Mean density of the soil material with the region (hc+H/2)*

Partical size distribution

$d_{50} := 20mm$ $d_{60} := 30mm$ $d_{10} := 3mm$

$\nu := 0.29$ *Poisson Ratio*

1.4. Partial coefficients

$\gamma_n := 1.1$

The safety class recommended for structures with a span less than 15 meters is 2, according to the natation section in Handbook.

Partial coefficients for material strength

$\gamma_{m.soil} := 1.3$ *According to the Handbook 2010, Appendix 2, Table B2.1*

$\gamma_{M1} := 1.0$ *According to the Handbook 2010, Section 5.3 (3)*

$\gamma_{Mf} := 1.35$ *For fatigue strength: Safe life, high consequence, Table 3.1, EN 1993-1-9*

Partial coefficients for loads

Ultimate limit state: *Table A 2.4(B), EN 1990*

$\gamma_{G.u} := \begin{pmatrix} 1.35 \\ 1.00 \end{pmatrix}$ $\gamma_{Q.u} := \begin{pmatrix} 1.35 \\ 0 \end{pmatrix}$ *Upper: Unfavorable*
Lower: Favorable

Serviceability limit state: *Table A 2.6, EN 1990*

$\gamma_{G.s} := \begin{pmatrix} 1.00 \\ 1.00 \end{pmatrix}$ $\gamma_{Q.s} := \begin{pmatrix} 1.00 \\ 0 \end{pmatrix}$ *Upper: Unfavorable*
Lower: Favorable

Fatigue limit state:

$\gamma_{Ff} := 1.0$

Section 9.3 (1), EN 1993-2

1.6. Live traffic load

Four load group types are considered:
(1) LM1 from EN 1991-2;
(2) LM2 from EN 1991-2;
(3) LM3 from EN 1991-2
(4) Typfordon from TRVK BRO 11, Publ nr 2011:085

The characteristic value of the equivalent line load for each of these 4 load types is obtained with the boussinesq method according to the Handbook, considering the most unfavorable loading position. The results of the equivalent line loads with different height of soil cover are shown in the figure below.

Figure* The equivalent line load on the culvert crown section at different depth h_c

Note: The Calculation and results of the equivalent line load are provided by the supervisor from the consultant company WSP in Gothenburg

The equivalent traffic line load for SLS and ULS

$$p_{traffic} := \begin{Vmatrix} \left(213.7 \frac{kN}{m}\right) & \text{if } h_c = 0.5m \\ \left(162.5 \frac{kN}{m}\right) & \text{if } h_c = 0.75m \\ \left(129.2 \frac{kN}{m}\right) & \text{if } h_c = 1m \\ \left(125.3 \frac{kN}{m}\right) & \text{if } h_c = 3m \\ \text{"Error"} & \text{otherwise} \end{Vmatrix}$$

$$p_{traffic} = 162.5 \cdot \frac{kN}{m}$$

The equivalent traffic line load due to LM3 for fatigue

$$p_{traffic.fatigue} := \begin{Vmatrix} \left(72.1\,\dfrac{kN}{m}\right) & \text{if } h_c = 0.5m \\[2mm] \left(57.1\,\dfrac{kN}{m}\right) & \text{if } h_c = 0.75m \\[2mm] \left(49.0\,\dfrac{kN}{m}\right) & \text{if } h_c = 1m \\[2mm] \left(42.6\,\dfrac{kN}{m}\right) & \text{if } h_c = 3m \\[2mm] \text{"Error"} & \text{otherwise} \end{Vmatrix}$$

$$p_{traffic.fatigue} = 57.1 \cdot \frac{kN}{m}$$

2. Calculation

2.1. Soil tangent modulus

- **Determination of relevant factors**

$$\rho_s := 26\,\frac{kN}{m^3}$$
True density of the soil material, Appendix 2, Handbook

$$e_1 := \frac{\rho_s}{\rho_1} - 1 = 0.301$$
Void ratio

$$C_u := \frac{d_{60}}{d_{10}} = 10$$
Uniformity coefficient

$$m_1 := 282 \cdot C_u^{-0.77} \cdot e_1^{-2.83} = 1.43 \times 10^3$$
Modulus ratio

$$\beta := 0.29 \cdot \log\left(\frac{d_{50}}{0.01mm}\right) - 0.065 \cdot \log(C_u) = 0.892$$
Stress exponent

$$\phi_k := 26deg + 10deg \cdot \frac{(RP - 75)}{25} + 0.4deg \cdot C_u + 1.6deg \cdot \log\left(\frac{d_{50}}{1mm}\right)$$

$$\phi_k = 40.882 \cdot deg$$
Characteristic angle of internal friction of the backfill material

$$\phi_{k.d} := \operatorname{atan}\left(\frac{\tan(\phi_k)}{\gamma_n \cdot \gamma_{m.soil}}\right) = 31.189 \cdot deg$$
Design value of friction angle

- **Arching effect**

$$S_{v1} := \frac{0.8 \cdot \tan(\phi_{k.d})}{\left(\sqrt{1 + \tan(\phi_{k.d})^2} + 0.45 \cdot \tan(\phi_{k.d})\right)^2} = 0.233$$

$$\kappa := 2 \cdot S_{v1} \cdot \frac{h_c}{D} = 0.028$$

$$S_{ar} := \frac{1 - e^{-\kappa}}{\kappa} = 0.986$$

- **Tangent modulus of soil material**

$$k_v := \frac{\sin(\phi_k) \cdot (3 - 2 \cdot \sin(\phi_k))}{2 - \sin(\phi_k)} = 0.823$$

$$E_{soil.k} := 0.42 \cdot m_1 \cdot 100 kPa \cdot k_v \cdot \left[\frac{(1 - \sin(\phi_k)) \cdot \rho_2 \cdot S_{ar} \cdot \left(h_c + \frac{H}{2} \right)}{100 kPa} \right]^{1-\beta}$$

$$E_{soil.k} = 40.099 \cdot MPa$$

Characteristic value of the tangent modulus

$$E_{soil.d} := \frac{E_{soil.k}}{\gamma_n \cdot \gamma_{m.soil}} = 28.041 \cdot MPa$$

Design value of the tangent modulus

2.3. Relative stiffness between the culvert and the surrounding soil

$$E_{soil.d} \cdot D^3 = 5.18 \times 10^{10} \, J$$

$$\lambda_f := \frac{E_{soil.d} \cdot D^3}{EI_{FRP}} = 13769.2$$

The main limitation of stiffness number is:
$100 < \lambda_f < 100,000$

2.4. Reduction of the effective height of soil cover

$$h_{c.red} := h_c - 0.015 \cdot D = 565.95 \, mm$$

2.5. Dynamic amplification factor

If loads from Swedish bridge code Bro 2004 are applied, a reduction is introduced provided that the cover depth is high.

$$r_d := \begin{cases} 1 & \text{if } h_{c.red} \le 2m \\ \left(1.1 - 0.05 \cdot \frac{h_{c.red}}{m} \right) & \text{if } 2m < h_{c.red} \le 6m \\ 0.8 & \text{if } 6m < h_{c.red} \end{cases}$$

$$r_d = 1$$

For loads from Eurocode, the consideration about reduction factor is not needed.

2.6. Determination of normal forces

- **Normal force due to the surrounding soil**

$$N_{surr} := 0.2\frac{H}{D}\cdot\rho_1\cdot D^2 = 134.603\cdot\frac{kN}{m}$$

When the backfilling reaches the crown level

$$N_{cover} := S_{ar}\cdot\left(0.9\cdot\frac{h_{c.red}}{D} - 0.5\cdot\frac{h_{c.red}}{D}\cdot\frac{H}{D}\right)\cdot\rho_{cv}\cdot D^2$$

Due to the soil cover only

$$N_{cover} = 107.818\cdot\frac{kN}{m}$$

- **Normal force due to live traffic loads**

Since the distributed live load q in the equation below is taken into consideration in the calculation of equivalent line load with the Boussinesq method, so

$$q := 0\,\frac{kN}{m}$$

$$N_t := \begin{vmatrix} \left[p_{traffic} + \left(\frac{D}{2}\right)\cdot q\right] & \text{if } \frac{h_{c.red}}{D} \leq 0.25 \\[2mm] \left[\left(1.25 - \frac{h_{c.red}}{D}\right)\cdot p_{traffic} + \left(\frac{D}{2}\right)\cdot q\right] & \text{if } 0.25 < \frac{h_{c.red}}{D} \leq 0.75 \\[2mm] \left[0.5\cdot p_{traffic} + \left(\frac{D}{2}\right)\cdot q\right] & \text{otherwise} \end{vmatrix}$$

$$N_t = 162.5\cdot\frac{kN}{m}$$

$$N_{t.fatigue} := \begin{vmatrix} \left[p_{traffic.fatigue} + \left(\frac{D}{2}\right)\cdot q\right] & \text{if } \frac{h_{c.red}}{D} \leq 0.25 \\[2mm] \left[\left(1.25 - \frac{h_{c.red}}{D}\right)\cdot p_{traffic.fatigue} + \left(\frac{D}{2}\right)\cdot q\right] & \text{if } 0.25 < \frac{h_{c.red}}{D} \leq 0.75 \\[2mm] \left[0.5\cdot p_{traffic.fatigue} + \left(\frac{D}{2}\right)\cdot q\right] & \text{otherwise} \end{vmatrix}$$

$$N_{t.fatigue} = 57.1\cdot\frac{kN}{m}$$

2.7. Determination of bending moments

- **Bending moment due to the surrounding soil**

$$f_1 := \begin{vmatrix} \left[0.67 + 0.87\left(\frac{H}{D} - 0.2\right)\right] & \text{if } 0.2 < \frac{H}{D} \leq 0.35 \\[2mm] \left[0.8 + 1.33\cdot\left(\frac{H}{D} - 0.35\right)\right] & \text{if } 0.35 < \frac{H}{D} \leq 0.5 \\[2mm] \left(2\cdot\frac{H}{D}\right) & \text{if } 0.5 < \frac{H}{D} \leq 0.6 \end{vmatrix}$$

$$f_1 = 0.691$$

$$f_{2.surr} := \begin{cases} \left(0.0046 - 0.001 \cdot \log\left(\lambda_f\right)\right) & \text{if } \lambda_f \leq 5000 \\ 0.0009 & \text{otherwise} \end{cases}$$

$$f_{2.surr} = 9 \times 10^{-4}$$

$$f_3 := 6.67 \cdot \frac{H}{D} - 1.33 = 0.162$$

$$M_{s.surr} := -\rho_1 \cdot f_1 \cdot f_3 \cdot f_{2.surr} \cdot D^3 = -3.721 \cdot \frac{kN \cdot m}{m}$$ *When the backfilling reaches the crown level*

$$f_{2.cover} := \begin{cases} \left(0.018 - 0.004 \cdot \log\left(\lambda_f\right)\right) & \text{if } \lambda_f \leq 5000 \\ 0.0032 & \text{otherwise} \end{cases}$$

$$f_{2.cover} = 0.003$$

$$M_{s.cover} := S_{ar} \cdot \rho_{cv} \cdot \frac{h_{c.red}}{D} \cdot \left(\frac{R_t}{R_s}\right)^{0.75} \cdot f_1 \cdot f_{2.cover} \cdot D^3$$

$$M_{s.cover} = 22.787 \cdot \frac{kN \cdot m}{m}$$ *Moment value due to soil cover only*

- **Bending moment due to live traffic**

$$f_{4'} := 0.65 \cdot \left(1 - 0.2\log\left(\lambda_f\right)\right) = 0.112$$

$$f_{4''} := \begin{cases} \left[0.12 \cdot \left(1 - 0.15 \cdot \log\left(\lambda_f\right)\right)\right] & \text{if } \lambda_f \leq 100000 \\ 0.03 & \text{otherwise} \end{cases}$$

$$f_{4''} = 0.045$$

$$f_{4'''} := 4 \cdot 0.01^{\left(\frac{h_{c.red}}{D}\right)} + 0.4 = 3.635$$

$$check := \begin{cases} \text{"OK"} & \text{if } f_{4'} \cdot f_{4'''} < 1 \\ \text{"ERROR"} & \text{otherwise} \end{cases}$$

$$check = \text{"OK"}$$

$$f_{4.IV} := \left(\frac{R_t}{R_s}\right)^{0.25} = 1.831$$

Moment value due to traffic only

$$M_t := f_{4'} \cdot f_{4''} \cdot f_{4'''} \cdot f_{4.IV} \cdot D \cdot p_{traffic} + S_{ar} \cdot \left(\frac{R_t}{R_s}\right)^{0.75} \cdot f_1 \cdot f_{2.cover} \cdot q \cdot D^2 = 67.598 \cdot \frac{kN \cdot m}{m}$$

CHALMERS, Civil and Environmental Engineering, Master's Thesis 2014:123

$$M_{t.fatigue} := f_4 \cdot f_4'' \cdot f_4''' \cdot f_{4.IV} \cdot D \cdot p_{traffic.fatigue} + S_{ar} \cdot \left(\frac{R_t}{R_s}\right)^{0.75} \cdot f_1 \cdot f_{2.cover} \cdot q \cdot D^2 = 23.753 \cdot \frac{kN \cdot m}{m}$$

3. Design value of normal forces and bending moments

3.1. Normal forces

Regarding normal forces, the loads due to both the soil and the live traffic are unfavorable.

- **Scenario 1: Backfilling reaches the crown level**

The load due to surrounding soil is considered as a live load in this stage.

$$N_{d.SLS.1} := \max(\gamma_{Q.s}) \cdot N_{surr} = 134.603 \cdot \frac{kN}{m}$$

- **Scenario 2: Backfilling completed**

SLS

$$N_{d.SLS.2} := \max(\gamma_{G.s}) \cdot (N_{surr} + N_{cover}) + \max(\gamma_{Q.s}) \cdot N_t$$

$$N_{d.SLS.2} = 404.922 \cdot \frac{kN}{m}$$

ULS

$$N_{d.ULS.2} := \max(\gamma_{G.u}) \cdot (N_{surr} + N_{cover}) + \max(\gamma_{Q.u}) \cdot N_t$$

$$N_{d.ULS.2} = 546.644 \cdot \frac{kN}{m}$$

$$N_{d.ULS.2.soil} := \max(\gamma_{G.u}) \cdot (N_{surr} + N_{cover})$$

$$N_{d.ULS.2.traffic} := \max(\gamma_{Q.u}) \cdot N_t$$

3.2. Bending moment

Definition:
Negative bending moments at the crown are due to surrounding soil till crown level;
Positive bending moments at the crown are due to cover soil and live traffic load.

Thus, for the calculation of each bending moment, there are two possible load combinations:
1) when the negative bending moment is dominant
: the load due to **surrounding soil** is **unfavorable**
: the load effects due to **cover soil** and **live traffic** are **favorable**
2) when the positive bending moment is dominant
: the load due to **surrounding soil** is **favorable**
: the load effects due to **cover soil** and **live traffic** are **unfavorable**;

- **Scenario 1: Backfilling reaches the crown level**

The load due to surrounding soil is considered as a live load in SLS:

$$M_{d.SLS.1} := \max(\gamma_{Q.s}) \cdot M_{s.surr} = -3.721 \cdot \frac{kN \cdot m}{m}$$

- **Scenario 2: Backfilling completed**

SLS

$$M_{d.SLS.2} := \begin{bmatrix} \max(\gamma_{G.s}) \cdot M_{s.surr} + \min(\gamma_{G.s}) \cdot M_{s.cover} + \min(\gamma_{Q.s}) \cdot \left(\frac{-M_t}{2}\right) \\ \min(\gamma_{G.s}) \cdot M_{s.surr} + \max(\gamma_{G.s}) \cdot M_{s.cover} + \max(\gamma_{Q.s}) \cdot M_t \end{bmatrix}$$

$$M_{d.SLS.2} = \begin{pmatrix} 19.066 \\ 86.664 \end{pmatrix} \cdot \frac{kN \cdot m}{m} \qquad \begin{array}{l} \textit{Upper: Negative bending moment is dominant} \\ \textit{Lower: Positive bending moment is dominant} \end{array}$$

ULS

$$M_{d.ULS.2} := \begin{pmatrix} \max(\gamma_{G.u}) \cdot M_{s.surr} + \min(\gamma_{G.u}) \cdot M_{s.cover} + \min(\gamma_{Q.u}) \cdot M_t \\ \min(\gamma_{G.u}) \cdot M_{s.surr} + \max(\gamma_{G.u}) \cdot M_{s.cover} + \max(\gamma_{Q.u}) \cdot M_t \end{pmatrix}$$

$$M_{d.ULS.2} = \begin{pmatrix} 17.764 \\ 118.299 \end{pmatrix} \cdot \frac{kN \cdot m}{m} \qquad \begin{array}{l} \textit{Upper: Negative bending moment is dominant} \\ \textit{Lower: Positive bending moment is dominant} \end{array}$$

$$M_{d.ULS.2.soil} := \begin{pmatrix} \max(\gamma_{G.u}) \cdot M_{s.surr} + \min(\gamma_{G.u}) \cdot M_{s.cover} \\ \min(\gamma_{G.u}) \cdot M_{s.surr} + \max(\gamma_{G.u}) \cdot M_{s.cover} \end{pmatrix}$$

$$M_{d.ULS.2.traffic} := \begin{pmatrix} \min(\gamma_{Q.u}) \cdot M_t \\ \max(\gamma_{Q.u}) \cdot M_t \end{pmatrix}$$

$$M_{d.ULS.2.cor} := \begin{bmatrix} \frac{2}{3}\left(\max(\gamma_{G.u}) \cdot M_{s.surr} + \min(\gamma_{G.u}) \cdot M_{s.cover}\right) + \frac{1}{3}\min(\gamma_{Q.u}) \cdot M_t \\ \frac{2}{3}\left(\min(\gamma_{G.u}) \cdot M_{s.surr} + \max(\gamma_{G.u}) \cdot M_{s.cover}\right) + \frac{1}{3}\max(\gamma_{Q.u}) \cdot M_t \end{bmatrix}$$

$$M_{d.ULS.2.cor} = \begin{pmatrix} 11.843 \\ 48.447 \end{pmatrix} \cdot \frac{kN \cdot m}{m} \qquad \begin{array}{l} \textit{Upper: Negative bending moment is dominant} \\ \textit{Lower: Positive bending moment is dominant} \end{array}$$

$$M_{d.ULS.2.cor.soil} := \begin{bmatrix} \frac{2}{3}\left(\max(\gamma_{G.u}) \cdot M_{s.surr} + \min(\gamma_{G.u}) \cdot M_{s.cover}\right) \\ \frac{2}{3}\left(\min(\gamma_{G.u}) \cdot M_{s.surr} + \max(\gamma_{G.u}) \cdot M_{s.cover}\right) \end{bmatrix}$$

$$M_{d.ULS.2.cor.traffic} := \begin{pmatrix} \frac{1}{3}\min(\gamma_{Q.u}) \cdot M_t \\ \frac{1}{3}\max(\gamma_{Q.u}) \cdot M_t \end{pmatrix}$$

4. Summary

- **Geometry**

Culvert profile   profile = "G: Box Culvert"   case = 14

Span $D = 12.27 \cdot m$

Soil cover $h_c = 750 \, mm$

- **Loads**

Traffic load $p_{traffic} = 162.5 \cdot \dfrac{kN}{m}$

- **Stiffness**

$EI_{FRP} = 3.762 \times 10^6 \cdot N \cdot m$

- **Sectional forces**

$N_{d.SLS.1} = 134.603 \cdot \dfrac{kN}{m}$

$N_{d.SLS.2} = 404.922 \cdot \dfrac{kN}{m}$

$N_{d.ULS.2} = 546.644 \cdot \dfrac{kN}{m}$

$N_{d.ULS.2.soil} = 327.269 \cdot \dfrac{kN}{m}$

$N_{d.ULS.2.traffic} = 219.375 \cdot \dfrac{kN}{m}$

$M_{d.SLS.1} = -3.721 \cdot kN$

$M_{d.SLS.2} = \begin{pmatrix} 19.066 \\ 86.664 \end{pmatrix} \cdot \dfrac{kN \cdot m}{m}$

$M_{d.ULS.2} = \begin{pmatrix} 17.764 \\ 118.299 \end{pmatrix} \cdot \dfrac{kN \cdot m}{m}$

$M_{d.ULS.2.soil} = \begin{pmatrix} 17.764 \\ 27.042 \end{pmatrix} \cdot \dfrac{kN \cdot m}{m}$

$M_{d.ULS.2.traffic} = \begin{pmatrix} 0 \\ 91.257 \end{pmatrix} \cdot \dfrac{kN \cdot m}{m}$

$M_{d.ULS.2.cor} = \begin{pmatrix} 11.843 \\ 48.447 \end{pmatrix} \cdot kN$

$M_{d.ULS.2.cor.soil} = \begin{pmatrix} 11.843 \\ 18.028 \end{pmatrix} \cdot \dfrac{kN \cdot m}{m}$

$M_{d.ULS.2.cor.traffic} = \begin{pmatrix} 0 \\ 30.419 \end{pmatrix} \cdot \dfrac{kN \cdot m}{m}$

Appendix B.3 Mathcad Routine for Design of FRP Culverts

-- *Mathcad No.3 Failure Prediction of FRP laminate*

$\mathrm{ORIGIN} =: 1$

1. Programming of strength calculation for a FRP laminate

$\sigma\left(E_{11}, E_{22}, v_{12}, G_{12}, \theta, t, no, NF, \Delta N, \sigma_{d.11.c}, \sigma_{d.11.t}, \sigma_{d.22.c}, \sigma_{d.22.t}, \tau_{d.12}\right) :=$

$$v_{21} \leftarrow \frac{E_{22}}{E_{11}} \cdot v_{12}$$

$$Q_{11} \leftarrow \frac{E_{11}}{1 - v_{12} \cdot v_{21}}$$

$$Q_{22} \leftarrow \frac{E_{22}}{1 - v_{12} \cdot v_{21}}$$

$$Q_{12} \leftarrow \frac{v_{12} \cdot E_{22}}{1 - v_{12} \cdot v_{21}}$$

$$Q_{21} \leftarrow \frac{v_{21} \cdot E_{11}}{1 - v_{12} \cdot v_{21}}$$

$$Q_{66} \leftarrow G_{12}$$

$$U_1 \leftarrow \frac{1}{8} \cdot \left(3 \cdot Q_{11} + 3 \cdot Q_{22} + 2 \cdot Q_{12} + 4 Q_{66}\right)$$

$$U_2 \leftarrow \frac{1}{2} \cdot \left(Q_{11} - Q_{22}\right)$$

$$U_3 \leftarrow \frac{1}{8} \cdot \left(Q_{11} + Q_{22} - 2 \cdot Q_{12} - 4 Q_{66}\right)$$

$$U_4 \leftarrow \frac{1}{8} \cdot \left(Q_{11} + Q_{22} + 6 \cdot Q_{12} - 4 Q_{66}\right)$$

$$U_5 \leftarrow \frac{1}{2} \cdot \left(U_1 - U_4\right)$$

$$QQ_{11} \leftarrow U_1 + U_2 \cdot \cos(2 \cdot \theta) + U_3 \cdot \cos(4 \cdot \theta)$$

$$QQ_{12} \leftarrow U_4 - U_3 \cdot \cos(4 \cdot \theta)$$

$$QQ_{22} \leftarrow U_1 - U_2 \cdot \cos(2 \cdot \theta) + U_3 \cdot \cos(4 \cdot \theta)$$

$$QQ_{16} \leftarrow \frac{1}{2} \cdot U_2 \cdot \sin(2 \cdot \theta) + U_3 \cdot \sin(4 \cdot \theta)$$

$$QQ_{26} \leftarrow \frac{1}{2} \cdot U_2 \cdot \sin(2 \cdot \theta) - U_3 \cdot \sin(4 \cdot \theta)$$

$$QQ_{66} \leftarrow U_5 - U_3 \cdot \cos(4 \cdot \theta)$$

$$QQ \leftarrow \begin{pmatrix} QQ_{11} & QQ_{12} & QQ_{16} \\ QQ_{12} & QQ_{22} & QQ_{26} \end{pmatrix}$$

$$\begin{pmatrix} QQ_{16} & QQ_{26} & QQ_{66} \end{pmatrix}$$

$\text{for } i \in 1 .. (no + 1)$

$\qquad h_i \leftarrow \left[\dfrac{-(t \cdot no)}{2} + (i-1) \cdot t \right]$

$\text{for } i \in 1 .. no$

$\qquad ha_i \leftarrow \left[h_{(i+1)} - h_i \right]$

$\qquad hb_i \leftarrow \left[\left(h_{i+1} \right)^2 - \left(h_i \right)^2 \right]$

$\qquad hd_i \leftarrow \left[\left(h_{i+1} \right)^3 - \left(h_i \right)^3 \right]$

$\text{while } (\max(ha) > 0)$

$\qquad \text{for } i \in 1 .. 3$

$\qquad\qquad \text{for } j \in 1 .. 3$

$\qquad\qquad\qquad A_{i,j} \leftarrow QQ_{i,j} \, ha$

$\qquad\qquad\qquad B_{i,j} \leftarrow (QQ)_{i,j} \, hb \cdot \dfrac{1}{2}$

$\qquad\qquad\qquad D_{i,j} \leftarrow (QQ)_{i,j} \, hd \cdot \dfrac{1}{3}$

$\qquad D1 \leftarrow \left(D - B \cdot A^{-1} \cdot B \right)^{-1}$

$\qquad A1 \leftarrow A^{-1} + A^{-1} \cdot B \cdot D1 \cdot B \cdot A^{-1}$

$\qquad C1 \leftarrow -D1 \cdot B \cdot A^{-1}$

$\qquad \varepsilon_{mid} \leftarrow A1 \cdot NF$

$\qquad k_{mid} \leftarrow C1 \cdot NF$

$\qquad \text{for } i \in 1 .. no$

$\qquad\qquad z_i \leftarrow \left[\dfrac{-(t \cdot no) - t}{2} + i \cdot t \right]$

$\qquad\qquad \varepsilon_i \leftarrow \varepsilon_{mid} + z_i \cdot k_{mid}$

$\qquad \text{for } i \in 1 .. no$

$\qquad\qquad Q_i \leftarrow \begin{pmatrix} 0 & 0 & 0 \\ 0 & 0 & 0 \\ 0 & 0 & 0 \end{pmatrix}$

$\qquad\qquad \text{for } x \in 1 .. 3$

$\qquad\qquad\qquad \text{for } y \in 1 .. 3$

$\qquad\qquad\qquad\qquad \left(Q_i \right)_{x,y} \leftarrow \left(QQ_{x,y} \right)_i$

$\qquad \text{for } i \in 1 .. no$

$\qquad\qquad stress_i \leftarrow Q_i \cdot \varepsilon_i$

$\qquad\qquad R1 \leftarrow \cos\left(\theta_i \right)^2$

$\qquad\qquad R2 \leftarrow \sin\left(\theta_i \right)^2$

$$R3 \leftarrow \cos\left(\theta_i\right) \cdot \sin\left(\theta_i\right)$$

$$\text{stresslocal}_i \leftarrow \begin{pmatrix} R1 & R2 & 2 \cdot R3 \\ R2 & R1 & -2 \cdot R3 \\ -R3 & R3 & R1 - R2 \end{pmatrix} \cdot \text{stress}_i$$

$$\sigma_{d.11} \leftarrow \begin{vmatrix} \sigma_{d.11.c} & \text{if } \left(\text{stresslocal}_i\right)_1 \leq 0 \\ \sigma_{d.11.t} & \text{otherwise} \end{vmatrix}$$

$$\sigma_{d.22} \leftarrow \begin{vmatrix} \sigma_{d.22.c} & \text{if } \left(\text{stresslocal}_i\right)_2 \leq 0 \\ \sigma_{d.22.t} & \text{otherwise} \end{vmatrix}$$

$$\text{check}_i \leftarrow \left[\left[\frac{\left(\text{stresslocal}_i\right)_1}{\sigma_{d.11}} \right]^2 - \left[\frac{\left(\text{stresslocal}_i\right)_1}{\sigma_{d.11}} \cdot \frac{\left(\text{stresslocal}_i\right)_2}{\sigma_{d.22}} \right] \dots \\ + \left[\frac{\left(\text{stresslocal}_i\right)_2}{\sigma_{d.22}} \right]^2 + \left[\frac{\left(\text{stresslocal}_i\right)_3}{\tau_{d.12}} \right]^2 \right]$$

$$\text{NF} \leftarrow \begin{vmatrix} (\text{NF} + \Delta\text{N}) & \text{if } \max(\text{check}) < 1 \\ \text{NF} & \text{otherwise} \end{vmatrix}$$

$$\text{for } i \in 1..\text{no}$$
$$\quad \text{for } x \in 1..3$$
$$\quad\quad \text{for } y \in 1..3$$
$$\quad\quad\quad \left(QQ_{x,y}\right)_i \leftarrow 0 \text{ if } \text{check}_i > 1$$
$$\quad\quad\quad (\text{ha})_i \leftarrow 0 \text{ if } \text{check}_i > 1$$
$$\quad\quad\quad \left(QQ_{x,y}\right)_i \leftarrow \left(QQ_{x,y}\right)_i \text{ otherwise}$$

$$\text{return } \left(\frac{\text{NF}}{\text{no} \cdot t} \right)$$

2. Design of the FRP laminate

2.1 FRP material

Material   Fiber: E-glass   Matrix: Epoxy   Fiber/Matrix: 45%

$$E_{k.11} := 38.6\,\text{GPa} \qquad E_{k.22} := 8.27\,\text{GPa} \qquad G_{k.12} := 4.14\,\text{GPa}$$

$$\upsilon_{12} := 0.26$$

Characteristic value of strengths

$$\sigma_{k.11.c} := 610\,\text{MPa} \qquad \sigma_{k.11.t} := 1062\,\text{MPa}$$

$$\sigma_{k.22.c} := 118\,\text{MPa} \qquad \sigma_{k.22.t} := 31\,\text{MPa}$$

$$\tau_{k.12} := 72\text{MPa}$$

Paritial factor for FRP laminate according to Eurocomp Design Code

$\gamma_{M1} := 1.5$ *Derivation of properties*

$\gamma_{M2} := 1.2$ *Method of manufacture: Resin transfer moulding*

$\gamma_{M3} := 2.5$ *1.0 for long-term loading in ULS;*
2.5 for short-term loading in SLS

$\gamma_M := \gamma_{M1} \cdot \gamma_{M2} \cdot \gamma_{M3} = 4.5$

Design value

$$E_{11} := \frac{E_{k.11}}{\gamma_M} \qquad E_{22} := \frac{E_{k.22}}{\gamma_M} \qquad G_{12} := \frac{G_{k.12}}{\gamma_M}$$

$$\sigma_{d.11.c} := \frac{\sigma_{k.11.c}}{\gamma_M} \qquad \sigma_{d.11.t} := \frac{\sigma_{k.11.t}}{\gamma_M}$$

$$\sigma_{d.22.c} := \frac{\sigma_{k.22.c}}{\gamma_M} \qquad \sigma_{d.22.t} := \frac{\sigma_{k.22.t}}{\gamma_M}$$

$$\tau_{d.12} := \frac{\tau_{k.12}}{\gamma_M}$$

2.2 Geometry

Geometry $t := 3\text{mm}$ *Thickness of each ply*

Construction of the FRP laminate   *Fiber orientation for each ply*

$$\theta := \text{stack}(0\text{deg}, 90\text{deg})$$

$\text{no} := \text{rows}(\theta) = 2$ *Number of plies*

---

3. Ultimate strength of the designed laminate

Assume a proper value of applied normal force with certain increment

$$\Delta N := \begin{pmatrix} 5 \\ 0 \\ 0 \end{pmatrix} \frac{kN}{m}$$

$$NF := \begin{pmatrix} 20 \\ 0 \\ 0 \end{pmatrix} \frac{kN}{m}$$

N.xx   *Positive value for tensile forces*
N.yy   *Negative value for compressive forces*
N.xy

$$\sigma\left(E_{11}, E_{22}, \upsilon_{12}, G_{12}, \theta, t, no, NF, \Delta N, \sigma_{d.11.c}, \sigma_{d.11.t}, \sigma_{d.22.c}, \sigma_{d.22.t}, \tau_{d.12}\right) = \begin{pmatrix} 118.333 \\ 0 \\ 0 \end{pmatrix} \cdot MPa$$

Appendix B.4 Data for the FE analysis of FRP culverts in ABAQUS
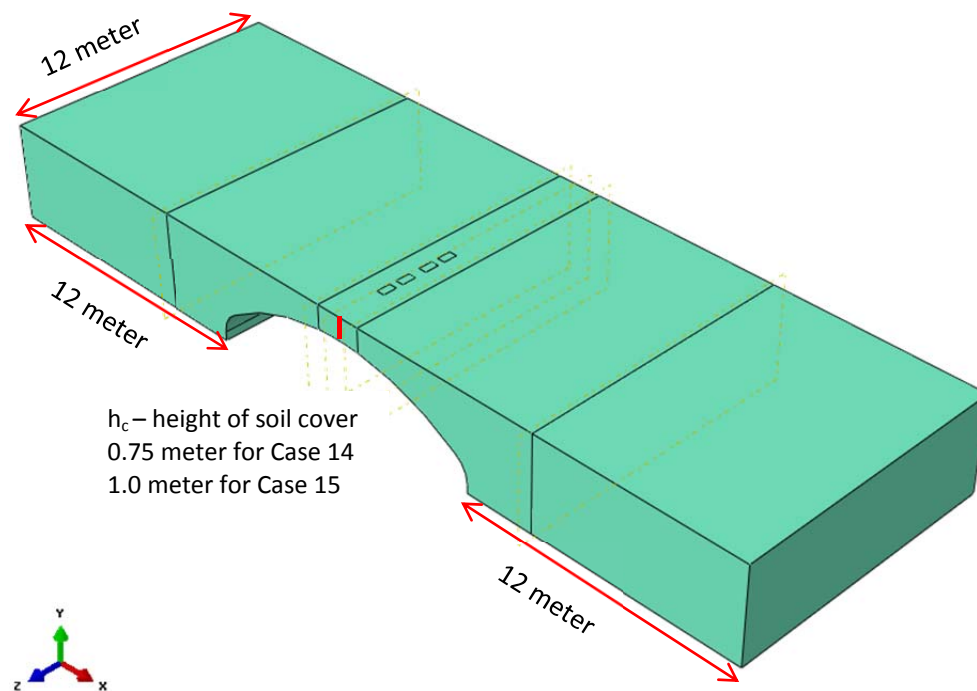
Dimension of the model

h$_c$ – height of soil cover
0.75 meter for Case 14
1.0 meter for Case 15

Figure B.4-1 Dimension of the surrounding soil material

FRP laminate
(E-glass&Epoxy) — 9 [mm]
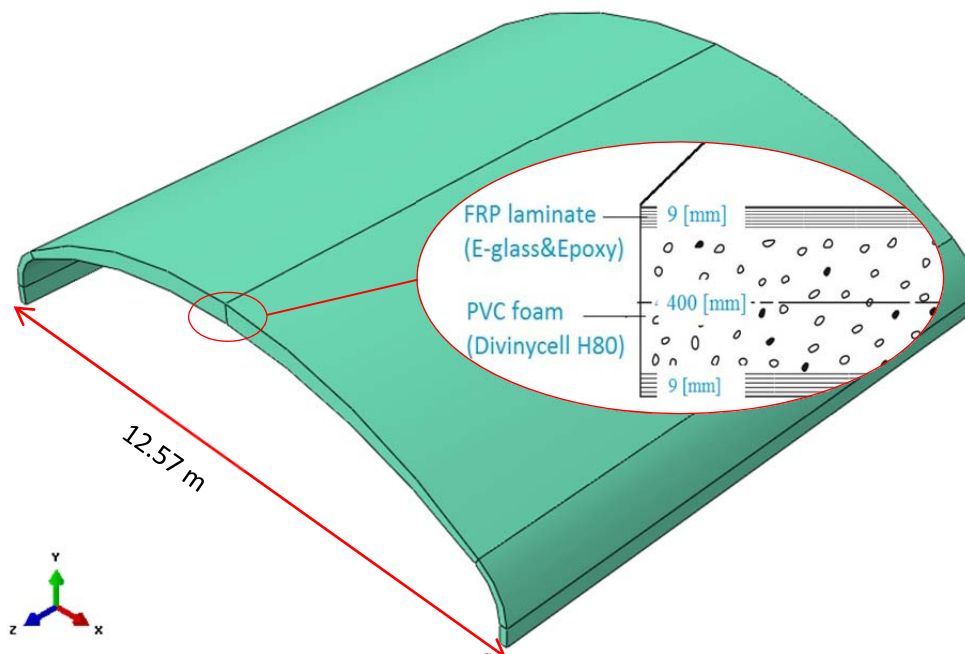
PVC foam
(Divinycell H80) — 400 [mm]

9 [mm]

Figure B.4-2 Dimension of the Box Culvert structure (same for both Case 14 and 15)

Mechanical properties

Building a model of the FRP culvert bridge in ABAQUS includes: 1) soil material surrounding the culvert structure, 2) FRP laminate face and PVC core that compose the culvert. Elastic constants used to define the mechanical properties in ABAQUS are shown in the Table B.4-1.

Table B.4-1 Define the mechanical properties of three parts

Soil	**Element type**	E_k [MPa]	υ [-]						
	Solid, Extrusion	40.1	0.29						
PVC foam	**Element type**	E_k [MPa]	υ [-]						
	Solid, Extrusion	80	0.33						
FRP laminate face	**Element type**	$E_{k.11}$ [GPa]	$E_{k.22}$ [GPa]	υ_{12} [-]	υ_{21} [-]	υ_{23} [-]	$G_{k.12}$ [GPa]	$G_{k.13}$ [GPa]	$G_{k.23}$ [GPa]
	Solid, Extrusion	38.6	8.27	0.26	0.06	0.33	4.41	4.41	3.10

Interaction

Table B.4-2 Interaction on the interfaces between different parts

Interaction	
Between soil and FRP culvert	Between FRP face and foam core
Surface to Surface Contact	Tie Constrain

Loads

The loads considered in the FE analysis are self-weight of soil material surrounding and live traffic load above the bridge. Since the height of soil covers in case 14 and case 15 are less than 1.0 meter, the traffic group LM2 is chosen to be applied. In Abaqus Model 1, the real LM2 is defined (Figure B.4-3), while in Abaqus Model 2 the equivalent line load converted from LM2 is applied in a conventional way (Figure B.4-4). The characteristic values of traffic loads are shown in Table B.4-3.

Table B.4-3 Define the traffic load in Abaqus models

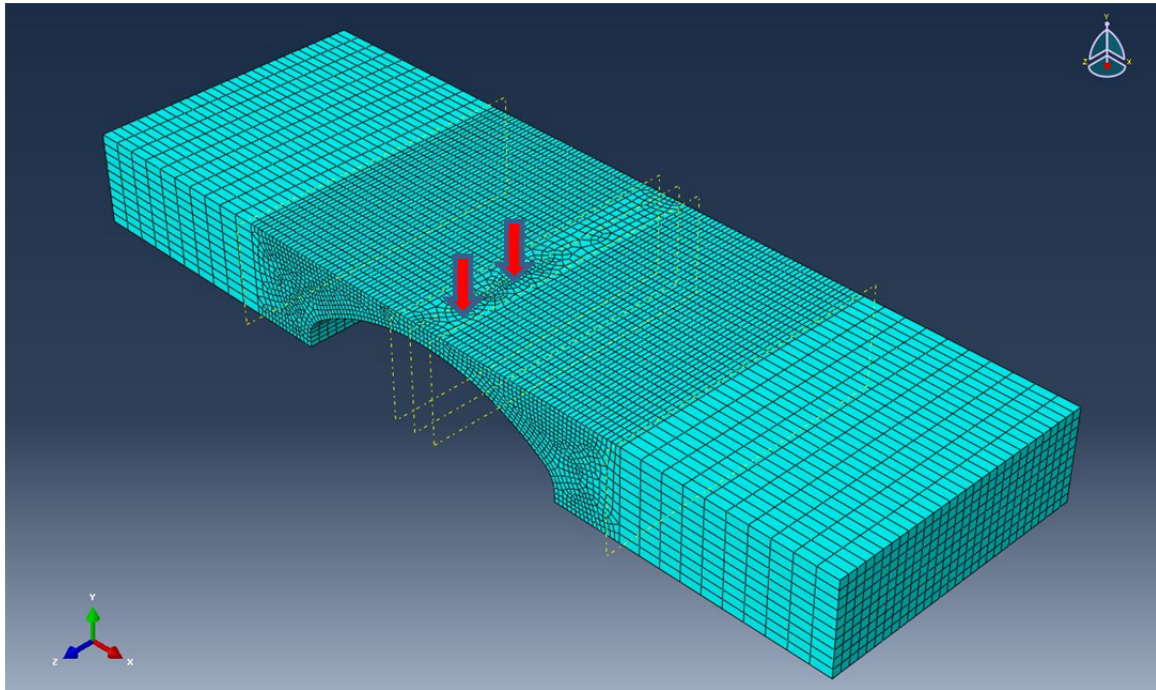| Real LM2	2×200 kN (on the area 0.35 m $\times$ 0.6 m)		Abaqus Model 1
Equivalent line load converted from LM2	Case 14: 213.7 kN/m	Case 15: 177.5 kN/m	Abaqus Model 2

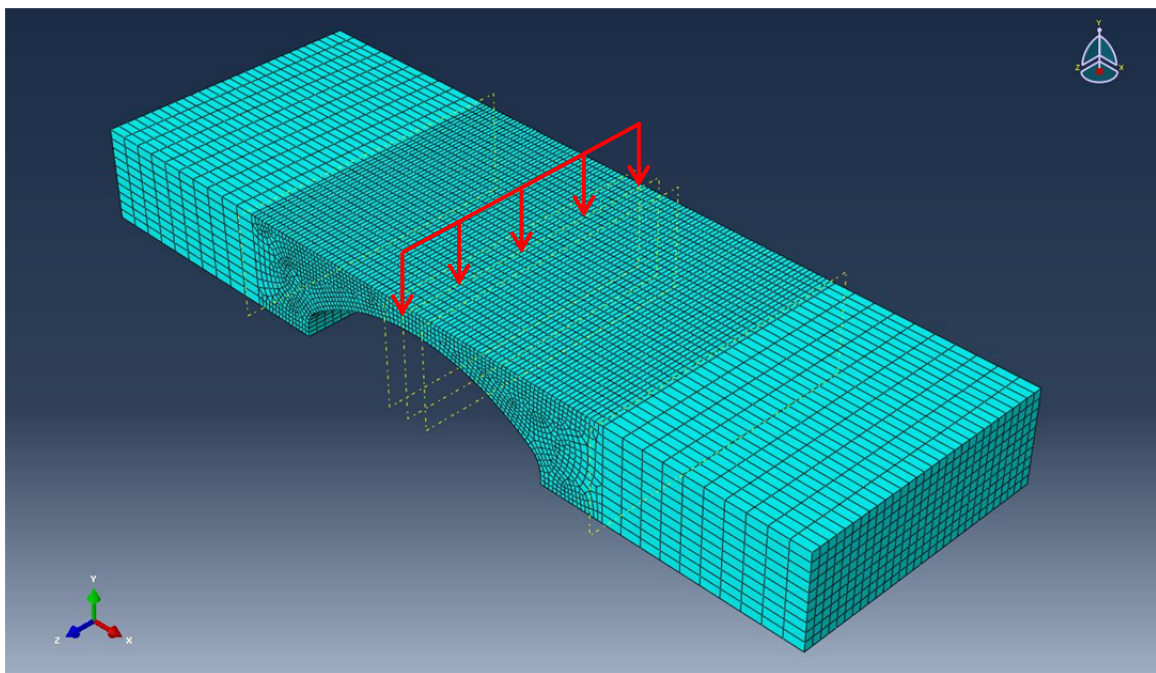*Figure B.4-3 Real traffic load LM2 defined in Abaqus Model 1*

Figure B.4-4 Equivalent line load converted from LM2 defined in Abaqus Model 2

Partial factors

Table B.4-4 Partial factors for materials and loads in ULS and SLS

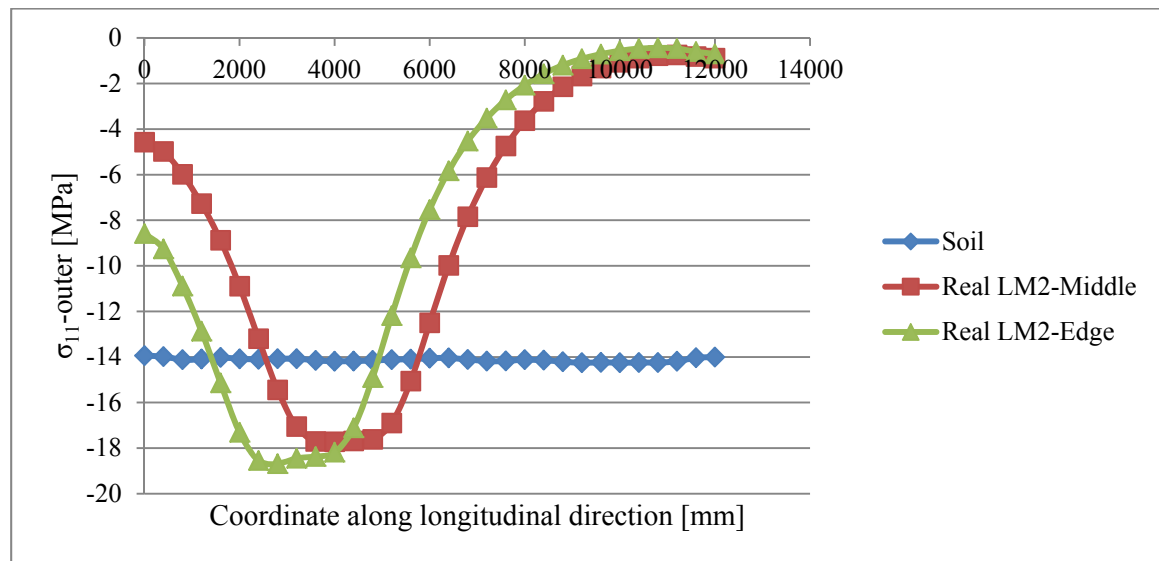| Partial factors	Materials		Load	
	Soil	FRP material	Self-weight of soil	Live traffic load
SLS	1.3	1.8	1.0	0.5
ULS	1.3	4.5	1.35	1.35

ABAQUS results of Case 14

Figure B.4-5 Stresses on the outer FRP laminate face, Case 14, ULS, Abaqus Model 1

Figure B.4-6 Stresses on the inner FRP laminate face, Case 14, ULS Abaqus Model 1

Figure B.4-7 Stresses on the outer and inner FRP laminate face, Case 14, ULS, Abaqus Model 2 with equivalent line load

Figure B.4-8 Deflection at the crown region along the longitudinal direction, Case 14, SLS

ABAQUS results of Case 15

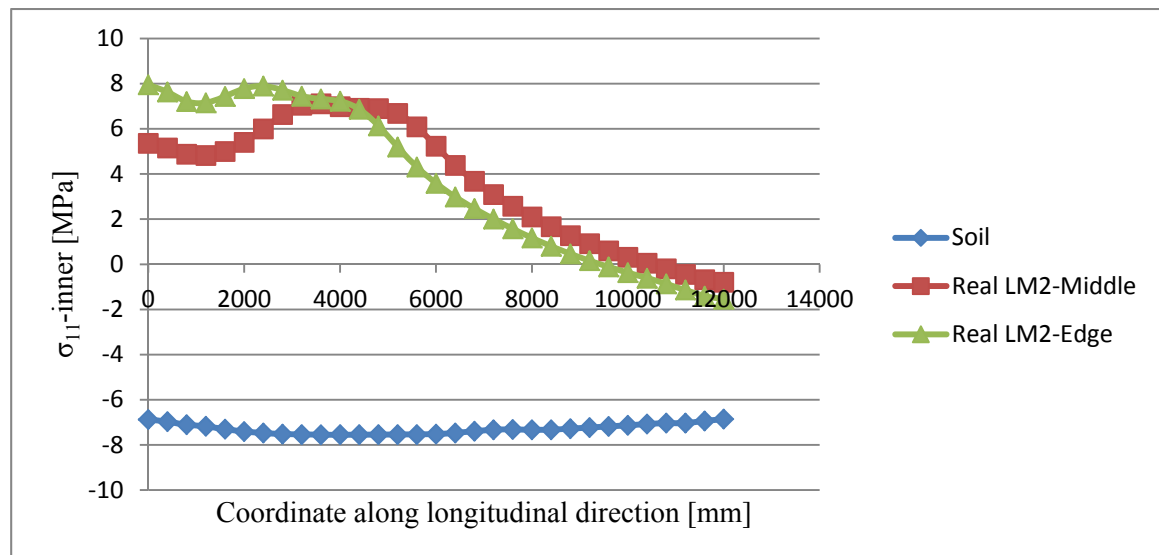*Figure B.4-9 Stresses on the outer FRP laminate face, Case 15, ULS, Abaqus Model 1*

Figure B.4-10 Stresses on the inner FRP laminate face, Case 15, ULS, Abaqus Model 1
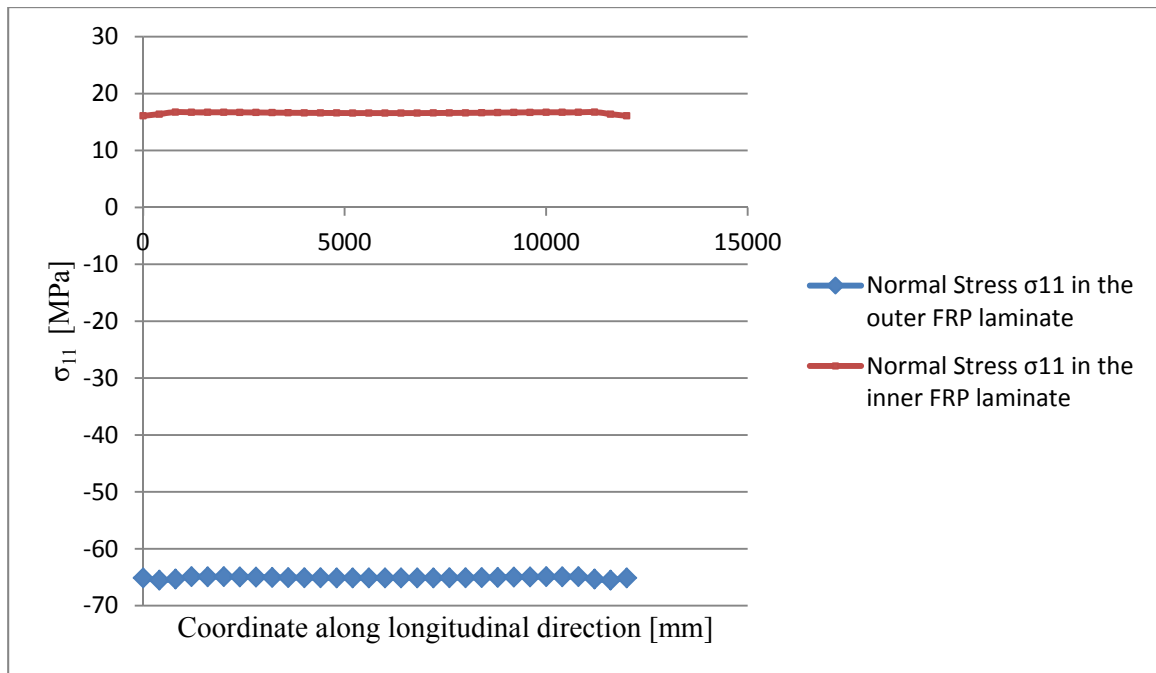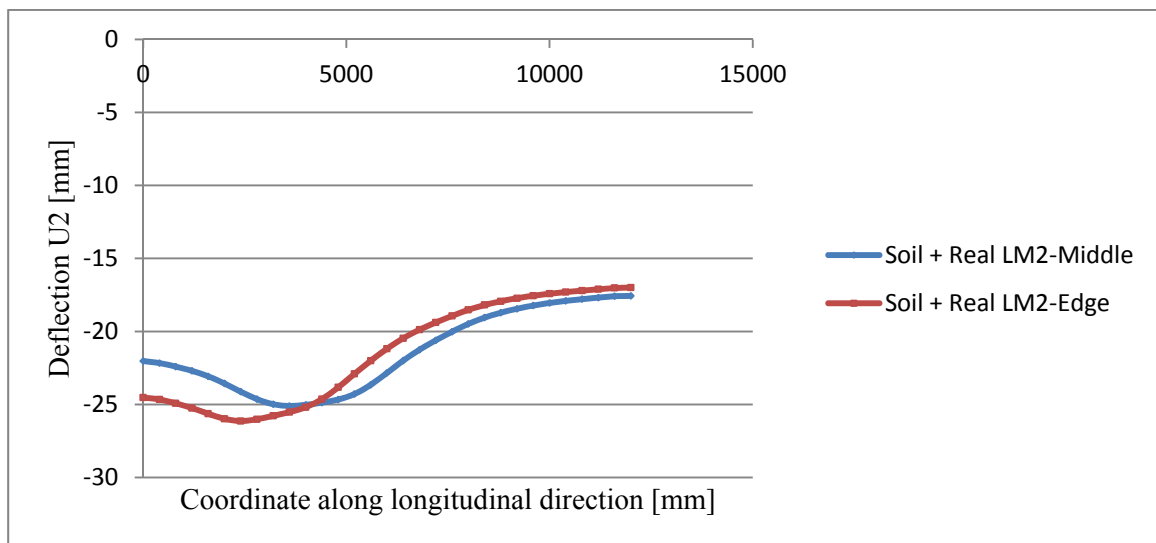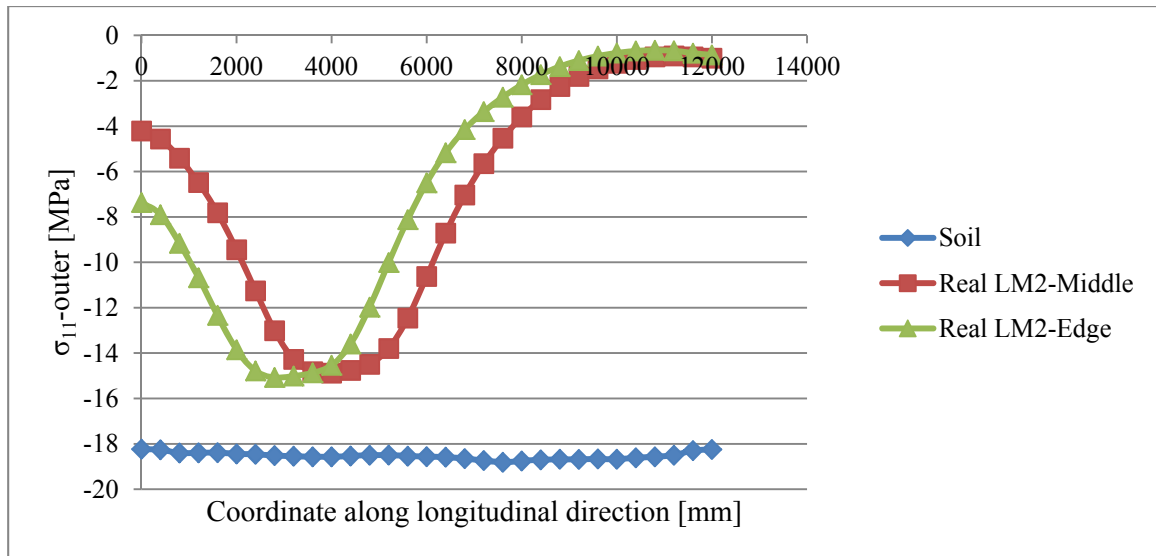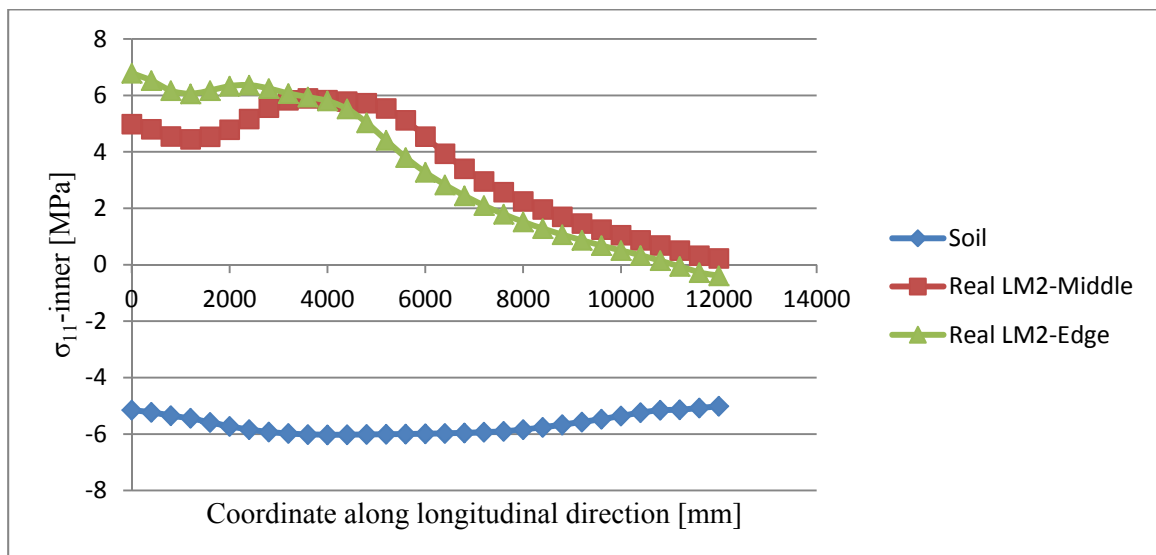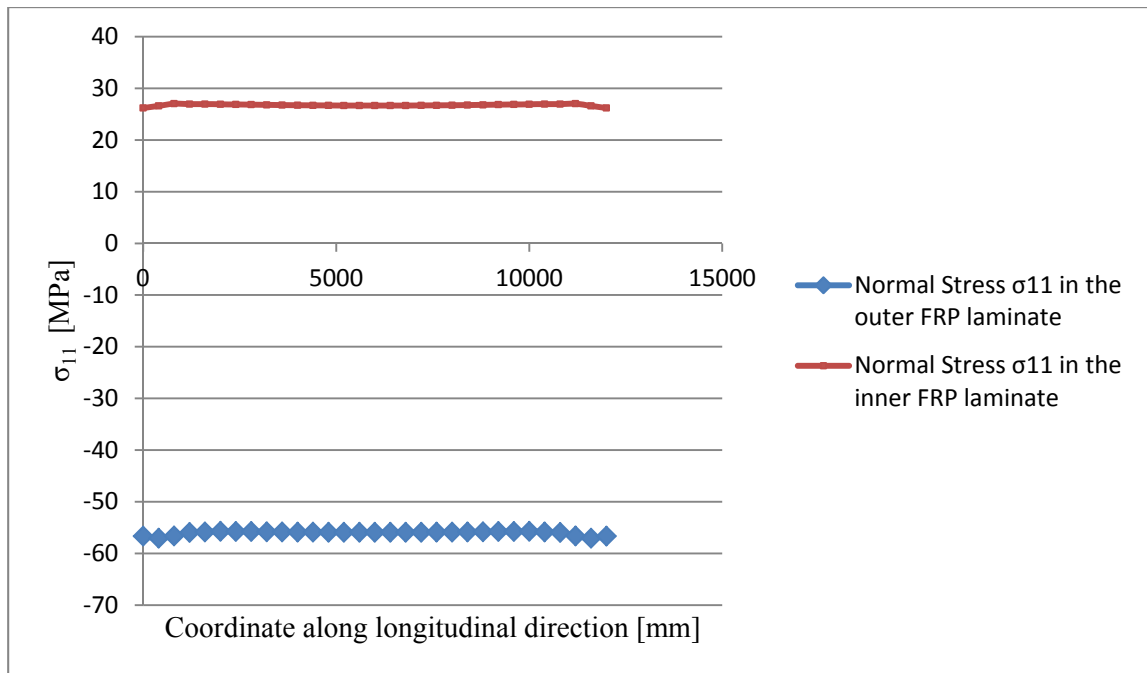
Figure B.4-11 Stresses on the outer and inner FRP laminate face, Case 15, ULS, Abaqus Model 2 with equivalent line load
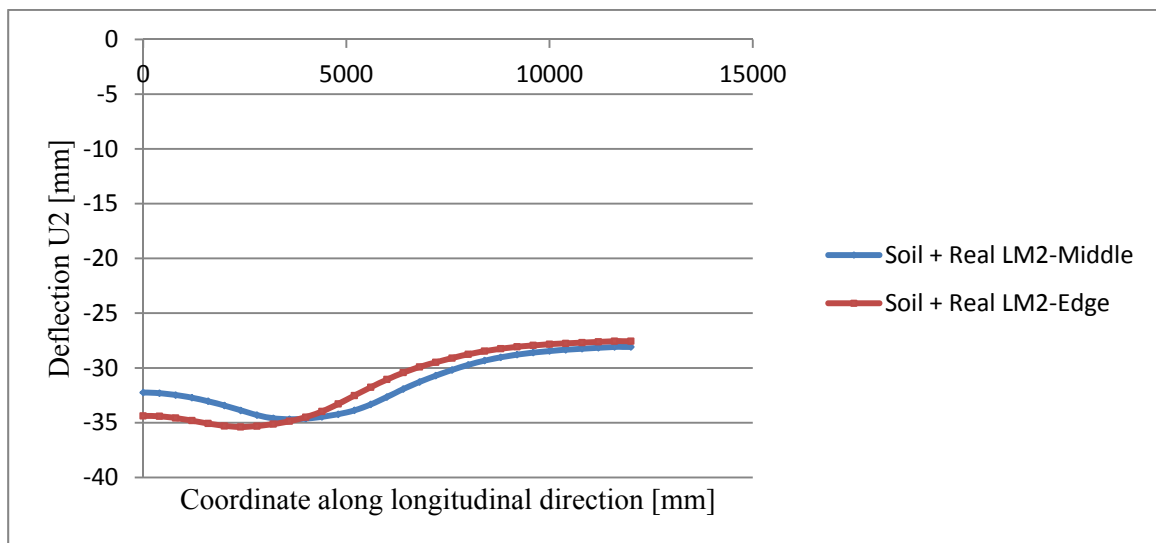

Figure B.4-12 Deflection at the crown region along the longitudinal direction, Case 15, SLS

Appendix C Data for LCC analysis

Table C.1 Total weight of the designed steel culvert structure in case 14

Surface area of culvert	[m^2]	176.000
Reinforcement area	[m^2]	66.400
Plate thickness	[m]	0.007
Number of bolts	[1/m^2]	15.000
Volume of the corrugated profile	[m^3]	1.720
Volume of corrugated reinforcement	[m^3]	0.650
Weight of the culvert	[ton]	13.416
Weight of the reinforcement	[ton]	5.070
Weight of fasteners	[ton]	0.800
Total weight, tons	[ton]	**19**

Table C.2 Initial costs of the designed steel culvert structure in case 14

	Cost category	**Sub-categories**	**Cost**	**%**
Initial construction costs	**Material costs**	Steel		
		Culvert structure	800,000	
	Total material costs		**800,000**	**51**
	Transportation and installation costs	Transportation	2,880	
		Installation (equipment, labour, etc.)	71,680	
	Total transportation & installation costs		**74,560**	**5**
Social costs	**User costs**	Driver delay	404,320	
		Vehicle operating	297,847	
	Total Social costs		**702,168**	**45**
	TOTAL initial costs		**1,576,728**	**100**

Table C.3 Total weight of the designed FRP culvert structure in case 14

Surface area of culvert	[m^2]	180.000
Area of foam in cross-section	[m^2]	4.200
Area of laminates in cross-section	[m^2]	0.270
Volume of the foam	[m^3]	50.400
Number of laminate's layers	[-]	9.000
One lamina's thickness	[m]	0.001
Volume fracture	[-]	0.450
Area of the top mould	[m^2]	23.000
Area of the bottom mould	[m^2]	22.000
Amount of epoxy in top skin	[litre]	910.800
Amount of epoxy in bottom skin	[litre]	871.200
Number of fasteners	[-]	500.000
Weight of the structure	[ton]	9.86
Weight of the fasteners	[ton]	0.11
Total weight	[ton]	**10**

Table C.4. Initial costs of the designed FRP culvert structure in case 14

	Cost category	Sub-categories	Cost [SEK]	%
Initial construction costs	**Material costs**	**FRP sandwich**		
		Moulds	26,960	
		Sandwich assembly	57,600	
		E-glass fibres	38,880	
		Epoxy resin	178,200	
		Foam	241,920	
		FRP fasteners	65,000	
	Total material		**608,560**	**44**
	Transportation and installation costs	Transportation	720	
		Installation (equipment, labour, etc.)	71,680	
	Total transportation & installation costs		**72,400**	**5**
Social costs	Driver delay		404,368	
	Vehicle operating		297,704	
	Total Social costs		**702,072**	**51**
TOTAL initial costs			**1,383,032**	**100**

Table C.5. Maintenance & operation costs

Maintenance & repair	Quantity [m2]	Cost [SEK/m^2]	Cost [SEK]	LCC cost
Steel				
M&R expenses per year	176	30	5,280	
M&R every 15 year	176		60,812	
Total life-cycle cost				**83,223**
FRP culvert				
Life-cycle expenses, 10% of steel				**8,322**

Table C.6 Demolition costs

	Cost categories	Cost	LCC cost
Steel			
	Demounting (labour, equipment, etc.)	71,680	**4,573**
	Transportation of materials, SEK/km	2,880	**184**
	Waste disposal, SEK	-8,717	**-556**
	Total	**65,843**	**4,200**
FRP			
	Demounting (labour, equipment, etc.)	71,680	**4,573**
	Transportation of materials, SEK/km	720	**46**
	Waste disposal, SEK	-11,271	**-719**
	Total	**61,129**	**3,900**

Table C.7 Summary of the results

	Comparison	Steel	%	FRP	%	Saving [%]
Initial	Material	800,000		608,560		31
	Installation & transport	74,560		72,400		
	Social	702,168		702,072		
	Total	1,576,728	95	1,383,032	99	14
M&R	Maintenance & repair	83,223	5	8,322	1	90
End of life	Disposal	4,200	0	3,900	0	
	TOTAL	**1,664,151**	100	**1,395,254**	100	19